energy&fuels

pubs.acs.org/EF Review

Advancements in In-Cylinder and After-Treatment Strategies for Mitigating Pollutants from Diesel Engines: A Critical Review

Samantha Da Costa, Kiran Raj Bukkarapu, Ravi Fernandes, Anand Krishnasamy,* and Pranay P. Morajkar*

Cite This: https://doi.org/10.1021/acs.energyfuels.4c00705 Read Online

ACCESS | Metrics & More | Article Recommendations

ABSTRACT: Although diesel after-treatment techniques demonstrate a substantial decrease in tailpipe emissions, the primary goal continues to be attaining nearly zero emissions to comply with current regulatory requirements and foreseeable imminent rigorous regulations. To achieve this objective, engine combustion systems and fuel formulations require fine-tuning. Taking insights from the recent literature, this review examines various processes, including homogeneous in situ methods, the incorporation of fuel-borne catalysts, and the use of biofuels. Despite progress in in-cylinder pollution mitigation techniques like low-temperature combustion, which exhibits substantial reductions in oxides of nitrogen (NO_x) and soot emissions, it is crucial to consistently advance technology to conform to evolving emission regulations and environmental concerns. A discussion is presented regarding the advantages and disadvantages of the homogeneous charge compression ignition (HCCI) mode and their potential for the future, focusing on biodiesel-fueled HCCI engines. The review assesses the effectiveness of thermal management strategies and engine design modifications that extend the operational range of HCCI engines powered by biodiesel in light of the inherent limitation of a restricted engine operating range. The review critically examines the merits and demerits of biofuels and HCCI systems and provides an essential analysis of current after-treatment approaches. With an imperative focus, the primary aim of this review is to ascertain modern catalysts designed explicitly for use in contemporary combustion systems. An exhaustive examination of the progress made in diesel oxidation catalysts, selective catalytic reduction techniques, lean NO_x traps, diesel particulate filters, and catalyst regeneration is presented. The concluding remarks analyze the catalytic characteristics necessary for smooth incorporation with modern technological developments in various combustion systems.

1. INTRODUCTION

The world is moving rapidly toward cleaner, greener, and sustainable forms of fuels and energy technologies owing to an urgent need to protect the global climate. Internal combustion engines, specifically diesel engines, have been known to be the most efficient workhorses since their invention in the 1890s. Their rugged nature and high torque production make them exceedingly reliable, and the absence of sparking reduces the maintenance costs of spark plugs. Diesel, as an energy-dense fuel, typically delivers great mileage with a higher usable energy content. However, all of these pros still fail to counterbalance the drawbacks. The abatement of derivational pollutants from these systems employing fossil fuels represents intriguing technological and scientific challenges, now more than ever, due to the present and upcoming stringent regulatory standards. While developed countries are planning to phase out direct injection (DI) engines, developing countries are heavily investing into more greener and sustainable fuels such as biofuels derived from valorization of biomass.

Present-day research and technology are focused on hydrogen fuels as the prospective solution to reduce the greenhouse emissions from the transport sector. Since hydrogen combustion temperatures are greater than 2500 °C,[1] cracking of atmospheric nitrogen and oxygen is easily viable, resulting in the formation of highly toxic greenhouse gases, oxides of nitrogen (NO_x). A computational fluid dynamics (CFD) model of diesel engine combustion, incorporating a complex reaction mechanism, was created by Zhang et al.[2] to investigate the effects of the nozzle diameter and spray cone angle on in-cylinder parameters and emissions of a hydrogen-diesel dual-fuel engine. Reducing the diameter of

Received: February 15, 2024
Revised: May 15, 2024
Accepted: May 15, 2024

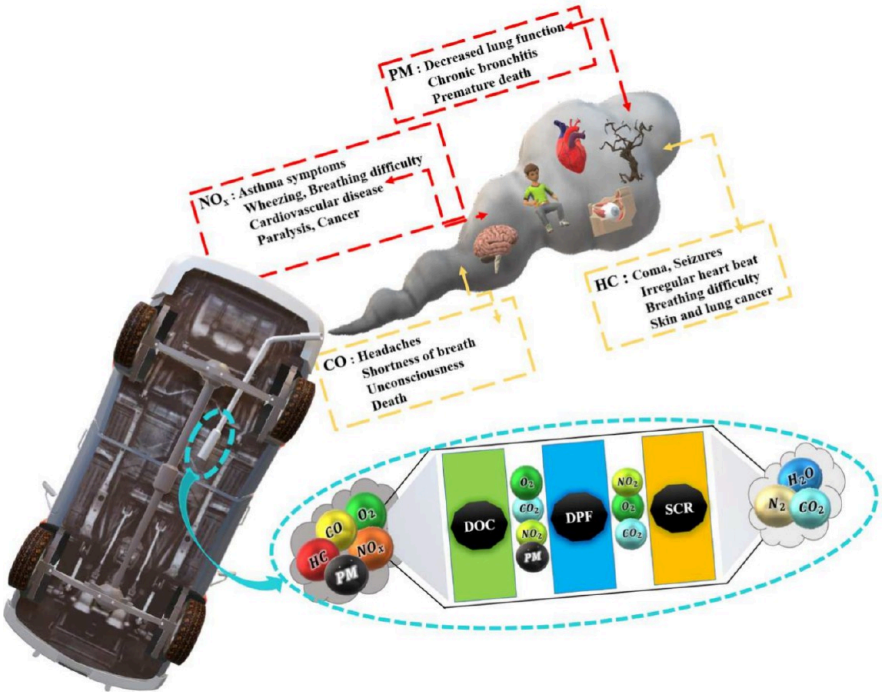

Figure 1. Schematic depiction of health risks and after-treatment strategies of exhaust fumes.

the nozzle results in greater pressure and temperature within the cylinder, thus reducing unburnt hydrocarbon (HC) and soot emissions while favoring NO_x emissions.[2] Smaller spray cone angles reduce HC and NO_x emissions but increase soot emissions.[2] In another study,[3] the researchers experimented to verify a diesel combustion model with an enhanced chemical kinetics mechanism. The authors studied the impact of different exhaust gas recirculation (EGR) rates on the engine's combustion, performance, and emissions. Response surface methodology (RSM) optimization revealed the most favorable operating conditions, demonstrating lower cylinder pressure, temperature, and NO_x emissions as the EGR rates increased.[3] However, along with being highly flammable, hydrogen generation and the infrastructure required for transport and storage raise concerns. Regardless of being most abundant, a significant amount of energy is needed for green hydrogen production, which does not equally balance out the energy that can be drawn from extracted fuel. This calls for extensive research and development to incrementally set up the demand and supply network. Therefore, because fossil fuels have existed for decades, the infrastructure required for producing and operating these systems is well established. Enhancing the existing systems with better pollution control strategies is a wiser approach for a technologically advanced future instead of refueling new infrastructure to develop a whole new fuel energy structure.

With industrialization expanding across rural, urban, suburban, and tribal areas, the exhaust gases from diesel-driven automobiles are widespread in the atmosphere and are absorbed into all living systems through direct or indirect pathways. The major pollutants emitted from conventional diesel combustion engines, such as particulate matter (PM), carbon monoxide (CO), HC, and NO_x, have been subjected to legislative limits as a repercussion of their adverse effects on the environment and the health of living organisms (Figure 1). On comparing the horsepower equated to a gasoline and diesel engine, the diesel exhaust notably resulted in greater environmental toxicity even after considering higher amounts of carbon monoxide emissions in gasoline-operated engines. With every scientific advancement, an avalanche of prospective health effects of exhaust emissions has come to light. A couple of decades ago, lung cancer was listed as the dominant emission related disease encountered only as an occupational hazard. But today, a steep shift in the scenario indicates consequential effects even on an unborn child. Once the exhaust gas enters the lungs, the radicals formed in the exhaust gas mixture at high temperatures, along with PM and other minacious components, undergo particle deposition followed by the interaction with bioreactive gases. These abruptly induce local oxidative stress and pro-inflammatory signaling, which pave the way for respiratory diseases such as asthma, lung cancer, chronic obstructive pulmonary disease (COPD), etc. These PM and other gases travel deeper across airway channels into the circulatory system and into the bloodstream, distributing them throughout the body. The radicals have a potent malignant nature which is bottom-line responsible for various cancers and other systemic health problems such as thrombosis, strokes, accelerated aging, and heart disease.[4]

de Melo et al.[5] aimed to verify the effects of PM inhalation during and before pregnancy, and to do this, they exposed Wistar rats to filtered air and air having a load of PM. On assessing the leukocyte and blood platelet count postexposure, an increase in the interleukin-4 cytokine levels, which is a potent regulator of immunity, was observed in the placenta's fetal portion, suggesting a spontaneous inflammatory reaction. Another control experiment following up on the consequences of fetal exposure to diesel exhaust indicated significantly lower numbers of daily produced sperm, spermatids, and sertoli cells in mature rats. The effect was attributed to the nasal ingestion of gases having ultrafine particles of size less than 0.1 μm, which are easily absorbed through the lungs and extrapulmonary tissues.[6] A study by Bendtsen et al.[7] compared fuel types

https://doi.org/10.1021/acs.energyfuels.4c00705
Energy Fuels XXXX, XXX, XXX−XXX

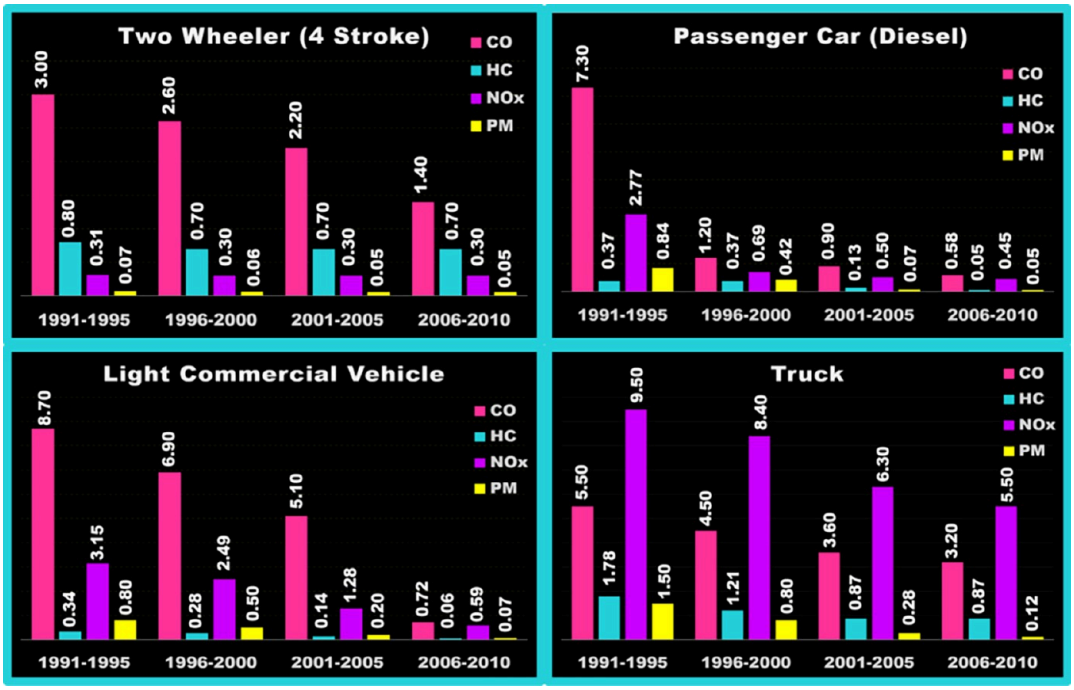

Figure 2. Pollutant emission factors for different categories of vehicles (Source: IndiaStat.com).

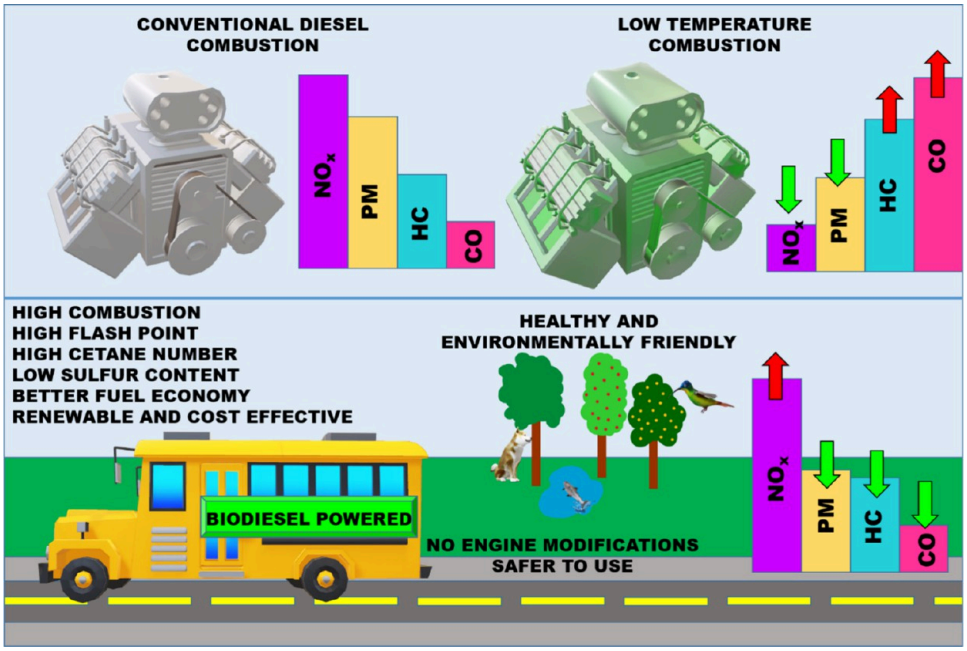

Figure 3. Schematic illustrating the precedence of LTC modes and use of biodiesels over conventional systems.

and combustion conditions with their consequences on the resulting toxicity. It was concluded that the reactive oxygen species in the exhaust are directly correlational toward genotoxicity in lung tissues, whereas the depositional surface area, elemental and organic carbon, and polycyclic aromatic hydrocarbons (PAH) correlated with neutrophil influx in a study conducted on mice. When zeroing in on NO_x, it majorly comprises nitrous oxide (N_2O), nitric oxide (NO), dinitrogen trioxide (N_2O_3), nitrogen dioxide (NO_2), dinitrogen tetroxide (N_2O_4), and dinitrogen pentoxide (N_2O_5).[8] Each of these has its environmental potency and quite easily participates in radical formation at higher temperatures. A facile route toward genotoxicity involves radical oxygen and nitrogen species which cause oxidative and alkylating deoxyribonucleic acid (DNA) damages via attack on double bonds of purine and pyrimidine bases followed by consequent DNA strand breaks.[9] To protect the environment and for the welfare of masses, government bodies have laid down stringent emission standards, as illustrated graphically in Figure 2. In order to surmount these present-day emission standards, alternative pathways such as the alternation of fuels, alternation of combustion processes, and augmented after-treatment strategies have been researched hitherto.[10,11]

https://doi.org/10.1021/acs.energyfuels.4c00705
Energy Fuels XXXX, XXX, XXX−XXX

After being signatories of the Paris Climate Agreement, environmentalists have a greater responsibility toward reducing the carbon footprint, primarily that of soot, NO_x, CO, and HC, which directly and indirectly contribute toward greenhouse gases. Renewable fuels such as biodiesels play a crucial role by reducing the burden on exhaustible fossil fuels and allowing the engineering of cleaner, greener fuels with enhanced pollutant mitigation properties.[12] The use of biodiesels is advantageous due to their convenient availability from biomass sources, representation of a simple carbon dioxide (CO_2) combustion cycle, and socioeconomic and consumer-friendly potential. The use of biodiesels and their emission characteristics are further discussed in section 2.2.

Given the substantial volatility of currency exchange rates on a global scale, it is critical to conduct a cost analysis for biodiesel production in the country of origin to ascertain its relative merits compared to conventional diesel fuel.[13] Native conditions comprise various elements—including climate, technological infrastructure, and available resources—that substantially impact production costs. The production of biodiesel generally entails the cultivation, refining, and distribution of feedstock.[14] Due to advantageous growing conditions and economies of scale, feedstock costs may be reduced in regions endowed with ample agricultural resources, such as specific areas in Southeast Asia or South America. However, costs associated with processing and distribution can fluctuate significantly due to labor costs, energy prices, and regulatory frameworks.[13] In contrast to diesel fuel, biodiesel production frequently exhibits enduring cost advantages in the face of fluctuating fossil fuel prices and increasingly stringent environmental regulations, notwithstanding the initial investment requirements.[15] Additionally, biodiesel presents the possibility of cost savings through mitigating greenhouse gas emissions and reducing dependence on imported fossil fuels, bolstering its economic feasibility amidst difficulties related to currency exchange. Hence, conducting a comprehensive cost analysis that considers local conditions is critical to arrive at well-informed decisions concerning the adoption of biodiesel and its comparative analysis with conventional diesel fuel.[15]

Although distinguished technological advancements are in play toward emission abatement, low-temperature combustion (LTC) and in-cylinder reduction techniques are the bottom line in the research and development of futuristic engine systems (Figure 3). The objectives here are fulfilled primarily by operating in air/fuel ratios greater than 1, i.e., a leaner mixture or by intensifying the EGR. LTC engine modes help diminish NO_x and PM levels simultaneously but drastically escalate HC and CO emissions. LTC modes integrate Homogeneous Charge Compression Ignition (HCCI) combustion, Premixed Charge Compression Ignition (PCCI) combustion, and Reactivity Controlled Compression Ignition (RCCI) combustion.[16,17] Lean mixtures and high temperatures (~1900 K) available in conventional combustion engines provide higher nitrogen (N_2) concentrations and sufficient activation energy for splitting the N_2 triple bond, providing nitrogen radicals for NO_x formation. Combustion generated PAHs, widely accepted as soot precursors, coagulate at adequately elevated temperatures (~1500 K) in rich fuel mixture zones to form soot particles. The application of EGR drops combustion temperatures and thereby results in a plunge in soot oxidation rates. In LTC operational modes, therefore, the oxidation of aromatics to CO and CO_2 is a chance hit, but the coagulation of PAHs for soot formation is quite rare in LTC temperature ranges. Thereby allowing LTC systems to achieve reduced soot and NO_x emissions successfully, which is a major concern when using biodiesels.[18,19]

Hybrid vehicles have shown great potential in replacing diesel engines due to their ability to reduce emissions and improve fuel efficiency. Various studies highlight the advantages of hybrid vehicles, emphasizing their essential contribution to reducing harmful emissions and improving fuel efficiency, especially in city driving conditions.[20] Methods such as utilizing fuzzy logic algorithms to optimize power control have been proposed to enhance the effectiveness and reduce exhaust emissions of hybrid electric vehicles. This results in a 5% decrease in fuel consumption and a 50% reduction in CO emissions.[21] In addition, using green hydrogen as a fuel in hybrid vehicles has shown an average increase in engine efficiency of around 17% and a decrease in energy consumption of about 15% during driving cycles. This highlights the potential for significant improvements in reducing emissions and increasing fuel efficiency.[21] However, unlike hybrids that require additional components, such as batteries and electric motors, LTC engines operate solely on internal combustion principles. This simplifies vehicle design and reduces manufacturing complexities. As a result, despite the importance of hybridization in reducing emissions, LTC engines are becoming an increasingly attractive and potentially more effective solution for tackling pollution issues in the automotive industry.[22]

The long-established engines, in their exhaust mixtures, let out HCs, which form when fuel gets trapped in nooks and crannies of the combustion chamber during excessively rich or lean fuel mixtures and ineffective evaporation and ignition of fuel. During combustion of overly lean mixtures, the fuel cannot blend homogeneously, and this inefficient propagation of flame front and partial pyrolysis leads to the formation of HC and CO. Moving over to overly rich fuel mixtures, inefficient mixing of fuel with air and even in case mixing occurs homogeneously, the fuel does not oxidize thoroughly, again resulting in the formation of HCs and CO. Thus, the LTC system comes with its setbacks that yearn for painstaking attention. Reduced combustion temperature, excessively lean mixtures, prompt ignition and combustion, and diminished oxygen concentrations increase HC and CO levels.[23,24] Literature and past research demonstrate a reduction in HC and CO emissions using biodiesels and a simultaneous increase in NO_x emissions, which conflict with the emission features exhibited by LTC modes. Centered on this, it could be speculated that using biodiesels and their blends in low temperature engine systems has the utmost potential to reduce emissions comprehensively and, if engineered fittingly, could be the most reliable engine and fuel system for future applications.

Meticulous and decisive control of engine operation and fuel type and quality can attenuate pollution emissions, but after-treatment is essential to attain near-zero pollution emissions at the tailpipe of the vehicle, even in LTC systems, as no technique can independently reduce emissions to near zero values. While LTC reduces NO_x and soot, biodiesels reduce HC and CO, which are prominent pollutants in LTC modes. Toggling between these two allows one to find a balance to reduce pollutants in the engine itself. Once beyond the engine, the after-treatment pollution control involves passing the warm engine exhaust over a catalyst or a series of catalysts based on the requirement to increase the reaction rate of chemical

https://doi.org/10.1021/acs.energyfuels.4c00705
Energy Fuels XXXX, XXX, XXX−XXX

Table 1. Comprehensive Table Listing Key Review Articles

author	title (year)	research status
ul Haq et al.[283]	Influence of nano additives on Diesel-Biodiesel fuel blends in diesel engine: A spray, performance, and emissions study (2024)	Addition of nanoparticles enhances cetane number, calorific value, heat transfer properties along with improving atomization, widening of spray cone angle, longer penetration length and better fuel-air mixing. Addition of metal oxide and oxygenated additives decreases viscosity, density and flash point along with increasing oxygen content. Positive effect on BTE and BSFC. Influence of these on exhaust gas temperatures and NO_x emissions have inconclusive results in literature.
Gad et al.[284]	A comprehensive review on the usage of the nanosized particles along with diesel/biofuel blends and their impacts on engine behaviors (2023)	Nanoparticle addition enables secondary oxidation for unburnt fuels, improve mixing of fuel with air, improve combustion efficiency, heat transfer rate, evaporation rate, combustion properties, thermal efficiency, specific fuel consumption, and thermophysical properties. they reduce ignition delay, decrease burning rate and improve cylinder pressure. Metal organic frameworks are good fuel additives with high porosity, surface area, consistent pore size, structural tunability etc.
Azad et al.[285]	A landscape review on biodiesel combustion strategies to reduce emission (2023)	Better biodiesel combustion could result from adjustment of injection pressure, piston bowl geometries and injection sprays. LTC strategies with homogeneous combustion reduce NO_x but reduce oxidation rates of hydrocarbons and CO.
Altarazi et al.[286]	Effects of biofuel on engines performance and emission characteristics: A review (2022)	Blending biodiesels is essential toward prevention of engine failure. Also, spherical combustion chambers improve results. With biodiesel blends BSFC is higher, while, BTE and engine torque are lower.
Kumar and Rehman[287]	Biodiesel in homogeneous charge compression ignition (HCCI) combustion (2016)	Though the title is Biodiesel in HCCI combustion, it covers a minimal discussion on biodiesel-HCCI studies. Out of 7 studies reviewed, one corresponds to PFI-HCCI combustion of the biodiesel−diesel blends. Biodiesel blends coupled with HCCI, reduce emissions simultaneously while maintaining the performance of a CI engine.
Saiteja and Ashok[288]	A critical insight review on homogeneous charge compression ignition engine characteristics powered by biofuels. (2021)	Discusses two studies related to PFI-HCCI of biodiesel−diesel blends, with a focus on the effect of biodiesel fraction on HCCI engine performance characteristics. Incorporation of stratified charge combustion techniques deflates HC and widens operation range.
Riyadi et al.[104]	Biodiesel for HCCI engine: Prospects and challenges of sustainability biodiesel for energy transition. (2023)	Focuses on studies related to various HCCI strategies for biodiesel combustion. HCCI combines merits of gasoline and diesel engines to achieve high thermal efficiency and lower emissions simultaneously. Primary objective is to lower NO_x and PM while maintaining high fuel efficiency.
Karre et al.[289]	State of the art developments in oxidation performance and deactivation of diesel oxidation catalyst (DOC) (2023)	Presence of H_2 increases adsorption of CO and hydrocarbons on Pt as well as Pt:Pd catalysts along with maintaining Pt in its metallic form thus increasing activity. SO_2 poisoning could be reduced using supports such as TiO_2, Si, Zr and w or using promoters like Vanadia.
Doppalapudi et al.[290]	Advanced strategies to reduce harmful nitrogen-oxide emissions from biodiesel fueled engine (2023)	Longer ignition delay and combustion duration shows reduction in NO_x emissions when using biodiesels. Higher EGR in LTC modes help attain near-zero NO_x emissions. Higher density, viscosity and unsaturation and polysaturated fuels increase emissions due to fuel accumulation inside the combustion chamber.
Shi et al.[291]	Mechanism, performance and modification methods for NH3-SCR catalysts: A review[291] (2023)	Introducing secondary metals, replacing carriers, adjusting redox and adsorption capacity of the catalyst are beneficial. Cu based zeolite catalysts show promising activity with high low-temperature performance and hydrothermal stability, however their poor SO_2 resistance could be solved by introducing secondary metals.
Luo et al.[292]	The evaluation of catalytic activity, reaction mechanism and catalyst classification in diesel particulate filter: a review (2024)	The morphology, pore size, pore structure and orderliness of microporous structures are essential to improve good contact between soot and catalyst. 3-dimensional ordered microporous catalysts are found to be effective. Ceramic paper and wire mesh as catalytic carriers show optimal filtration efficiency, regeneration frequency and balances pressure drop.
Zhang et al.[293]	Diesel particulate filter regeneration mechanism of modern automobile engines and methods of reducing PM emissions: a review (2023)	Soot produced at low-load, low-speed, oxygen enriched fuel and post injection operating parameters have stronger reactivity. The best after treatment system comprises of DOC, DPF and SCR along with LNT and EGR to alter configurations as per a given set of working conditions.

https://doi.org/10.1021/acs.energyfuels.4c00705
Energy Fuels XXXX, XXX, XXX−XXX

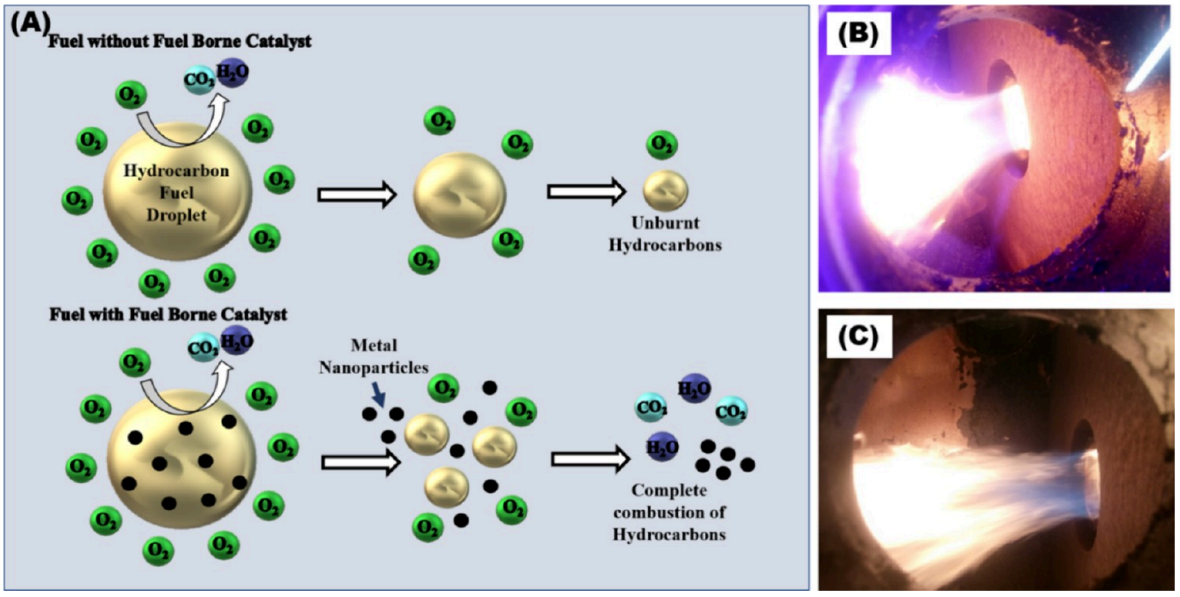

Figure 4. (A) Combustion of hydrocarbon rich fuel droplets in the presence of oxygen-rich air over the residence time of the fuel in the combustion chamber. Photographic illustration of combustion with (B) neat fuel and (C) fuel doped with fuel borne catalyst. (B) and (C) Reproduced with permission from ref 39. Copyright (2018) with permission from Elsevier.

reactions to consume the pollutant. The catalysts used should be able to function, survive, and regenerate in exhaust gas conditions over tens of years and a hundred thousand miles of operation and sustain the attack by catalyst poisons. Customarily, a catalyst system is composed of a substrate coated with metals or metal oxide composites. The active material is bound onto the substrate, providing a greater surface area to maximize interactions. This substrate is mounted onto a metal that can withstand vibrations and shocks and provide sufficient insulation to the active catalytic species. The vital catalytic mitigation systems include diesel oxidation catalysts (DOC), selective catalytic reduction (SCR), lean NO_x traps (LNT), and diesel particulate filters (DPF).[25]

A number of review papers are available in the literature (Table 1), and they concisely provide individual studies on fuel modifications, LTC, DOC for HC and CO, SCR for NO_x along with direct NO_x decomposition and LNT and finally, the DPF for soot. However, to the best of our knowledge, there is not a critical review analyzing which combinations of these strategies are to be used and what are the possible technological challenges that would be required to be addressed to possibly achieve near zero emissions for a sustainable transportation system in the future. To be able to achieve the ultimate objective of nearly zero emissions (NO_x, HC, soot, CO mitigation) without compromising on engine efficiencies, a strategic combination of advanced in-cylinder combustion with advanced after-treatment strategies is essential for mitigating pollutants. This review aims to understand the working principle of each of these systems along with their fundamentals, critically evaluate the advancements being researched in these systems, and put forward effective strategies for designing next-generation clean and sustainable energy technologies. Optimal properties for catalysts to prepare next-generation after-treatment systems have also been highlighted concisely. Therefore, this review is expected to provide students, researchers, and policymakers a guiding platform not just to understand the intricate challenges in existing combustion technology but also make them aware of the possible challenges the modern technologies such as biofuel combustion and present after-treatment modes would bring in the future.

2. CLEAN COMBUSTION VIA FUEL MODIFICATION STRATEGIES

2.1. Evaluating Fuel Borne Additives. Fuel borne catalysts (FBC) serve as homogeneous combustion catalysts that elevate peak cylinder pressure and fasten the heat release rate (HRR), while simultaneously reducing the combustion duration of the fuel and ignition delay. Concurrently, addition of FBCs increased the brake thermal efficiency (BTE) and decreased the brake specific fuel consumption (BSFC).[26] They effectively enhance the passive regeneration of DPFs, by providing an oxygen-rich environment for PM conversion to CO_2. While active regeneration targets an increase in exhaust temperature or, by some means, attains the soot oxidation temperature, passive regeneration is pulled off by reducing the ignition temperature of the soot itself. This is very well achieved by dosing the fuel with FBCs. A FBC is expected to reduce the oxidation temperature of soot by altering the physicochemical properties of the fuel (Figure 4(A)).[27] They may either react with carbonaceous matter directly or react with water vapor and form hydroxyl radicals, which are superb soot oxidation agents, or they may alter the performance and emissions of burners. FBCs first reduce soot formation inherently in the fuel, and once they reach the DPF filter, provide a homogeneous dispersion of the catalyst in the soot bed which further hastens the oxidation process. These nanoparticles alter engine performance characteristics such as BSFC, BTE, exhaust gas temperature, etc.[28] Several studies have been conducted to investigate the effects of metal-based catalysts in the form of oxides, organometallic or organo-soluble compounds, etc. Their consequential effect on the formation, oxidation, and mass emission of soot has been explored, along with their repercussions on engine performance and emissions.

https://doi.org/10.1021/acs.energyfuels.4c00705
Energy Fuels XXXX, XXX, XXX−XXX

FBCs mainly consist of compounds containing metals, especially alkali and alkaline earth metals and transition metals. Their presence could potentially reduce the ignition temperature of soot, thus reducing it to conventional exhaust temperatures, which reduces activation energy required for soot oxidation. They are also known to shorten the ignition delay, thus accelerating the rate of combustion. The main focus has been on Fe and Ce compounds, although others owing to their variable oxidation states have also been radically explored. The doping procedures usually involve weighing the required quantity of the FBC and sonicating the catalyst in the required fuel, producing a uniform suspension and further heat treatment if required, followed by dilutions to achieve the required concentrations.[29,30] Zhang et al.[31] methodically scrutinized the consequences of the addition of CeO_2 and $Fe(C_5H_5)_2$ (ferrocene) to ultralow sulfur diesel fuel and its impact on the physicochemical and toxicological features of soot. Summarily, on addition of ferrocene, the organic components decompose at early stages owing to their low melting points, and the metal ions left behind move into their most stable oxidation state which in the case of iron is Fe(III) oxide crystallizing toward hematitic α-Fe_2O_3. These nuclei and nanoparticles of Fe are known to reduce soot emissions, particularly for lighter load operations. Fe was chosen initially due to its favorable mutual solubility in diesel. On addition of powder additives to a fuel, a desired amount of solubilizer needs to be added for efficient dissolution. However, this may further deteriorate fuel quality, and thus, inevitably solvent phase FBCs are preferred, which will not lead to any stratification on blending.[32] Fennell et al.[33] contributed toward elucidation of a mechanistic pathway wherein NO_x follows a dissociative pathway at the soot-catalyst interface. The dissociated oxygen (O_2) atoms from NO_x make themselves available for soot oxidation, while a simultaneous recombination of nitrogen atoms takes place and they diffuse out. These reactions readily occur on the surface of Fe_2O_3 under an excess of O_2. Further, nanostructural studies of soot emitted postcombustion with Fe-catalyzed fuel suggested a change in shape of primary particles, wherein they appeared jagged and irregular instead of spherical. Also, a higher degree of disorder was observed in these particles, which will enhance soot oxidation in the DPF, and a reduction could be highlighted in the amount of total elemental carbon in the soot produced. Conversely, the presence of these metal nanoparticles affects soot formation by functioning as condensation nuclei for earlier than usual soot inception and hence increasing soot formation. Fe nanoparticles with a smaller size and greater mobility have a greater number of soot/catalyst contact points, thus increasing efficiency under exhaust conditions.[34,35] Even though Fe possesses an inordinately large bulk oxygen capacity, its oxygen conducting rate is relatively low, which limits its utilization. Grafting Fe with another metal oxide with greater oxygen storage and release (OSR) capabilities could act as a portal for increased oxygen transfer by Fe nanoparticles.

Now shifting the focus onto CeO_2 as a fuel additive, its nanoparticulate structure will remain unmodified and will be unchanged under the exhaust conditions as a consequence of its high thermal stability. CeO_2 is a well-known redox catalyst and has abundant lattice oxygen species, which can be easily transferred to carbonaceous matter for soot oxidation, while the metal oxide species simultaneously take up gaseous oxygen and replenish themselves to promptly continue the mechanistic oxygen cycle. In this regard, it could be concluded that for CeO_2, a higher surface area of the catalyst is essential toward higher soot oxidation, and dosing with Ce also drastically decreases the activation energy of the said oxidation reaction. Contrarily, an increase in the concentration of Ce has a consequential reduction in the ignition temperature, and this ends up in a greater amount of unburnt fuel left to condense on the soot surface leading to excessive organic carbon emissions. Thus, even the two extensively apprehended FBCs have competing repercussions, and further a momentary discussion on other metals serving as FBCs is crucial.

Ce, Pt, Ce-Pt, and Fe-soot generated from their corresponding FBCs were studied by Krishna and co-workers,[36] of which, Pt-Ce soot is oxidized at much lower temperatures (275−300 °C) with O_2 in comparison to the other soot samples. Although ceria by itself can show great oxidative activity, the synergistic effect arising due to the combination of Pt with Ce seems to enhance the reaction rates. The O_2 storage and release capacity of ceria provides active oxygen species at local contact sites. As the CeO_2 species supplies lattice oxygen to carbonaceous soot resulting in oxygen vacancies, these are rapidly filled by gas-phase oxygen, which is a driving force to enhance soot oxidation. Pt catalysts do not outperform ceria due to sintering in the absence of a catalyst support, and on integrating Pt with Ce, the Pt crystallites seemed to stabilize, which resulted in a higher impact on the oxidation rates. It is often highlighted that the major drawback of DPF traps arise from their inability to provide sulfur resistance, although in the case of FBCs the durability in the presence of sulfur groups has been observed to be not quite an issue in conventional engines.[37] This is the result of regeneration cycles that the catalyst undergoes during engine operation. The catalyst is subjected to high temperatures in the combustion chamber, which can help desorb or decompose sulfur-containing groups. Most catalysts used as FBCs possess high oxygen storage capabilities (OSC) and are able to oxidize sulfur dioxide (SO_2) to less harmful sulfates which could then be carried away by the exhaust gas. In a compression engine study carried out by Shukla et al.,[38] diesel fuel mixed with Au/CeO_2 effectively reduced NO, the number of particulate matters decreased in nucleation mode, while an increase was observed in accumulation mode. Gold, once assumed to be catalytically inert, has now been widely explored and proven to have impressive activity. The favorable activity of this FBC could be attributed to the reversible Ce^{4+}/Ce^{3+} and Au^{3+}/Au^{1+} reactions.

Mixed modified Fe_2O_3-WO_3 catalysts were synthesized and dosed into biodiesel fuel by Bazooyar et al.[39] As discussed earlier, iron is known to produce highly reactive sites on its oxide surface for carbon particles to condense and almost completely oxidize during combustion. Fe compounds are also known to increase flame peak temperatures leading to lower activation energies for soot oxidation as discussed previously.[40] Tungsten is known to be a good selective reduction catalyst along with providing a higher tensile strength of its host and increasing its lifetime. The peculiar stable behavior of tungsten vaporizes it downstream of the flame compared to ferric ions, and thus these assist in reducing a large number of free oxidized radicals. It was also observed that the addition of the FBCs results in a change in color of the central region of the flame from yellow to blue, and the fuels combust with greater intensity and luminosity as compared to neat biodiesels as shown in Figure 4(B) and (C).[41]

https://doi.org/10.1021/acs.energyfuels.4c00705
Energy Fuels XXXX, XXX, XXX−XXX

Organic-based Mn fuel additives were tested by Celik et al.[42] by blending it with rapeseed methyl ester biodiesel. The fuel properties such as viscosity, density, and flash point decreased, while the calorific value increased with a corresponding increase in fuel atomization. These enhanced fuel characteristics resulted in a consequential decrease in CO, HC, and smoke emissions by 25.28%, 6.64%, and 6.5% respectively, however, with a substantial increase in NO_x emissions by 25.54%. In another study, carried out on a single-cylinder constant speed diesel engine, Mn-doped alumina were employed as fuel additives using avocado biodiesel with a 20% blending. The brake thermal energy increased, and a reduction in brake-specific fuel consumption was seen. This was accompanied with reduction in CO, HC, smoke, and NO_x emissions.[43] Hassan and co-workers[44] blended Ni and Al nanoparticles with a castor oil biodiesel-diesel blend and observed an increase in torque, brake power, and brake thermal efficiency with a corresponding decrease in brake specific fuel consumption. This also decreased CO and NO_x emissions.

Fe, Ce, and Pt are the main contenders among others (Table 2) to perform as efficient FBCs, and their modification with various other transition metals have a similar mechanistic pathway with differing activities. The bottom-line intention of FBCs is the reduction in exhaust gas pollutants mainly focusing on particulate matter, although the effect on NO_x is nonconclusive, since results differ in the literature as a consequence of fuels, engine, and other experimental variations. FBCs also preferentially alter engine related properties such as BTE, BSFC, fuel atomization, etc. at the same time enhancing the cetane number and calorific value of the fuel. Properties such as good solubility, temperature tolerance, small size, higher mobility along with a greater surface area of these FBCs with the potential to easily transfer and take up oxygen in a cyclic pathway could be highlighted during their fabrication. However, these lead to another environmental hazard, i.e., increased emissions of nanosized particles as the FBC-doped fuels facilitate formation of self-nucleated metallic nanoparticles. It was also observed that the soot produced had a greater amount of organic carbon fraction and water-soluble organic fraction which have greater probabilities of binding to vital cellular sections of human cells and other fauna leading to excessive in vitro toxicity. The seepage of such metals in higher amounts into the lungs along with particulate matter definitely has far worse consequences than merits.[45] The study of FBCs has been extensively carried out by blending with diesel fuels and recent studies with biodiesel fuels; however, these investigations need to be extrapolated to newer hybrid engine technologies which will be subsequently discussed in Section 3.

2.2. Key Challenges and Development in Biodiesel Combustion. Alternative fuels such as alcohols, biodiesels, natural gas, etc. have been tried and tested in diesel engines to reduce pollutants and enhance cost-effectiveness. The vaporization latent heat and self-ignition temperature of alcohols possessing fewer carbon atoms are higher in comparison to diesel, along with a lower octane number. As a prerequisite for combustion parameters, alcohols with lower latent heat are not preferable, and hence methanol, ethanol, etc. are favored over other higher alcohols and are also financially viable. The use of fuels with a low carbon number show lower soot emissions and since alcohols tolerate higher EGR, and NO_x production is also substantially abated. Natural gas has gained appreciation due to its low-greenhouse-gas emissions and cost-effectiveness. The

Table 2. Brief Summary of FBCs, Their Properties, and Effects on Combustion Characteristics

catalyst; synthesis method	engine specifications	catalyst characteristics	inference
Fe (F7994);[32] commercial Fe solvent FBC	Diesel engine under a rated speed of 2600 r/min, at engine loads.	Solubility in diesel fuel, heat stability	Decrease in BSFC, decrease in NO_x and smoke with an increase in the FBC blending ratio.
0.01% Au/CeO_2;[28] reduction method	Kirloskar TV-1 four-stroke water-cooled CI engine	OSC of CeO_2 reduces available O_2 for reaction with N_2; this property also reduces PM emissions in nucleation mode.	48.30% reduction in coke formation, small rise in in-cylinder pressure and BTE, along with a reduction in HRR and CO emissions. Decrease in NO_x and HC emissions.
CeO_2 nanoparticles (8−10 nm);[294] commercial	Single-cylinder direct injection research engine	CeO_2 can store and donate oxygen from its crystal lattice, which in an oxygen lean environment will pose as a catalytic oxygen donation.	Soot emission reduced by ∼50%, 2−5% reduction in NO_x at high load EGR, standard particulate matter size, and not a wide distribution as typically observed in LTC modes.
Barium ethoxide;[295] stirring	Three-cylinder direct injection INTER-IDE314NG diesel engine	Ba reacts with S forming $BaSO_4$ which reduces the total particulate mass emission rate.[296]	Decreased HC emissions for diesel but increased for biodiesel due to high viscosity and larger droplets of biodiesels. Smoke opacity decreased for diesel fuel.
TiO_2 (21 nm);[297] commercial	Vertical, water-cooled, monocylinder test engine	TiO_2 lowers the activation energy and increases thermophysical properties of fuels, increasing the temperature around fuel droplets and thus enhancing combustibility.	Biodiesel combustion with TiO_2 reduces the cylinder pressure and HRR along with BTE. Improves engine ouput and decreases emissions.
Alumina nanoparticles;[298] commercial	Kirloskar four stroke, single cylinder, direct injection, air cooled engine	Alumina enhances the rate of atomization, accelerates combustion, and increases heat transfer from combustion products, thus improving engine performance.	Higher cylinder pressure at full load with higher HRR. Reduction in major pollutants such as CO, CO_2, and HC.
Graphene oxide nanoparticles;[299] commercial	Lombardini DIESEL 3LD 510 air cooled single-cylinder engine	Graphene oxide has excellent mobility of charge carriers and unique electronic and mechanical properties.	Improvement in power, decreased CO and HC emissions, and a slight increase in CO_2 and NO_x emissions.

https://doi.org/10.1021/acs.energyfuels.4c00705
Energy Fuels XXXX, XXX, XXX−XXX

fuel can be applied to the in-use engines without major alterations, although a higher compression ratio would be needed to be applied due to the high-octane number of this fuel. These fuels can be used together with diesel in a dual fuel combustion system or could also be blended with diesel using cosolvents or emulsifiers if not readily soluble.[46,47]

A distinguished alternative fuel contender, biodiesel, derived from vegetable, animal, and other waste fats has been extensively used in heavy-duty and marine engines.[48] Reasons are a shortage in supply of fossil fuels, nonedible and waste matter having a great potential to be converted into biodiesel, and in the aspect of environmental protection they have proven to be less polluting and demanding on the environment. Biodiesels also back up the Renewable Fuel Standard (RFS) program, working toward reducing greenhouse gas emissions and expanding the renewable fuels sector while reducing reliability on fossil fuels.[49] B100 or neat biodiesel is not always quite favorable primarily due to its high viscosity owing to the excess fatty acid content resulting in poorer fuel atomization.[50] Also, biodiesel does not perform well in colder weather conditions as the viscosity of the fuel increases, further resulting in clogged filters and gelling up of fuel,[51] thereby concluding that an optimum % proportion of biodiesel within the biodiesel-diesel blend improves performance.[52] Every synthesized biodiesel contains fatty acid esters, and the combination of these saturated and unsaturated fatty acids is characteristic to a given raw material from which they have originated. These then have their own peculiar cetane number, density, kinematic viscosity, calorific value, etc.[53] The total fraction of fatty acids in the biodiesel corresponds to its chemical properties, and these can be further divided based on their dependency on the chain length and number of double and single bonds in and out of conjugation with *cis* or *trans* orientations.[54] The fuel bound oxygen species and lack of sulfur groups relatively improve emission quality. However, with long-term use, serious issues arise, such as those arising from oil thickening, injector depositions, and cold start in winter seasons, are observed. These small variations add up to alterations in performance and emissions of biodiesels.[55,56] The higher oxygen and aromatic content in the fuel, the higher the combustion temperature along with a high cetane number, and viscosity, with high bulk modulus being inherent characteristics of most biodiesels, and these just happen to be the properties triggering NO_x formation.[57]

While the complex reactions and combustion pathways adopted by biodiesels in automotive engines are highly networked due to their vast number and varied components, surrogate or representative molecules are used to comprehend these and devise predictive models for kinetic rate laws. The nature of their results can be extended to develop working principles of complex biodiesel fuels. The carbon chain lengths,[58,59] number and type of functionalities,[60,61] oxygen species,[62,63] position and extent of unsaturation,[64,65] and percentage blending of representative molecules[66,67] are altered to understand their impact on the fuel. These observations are further extended toward comprehending the fuel as a whole. The formation of reactive intermediates, such as stable and unstable radical species and cyclic structures, provides insight into the initial combustion products formed, which play a crucial role in pollutant formation. Resonance-stabilized or cyclized molecules or radicals have a higher lifetime and are involved in soot inception. Similarly, stabilized molecules generated in the gas phase form a part of hydrocarbon emissions. Therefore, such studies involving surrogate fuels are used for laboratory optimization along with setting up computational models for biodiesel combustion.[68,69] When correlating biodiesels to their sooting tendency, Wang et al.[70] compared biodiesel methyl esters obtained from different sources using engine experiments and simulations at differing operational conditions. Their study systematically backed up an existential idea that a lower sooting tendency could be observed for methyl esters with the lowest amount of unsaturated alkyl esters. Likewise, Da Costa et al.[71] observed similar results while scrutinizing the nanostructural characteristics and oxidative reactivity of soot obtained from two biodiesel surrogate blended diesel fuels wherein the surrogates differed from each other only by a single unsaturated bond. The saturated fuel blends showed lower sooting tendencies compared to the unsaturated diesel fuel blends. This study was done using diffusion flame generated soot which is a representative controlled method to avoid interferences by metal specs, engine oils, and lubricants.[72]

While focusing on pollutant emissions, certain engine related parameters need to be highlighted. First, the BTE, which is lowered in the case of biodiesels due to higher density and viscosity, leads to poor atomization and reduced fuel combustion. Also, certain biodiesels have lower calorific values, which add up to further lowering the BTE.[73] Further, the BSFC of biodiesels is higher than neat diesel fuel, resulting in varied exhaust gas temperatures. These temperatures are the primary parameters in optimizing emission mitigation strategies of a compression ignition (CI) internal combustion engine.[74] Multiple studies with different biodiesels synthesized from waste or feedstock end up with varied exhaust gas temperatures in biodiesel and diesel run engines depending upon the engine running conditions and composition of the biodiesel. Rahman and co-workers,[75] from their four-stroke engine run using biodiesel produced from water hyacinth biomass, concluded that the exhaust temperatures substantially increase with engine load and were even higher when the engine was run with diesel as compared to the biodiesel blend. A similar trend was followed in a study conducted by Rajak et al.[76] wherein the exhaust gas temperatures dropped on increasing the biodiesel blending ratios, while Emiroğlu et al.[77] established that diesel fuel has higher exhaust gas temperatures than biodiesel blended diesel fuel due to longer combustion durations observed for diesel fuels and also as a consequence of higher oxygen content in biodiesel blended fuels. Thus, this could be attributed to an effect of the high viscosity, low cetane number, and reduction in volatility leading to poor mixing, which may also lower exhaust temperatures in the case of biodiesels. Predominantly, density itself affects fuel atomization, cetane number, and heating values. Not just the physiochemical properties of the fuel but the combustion characteristics such as cylinder pressure, HRR, etc. also play a major role in effecting exhaust emissions. Hence, it is essential to tailor the characteristics of the fuel in order to reduce pollutants and maximize combustion efficiency by altering the primary properties of the fuel which consequently effect engine performance and emissions.[78,79]

CO emissions are a direct consequence of incomplete combustion and a deliberate result of local rich fuel mixtures. In the case of biodiesels, CO emissions arise due to high density, viscosity, and poor atomization. However, at increased engine loads or as speed increases, a larger amount of air enters

https://doi.org/10.1021/acs.energyfuels.4c00705
Energy Fuels XXXX, XXX, XXX−XXX

the combustion chamber facilitating the combustion process.[80] A comparison between the performance and emission of diesel engines using eucalyptus biodiesel blends was conducted by Ellappan et al.[81] which only further confirmed that CO emissions decreased when using biodiesels. This feature was explained based on excess of O_2 bound within the fuel in biodiesel, which leads to enhanced oxidation of CO to CO_2 as compared to that in neat diesel. As the discussion moves on to CO_2 emissions, with an increased amount of CO converting into CO_2 in biodiesels, it is apparent to expect a spike in the CO_2 emission values. Further, Shrivastava et al.[82] also correlated an increase in injection pressure and biodiesel ratios to an increase in percentages of CO_2 emissions. Also, higher molecular weight compounds in biodiesels along with their greater carbon content are said to have a greater effect on carbon dioxide emissions. Valente et al.[83] in a study indicated a decrease in CO_2 emissions on increasing engine loads in a diesel run engine; however, the effect was contrasting when the diesel fuel was replaced with biodiesel. Hoang,[84] Krishania et al.,[85] Ogunkunle et al.,[86] and many others had similar observations and concluded that the higher amount of fuel bound oxygen increases combustion efficiency thereby ending up in near complete carbon oxidation and an increase in percentage of CO_2 emissions. Since burning carbonaceous fuels will eventually result in some byproduct, a relatively less noxious CO_2 is preferential over CO, which poses greater toxicity.

Moving over to HC in exhaust gases results out of incomplete and inefficient combustion. Fuel or oil stuck up in cracks, crevices, or along cylinder walls will not be combusted uniformly. The higher oxygen content and high exhaust gas temperatures as a consequence of biodiesel combustion aid in ensuring near-complete combustion of the carbonaceous components of fuel, thereby overall decreasing HC emissions. A couple of studies also suggest minimal HC release when the percentage of biodiesel blending is increased.[87,88] The oxygen content in biodiesels inherently decreases formation of HC in the combustion chamber itself and this, coupled with advanced fuel injection timing, shorter and saturated carbon chains of the fuel, along with well-defined combustion timing all together contribute toward HC reduction.[89] On analysis of the exhaust emissions in biodiesel run engines it can be concluded in a nutshell that they are greatly dependent upon the oxygen content, saturation, and carbon chain length along with the viscosity, density, and combustion characteristics of the biodiesel under study.

Finally, the most dangerous component of exhaust gas is NO_x; it consists of ∼90 vol % NO, ∼5 vol % NO_2, and ∼5 vol % of other nitrogen oxides.[90,91] Its formation mechanism is highly complex and is dependent on a number of parameters such as operating points, combustion chamber design and temperature ranges, fuel and air ratios and system designs, oxygen concentration, etc. The difference in injection timings, adiabatic flame temperatures, ignition delays, and heat transfers rates in diesel and biodiesel fuels create all the changes in NO_x production rates of the two fuels.[92] Sayyed et al.,[93] Rajendran,[94] Baweja et al.,[95] and other researchers indicated that the use of biodiesels increases NO_x production and emissions for all loads. With increasing loads and near stoichiometric fuel-air mixtures, an increase in oxygen percentages with corresponding increase in in-cylinder temperatures is observed, which consequently increases NO_x production. Sathiyamoorthi et al.[96] also observed a similar trend, and How et al.[97] additionally suggested that the reduction in radiative heat dissipation when biodiesels are used could also be a contributing factor toward an increase in NO_x production. Mourad et al.[98] concluded that NO_x emissions could be decreased by increasing the amount of exhaust gas recirculation. As this would reduce the amount of excess air and primarily the amount of oxygen in the combustion chamber, there would be no sufficient oxygen in the reaction system for NO_x formation. On the other hand, Mubarak et al.[99] investigated Salvinia molesta oil biodiesel and suggested that due to the presence of a greater number of saturated fatty acids and lower heating value of this biodiesel, lower combustion temperatures are observed, which decrease NO_x formation. Similar was the trend with *Dunaliella tertiolecta* microalgae produced biodiesel which had a higher cetane number than diesel, thus resulting in shorter combustion intervals and a lesser amount of NO_x produced.[100] Hence, the increase or decrease in NO_x emissions with biodiesels is quite ambiguous and is subject to experimental procedures. Hence, until a standardized experimental model is put into play, putting forth a conclusion would be inaccurate.

While the CO, SO_x, HC, and soot content are known to relatively decrease, the percentages of NO_x and CO_2 are known to proportionally increase on combustion of biodiesels, yet a good balance between the two must be achieved to meet current emission norms. In order to control NO_x, major suggestions include lowering of combustion and exhaust gas temperatures and limiting the presence of oxygen. Although the latter is inevitable, reduction of exhaust temperatures is achievable by increasing the number of saturated groups and using fuels with higher cetane numbers. These properties can be achieved by tailoring biodiesel synthesis to produce fuels of this nature, and this could be achieved by carrying out transesterification of triglycerides into fatty acid methyl esters (FAME) using heterogeneous catalysts that drive the reaction forward in the direction to produce the desired products.[101,102] Although FAME comprises highly compounded mixtures, one can aim to produce the desired products in greater proportions to facilitate the desired combustion framework. Similarly, in the case of CO, which is easily oxidized to CO_2, due to the apparent increase in inherent oxygen bound to the fuel, a decrease in HC emissions is also observed due to the same reason. As observed, there are contradictory findings in the literature with respect to temperatures, physical properties, and heating values associated with combustion of biodiesels and their blends. These findings vary relative to the inherent properties of the biodiesel fuel along with the experimental parameters such as engine loads and functioning. It is therefore essential to further look into the consequences of this fuel blending with hybrid engines with a modernist approach in order to achieve the ultimate goal of near zero emissions.[103]

While diesel engines struggle to find a balance between NO_x and soot trade-offs, LTC modes such as HCCI have now emerged to overcome these fallouts. However, in the bargain, controlling combustion phasing is a concern which simultaneously increases HC and CO emissions. In order to achieve a good balance in LTC modes, Riyadi et al.[104] and many others have proposed the use of biodiesels. With alterations in inlet air temperatures, exhaust gas ratios, and recirculation along with injection pressures, LTC engines fuelled with biodiesels could not only improve engine performance and increase combustion efficiency but also be less of a burden on the environment. The silent majority of researchers have come to

https://doi.org/10.1021/acs.energyfuels.4c00705
Energy Fuels XXXX, XXX, XXX−XXX

terms with a fact that due to the higher oxygen content in biodiesels a well-accepted reduction is observed in emissions of CO, CO_2, HC, soot, and smoke. Internal oxygen in these fuels will inevitably lead to oxygen-rich combustion, which optimizes the air/fuel ratios, leading to less pollutant formation. However, the near complete combustion due to presence of a sufficiently high amount of fuel bound oxygen raises the in-cylinder temperature above the threshold adiabatic temperatures, which provides sufficient activation energy for reactions leading to NO_x formation.[105,106] This is where conventional systems are subjugated by LTC modes, as the exhaust temperatures in LTC run systems assist in reducing NO_x and soot formation. The next step in pollutant mitigation involves alterations in the engine working and modifications which can be altered to achieve greater control in pollutant emissions. These are discussed in the next section.

3. CLEAN COMBUSTION VIA ENGINE MODIFICATIONS

3.1. Brief Introduction to Conventional and LTC Modes. Higher thermal efficiency and better fuel economy of conventional diesel engines have made them the most preferred prime movers in transportation.[107] However, conventional diesel combustion (CDC) poses a severe problem regarding higher emissions of NO_x and soot owing to the higher combustion temperatures and heterogeneity in the fuel-air mixture.[108] In conventional diesel combustion, diesel fuel is injected into the combustion chamber just before the end of the compression stroke. The fuel-air mixture formed during the delay period autoignites rapidly, resulting in a premixed combustion phase followed by a predominant mixing-controlled combustion phase. The HRRs are higher in the premixed combustion phase due to the rapid combustion of the charge, leading to increased local temperatures that favor NO_x formation in near-stoichiometric regions.[104] Owing to the diffusion combustion of heterogeneous charge, soot formation occurs in regions with a local equivalence ratio (ϕ) between 2 and 4 and local combustion temperatures between 1800 and 2200 K.[109] Most in-cylinder strategies that attenuate NO_x formation favor soot formation.[110] Thus, despite being the most fuel-efficient engine, conventional diesel combustion poses challenges to simultaneously attaining ultralow NO_x and soot emissions.

Several low-temperature combustion strategies have been investigated extensively in the past decade to eliminate the NO_x-soot trade-off and achieve ultralow values of NO_x and soot[111] by decoupling the fuel-injection event from the start of combustion.[28] This approach ensures sufficient fuel-air premixing time by maintaining a positive ignition dwell (time elapsed between the end of fuel injection and the start of combustion), forming a lean, homogeneous fuel-air mixture.[112] The lean and homogeneous nature of the charge eliminates the scope for fuel-rich regions that favor soot formation. It simultaneously reduces NO_x emissions by lowering the combustion temperatures to below 1800 K.[113] The most commonly investigated LTC strategies include HCCI, PCCI, and RCCI.[114] The physical implementation of these strategies is fundamentally different in the fuel injection schedule. The combustion characteristics of these strategies, including combustion phasing, rate of pressure rise, and cylinder peak pressure, are also considerably different.[115] Thus, each LTC strategy is unique in terms of the load range achievable and emission formation.

3.2. Challenges in LTC Modes. The HCCI strategy generally involves port fuel injection during the intake stroke and, thus, has a very high positive ignition dwell with a higher degree of fuel-air premixing. The HCCI strategy is typically a hybrid between conventional spark ignition (SI) and compression ignition (CI) engines. A premixed fuel-air mixture is inducted into the cylinder in the HCCI combustion mode, which is compressed until autoignition. The resultant rapid and premixed combustion lasts for shorter combustion durations, lowering heat transfer losses and yielding thermal efficiency superior to or similar to conventional combustion.[116] Autoignition of lean and homogeneous fuel-air mixtures helps reduce NO_x and soot emissions by more than 90%.[117] However, achieving optimal combustion phasing and control in the HCCI is challenging because it is primarily governed by fuel molecular composition and associated chemical kinetics. The instant of autoignition is directly controlled by fuel injection timing in conventional CI engines and spark timing in SI engines. Fuel injection rate controls the heat release rate in conventional CI engines, whereas flame propagation controls it in SI engines. In the HCCI strategy, there is no direct control of the combustion event because the fuel injection schedule is completely separated from the instant of autoignition and the subsequent heat release rate.[118] Consequently, the resultant premixed combustion leads to a rapid peak pressure rise rate (PPRR), narrowing the load range achievable with the HCCI strategy.[119]

In the PCCI strategy, the fuel injection schedule and the start of combustion are not entirely separated as in HCCI. The fuel injection is timed during the compression stroke inside the cylinder,[120] so the duration of positive ignition dwell is relatively lower than in HCCI. Thus, the degree of fuel-air premixing is not as high as in HCCI. Fuel is injected early during the compression stroke to form a homogeneous fuel-air mixture, whose ignition is controlled by the injection timing and the chemical kinetics.[121] However, too advanced fuel injection leads to spray wall impingement and thus unacceptably high HC emissions.[122] The PCCI strategy has recently been implemented by prolonging the ignition delay period using excessive charge dilution and reduced compression ratio to prepare the homogeneous fuel-air mixture with the fuel injection event near the top dead center (TDC).[123] The literature confirms the application of all these PCCI strategies in achieving ultralow emissions of NO_x and soot.[124]

High reactivity fuels like diesel autoignite readily well before achieving proper fuel-air premixing, which is required to reduce the formation of NO_x and soot simultaneously. This situation necessitates utilizing a high EGR rate to delay the start of the combustion event. Thus, the major shortcoming of the PCCI combustion mode is the requirement for EGR, often higher than 50%.[125] Therefore, PCCI combustion is recommended for low-reactivity fuels like gasoline, which provides a sufficient premixing time before the start of combustion with relatively lower EGR rates than diesel PCCI.[111] However, the requirement of high EGR to delay the onset of the combustion in PCCI mode, regardless of fuel reactivity, poses challenges concerning the air-handling systems of the engine. Additionally, high EGR affects combustion stability, thermal efficiency, and fuel consumption.[126] Reducing oxygen concentration due to high EGR increases the unburnt hydrocarbon and carbon monoxide emissions.[127]

Researchers[128] have also explored alternative approaches to achieving the PCCI strategy without requiring heavy EGR.

https://doi.org/10.1021/acs.energyfuels.4c00705
Energy Fuels XXXX, XXX, XXX−XXX

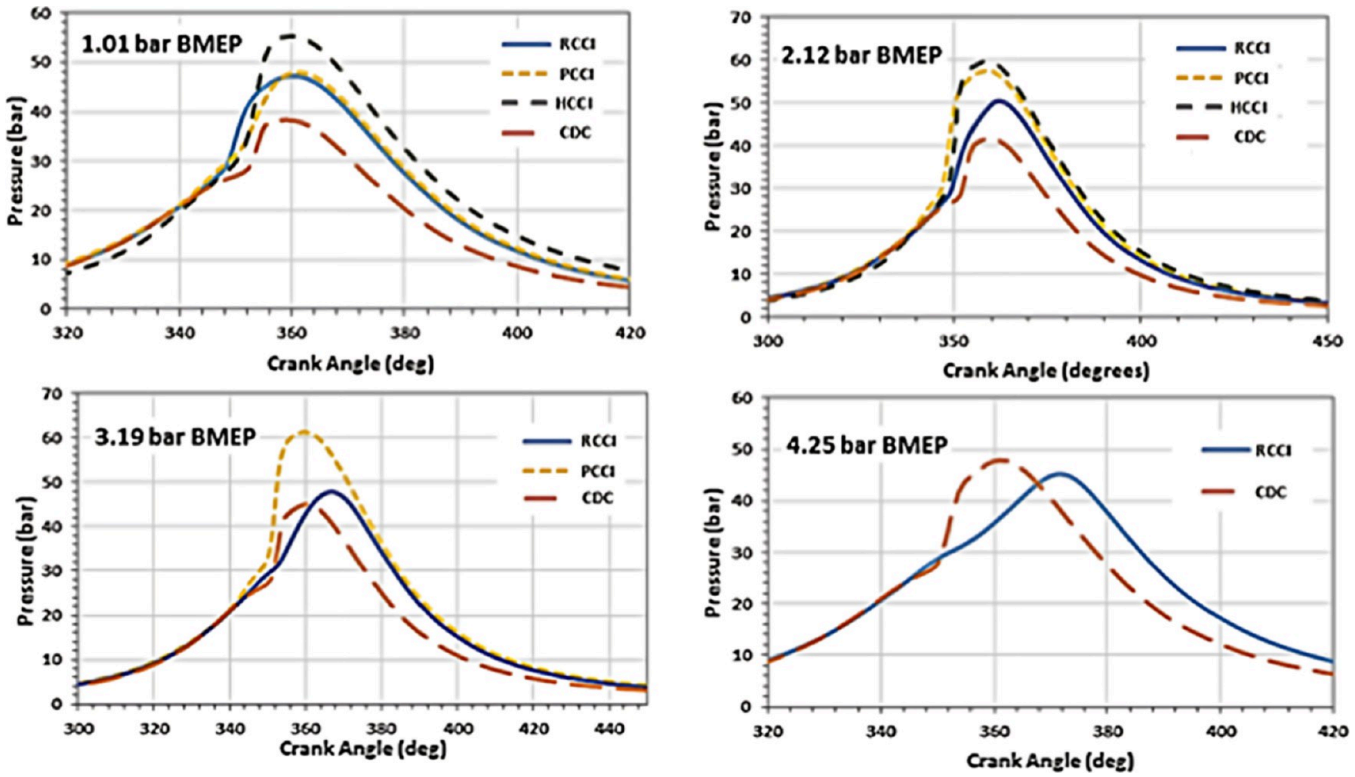

Figure 5. Comparison of cylinder pressure histories for diesel in CDC, HCCI, PCCI, and RCCI modes. Reproduced with permission from ref 117. Copyright (2018) with permission from Elsevier.

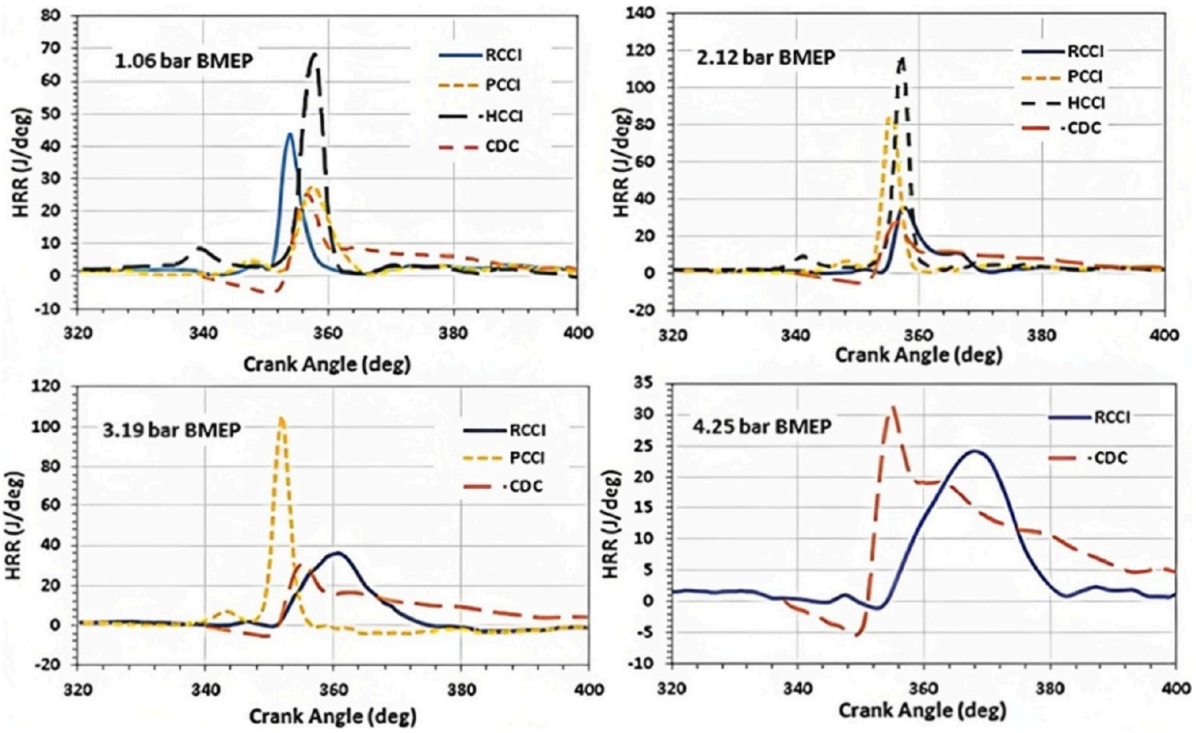

Figure 6. Comparison of heat release rates for diesel in CDC, HCCI, PCCI, and RCCI modes. Reproduced with permission from ref 117. Copyright (2018) with permission from Elsevier.

This approach is a hybrid of HCCI and CDC modes. Most fuel is premixed in this approach by using a port fuel injection system (PFI). The remaining fuel is injected directly into the cylinder during the early stages of the compression stroke. Direct injection timing and premixed fuel ratio, defined as port fuel to direct injection quantity, dictate the combustion event, not requiring high EGR.[129] Nevertheless, due to direct injection, the homogeneity levels achieved with the PCCI strategy are lower than those with the HCCI strategy. Consequently, a better reduction in NO_x and soot emissions

https://doi.org/10.1021/acs.energyfuels.4c00705
Energy Fuels XXXX, XXX, XXX−XXX

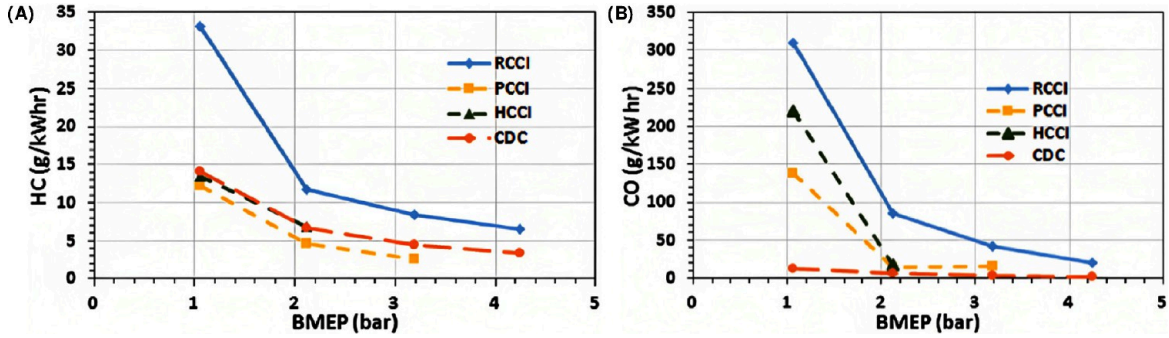

Figure 7. Comparison of (A) HC and (B) CO emissions for diesel in CDC, HCCI, PCCI, and RCCI modes. Reproduced with permission from ref 117. Copyright (2018) with permission from Elsevier.

is observed in HCCI than in PCCI. In addition, this approach results in combustion duration and PPRR similar to those of fully premixed HCCI, even with low-reactivity fuels like gasoline. This phenomenon is attributed to very little sensitivity of ignition delay of gasoline-like fuels to the charge equivalence ratio, especially when lower than 0.5.[130] Thus, a narrow achievable load range remains the primary limitation, even with a PCCI strategy. Solutions like multiple injections to reduce the PPRR, increased boost pressure,[131] high fuel injection pressures,[132] charge dilution using water vapor induction,[133] and fuel modifications using alternative fuels such as alcohols[126] are explored to extend the engine operating load range in PCCI mode.

RCCI is a dual fuel LTC strategy in which fuel with a lower reactivity is premixed by port fuel injection, and a higher reactivity fuel is directly injected into the cylinder during the compression stroke.[134] The reactivity stratification attained using fuels of opposite reactivity helps achieve lower PPRR and broader combustion duration, thus, higher engine loads.[135] Figures 5 and 6 show the cylinder pressure histories and heat release rate characteristics for diesel in CDC, HCCI, PCCI, and RCCI modes, wherein RCCI exhibits a slower pressure rise rate and broader combustion.[117] Similar to fully premixed HCCI, RCCI combustion is also controlled by chemical kinetics. The high-reactivity fuel is injected directly early in the compression stroke so that the equivalence ratio at the onset of combustion remains extremely low (<0.5). As a result, autoignition occurs initially at regions of higher reactivity, progressing toward the low reactivity, and a reactivity gradient is set up in the engine cylinder. Literature extensively demonstrates the applicability of the RCCI strategy in achieving moderate to higher engine loads with numerous low-reactivity fuels like gasoline, methanol, ethanol, butanol, and high-reactivity fuels like diesel, dimethyl ether, and biodiesel.[136] The low reactivity and high volatility of PFI fuels promote better fuel-air mixing and thus better premixing without early autoignition. Autoignition of the charge and combustion phasing may be controlled to some extent by using one or more pilot injections of DI fuels.[117]

The achievable higher load limit varies with the reactivity and heat of vaporization of the PFI fuel, which dictates the resistance the PFI fuel offers for the autoignition of the charge. It also depends on the injection scheduling and reactivity of the DI fuel. This is the primary advantage of the RCCI strategy, which facilitates modification of charge reactivity by varying the premixed ratio and DI timing as desired to reduce the PPRR at higher engine loads.[137] Optimized injection scheduling allows smooth operation over the entire engine load in RCCI.[138] Research suggests a change in the strategy with the increased engine load, starting from entirely premixed combustion at low load, followed by premixed and mixed combustion from medium to high load, and diffusion combustion at full load.[139] Dual-fuel RCCI combustion appears to be a promising solution for attaining clean combustion; however, the necessity to handle two fuels with separate fuel storage and injection systems impedes its practical implementation.[140] Some RCCI investigations have employed a single fuel (gasoline) and a cetane improver (ethylhexyl nitrate).[141] Gasoline that is injected directly is doped with a small tank of the additive. Gasoline that is injected through the port is not doped with the additive. This study revealed some encouraging findings, with emissions and efficiency levels comparable to gasoline-diesel RCCI.[141]

Besides the narrow operating load range, common limitations of LTC strategies include higher cycle-to-cycle combustion variation[142] and combustion noise than conventional diesel combustion.[143] Regardless of the LTC strategy, the HC and CO emissions are significantly higher than those of conventional diesel combustion as the in-cylinder combustion temperatures targeted to attenuate NO_x and soot affect the HC and CO oxidation (refer to Figure 7).[111] The high HC and CO emissions observed with the LTC strategies can be reduced using after-treatment control strategies, including a three-way catalytic converter and diesel oxidation catalyst.[111] Thus, LTC provides an affordable approach to achieving ultralow emissions and high-efficiency combustion.

3.3. Homogeneous Charge Compression Ignition.

LTC strategies such as HCCI benefit from the increasing popularity of cutting-edge technologies used in the production of diesel engines, such as variable valve timing, in terms of practicality. The HCCI concept can be categorized in many ways based on the method of premixed charge preparation. The fuel can be injected into the intake manifold using a suitable fuel injector to form a homogeneous mixture during suction and compression strokes. In this port fuel-injected homogeneous charge compression ignition (PFI-HCCI) strategy, fuel evaporation is an associated problem with low volatile fuels, along with common shortcomings such as narrow load range and higher HC and CO emissions.[144] The fuel can be injected directly into the cylinder during the early stages of compression strokes, providing sufficient time for premixing the fuel and air. This early in-cylinder fuel injection helps to attain the HCCI type of combustion. However, it results in issues such as fuel spray wall wetting.[145] The other category of HCCI combustion is the late in-cylinder injection of fuel, in

https://doi.org/10.1021/acs.energyfuels.4c00705
Energy Fuels XXXX, XXX, XXX−XXX

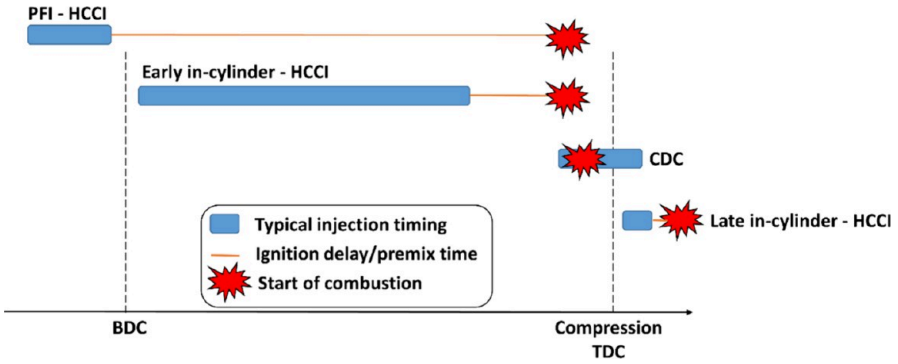

Figure 8. Classification of the HCCI strategy.

which fuel is injected after the top dead center to extend the delay period due to the downward motion of the piston and associated volumetric expansion that decreases the pressure and temperature inside the combustion chamber. Nevertheless, the mixture prepared in PFI-HCCI would have the highest degree of homogeneity compared with the other two methods. The typical injection strategy followed to achieve the above-said types of HCCI combustion is shown in Figure 8.

3.4. Homogeneous Charge Compression Ignition – Challenges. *3.4.1. No Direct Control over the Combustion Phasing.* Since the fuel injection schedule is separated from the instant of autoignition and the subsequent heat release rate, there is no direct control over the start and progress of the combustion event in the HCCI strategy.[104] PFI-HCCI presents a worst-case scenario regarding combustion control, wherein the fuel is injected outside the engine cylinder during the intake stroke. Diesel and biodiesel are high-reactivity fuels and ignite well-advanced during the compression stroke. Advanced autoignition of the charge in the compression stroke increases the negative work, affecting the overall efficiency.[115] Too advanced autoignition of the charge followed by a high heat release rate before the piston reaches TDC contributes to the high rate of pressure rise, leading to engine knock and limiting the higher load achievable.[119] The high peak pressure rise rate can lead to unacceptably high cylinder wall temperatures, head gasket failure, and mechanical damage to the engine. Due to the dependency on in-cylinder temperatures, HC and CO emissions are also affected by the instant the autoignition that occurs.[146] Therefore, it is essential to delay the start of combustion and control the heat release rate as required for a wider operating load range, higher power output, and overall efficiency.

3.4.2. Narrow Load Range of Operation. The limited operating range of HCCI engines is a significant impediment to their widespread commercialization. The low temperature and lean mixtures do not favor the combustion at low loads; thus, the charge misfires. The high peak pressure rise rate at high loads leads to knocking combustion. Therefore, HCCI operation is limited to a narrow intermediate load range below which the engine misfires and beyond which it knocks.[17] Gowrishankar et al.[147] and Bukkarapu and Krishnasamy[148] could achieve only 20% of the full load with neat biodiesel in HCCI operation, attributing it to the high reactivity of the biodiesel. Extending the operating range is critical for reaping the full benefits of HCCI engines.

3.4.3. High HC and CO Emissions. Lack of oxygen availability and low gas temperatures hinder CO oxidation in the CDC, paving the way for incomplete combustion of the fuel. In conventional CI engines, several factors contribute to HC emissions due to the heterogeneous nature of combustion. These include under- and overmixing fuel and air, spray wall wetting, and poor fuel atomization. The factors contributing to HC emissions in conventional SI engines include flame quenching in cold regions and crevices, incomplete fuel vaporization inside the cylinder, fuel leakage through exhaust valves, and misfired combustion.[149] Since the HCCI strategy combines the features of conventional SI and CI engines, HC formation can occur through any of these sources. Lean operation and lower combustion temperatures result in higher HC and CO emissions in HCCI engines than those in conventional CI and SI engines. Other sources of HC emissions in HCCI engines are crevices and liquid fuel due to improper vaporization and poor premixing. In the case of early DI-type HCCI engines, spray wall-wetting also contributes to high HC emissions.[17]

3.4.4. Homogeneous Mixture Preparation. In HCCI engines, lean and homogeneous fuel-air mixture must be prepared to bypass NO_x and soot favorable conditions. However, preparing the desired homogeneous fuel-air mixture is challenging as the thermodynamic cycle time in an internal combustion engine is too short. The effects of poor mixture preparation are oil dilution and wall wetting, thereby increasing HC emissions and fuel consumption.[150] Allowing more time for mixture preparation results in greater homogeneity of the fuel-air mixture. On that note, PFI-HCCI is better than other types of HCCI mixture preparation strategies.[151] However, mixture preparation remains a difficult task in the case of low-volatility fuels like diesel and biodiesel.[146]

3.4.5. Cold-Start Operation. In geographically cold regions, the fuel-air mixture in an HCCI engine cools due to the cold combustion chamber walls and intake conditions. Low-charge temperatures do not favor the initiation of autoignition, resulting in an engine misfire. Thus, it is challenging to achieve cold-start operation in HCCI engines.[104]

3.5. Engine Design Modifications and Thermal Management Strategies to Overcome Limitations of HCCI. The successful operation of the HCCI engines requires delaying the autoignition and controlling the subsequent heat release event. It emphasizes maintaining the peak pressure rise rate below acceptable levels for extended load ranges in HCCI engines. Delaying the start of combustion also helps to provide more time for the preparation of a fuel-air mixture with a higher degree of homogeneity. Though there is no direct control over the start of combustion, combustion phasing can be controlled by using suitable strategies to achieve HCCI combustion. These control strategies are based on engine

https://doi.org/10.1021/acs.energyfuels.4c00705
Energy Fuels XXXX, XXX, XXX−XXX

design modifications and the adoption of suitable thermal management strategies, which will be discussed next.

3.5.1. Strategies to Control the Combustion Phasing. 3.5.1.1. Engine Design Modifications - Compression Ratio Modifications. Autoignition of the charge depends on fuel reactivity and the in-cylinder conditions. The evolution of the in-cylinder temperature and pressure relies on the engine geometry, viz., the compression ratio. Lowering the compression ratio of a diesel engine reduces the in-cylinder temperatures, delaying the preflame oxidation and low-temperature pathways and, thereby, delaying the start of combustion. Also, the peak pressure rise rate can be reduced by lowering the compression ratio, which helps extend the load range. Reportedly, the HCCI operation cannot be achieved beyond 20% of the load range for a diesel engine of 4.4 kW rated power at a compression ratio of 17.5:1 with 47-cetane diesel fuel. Lowering the compression ratio to 15:1 could extend the load range to 40%.[117] Ryan et al.[152] investigated the effects of reducing the compression ratio on the HCCI operation with 47-cetane diesel fuel. Reducing the compression ratio from 12:1 to 8:1 delayed the start of combustion remarkably, as illustrated in Figure 9. The authors[152] concluded that the range of the compression ratio to achieve HCCI combustion in the case of a single cylinder four stroke water cooled diesel engine is 8:1 to 14:1. Several studies conducted using biodiesel-diesel blends and neat biodiesel also confirm the necessity of compression ratio modification to achieve stable HCCI combustion.[153] Using methyl decanoate as a representative of biodiesel to understand its combustion in HCCI mode, Xu et al.[154] reported an optimal compression ratio between 7:1 and 13:1. Bunting et al.[155] reduced the compression ratio from 20 to 10.5 to ensure the desired combustion phasing in their attempts to optimize the biodiesel-diesel blends chemistry for HCCI combustion. Similarly, Bukkarapu and Krishnasamy[148] reduced the compression ratio from 17.5:1 to 15:1 to achieve higher engine loads with neat biodiesel in an HCCI engine.

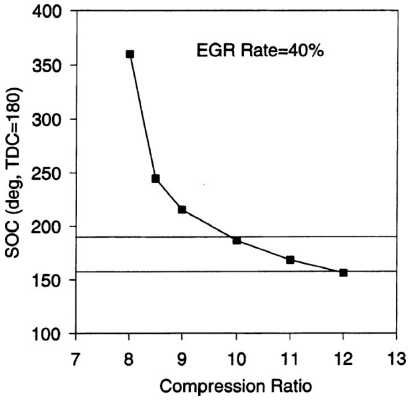

Figure 9. Effect of compression ratio on the start of combustion. Reproduced with permission from ref 152. Copyright (1996) with permission from SAE International.

In the case of conventional SI engines that needed to be converted to HCCI engines, increasing the compression ratio is suggested to achieve HCCI combustion with low-reactivity fuels. Variable compression ratio (VCR) and variable valve timing (VVT) techniques can modify the geometric and effective compression ratio, as required, based on the fuel reactivity. Different blends of low-reactivity (gasoline) and high-reactivity (diesel) fuels were tested by Christensen et al.,[156] varying the compression ratio from 9.6:1 to 22.5:1 using a variable compression ratio engine. The authors[156] confirmed the multifuel potential of an HCCI engine with the VCR technique. Similar studies with natural gas[157] and gasoline of varying octane numbers[158] confirmed the applicability of VCR-HCCI engines to extend the operating range. Thus, compression ratio modifications provide fuel flexibility with extended load range operation of HCCI engines.[159]

3.5.2. Thermal Management Strategies – Intake Charge Temperature. Intake charge temperature in the case of external mixture preparation-based HCCI (PFI-HCCI) and intake air temperature in early and late DI-type HCCI engines provide additional control over the onset of combustion. A higher intake temperature advances the start of combustion during the compression stroke, causing significant negative work penalties and affecting the engine's thermal efficiency.[160] Due to advanced combustion, the heat release rate accelerates, resulting in a high peak pressure rise rate, limiting the load range. Thus, lowering the intake temperature is inevitable to delay the start of combustion.[161] However, it cannot be reduced to an extent where the engine misfires. Gray et al.[116] varied the intake charge temperature between 130 and 205 °C and achieved controlled HCCI combustion. The authors[116] suggest lower intake charge temperatures of 130 °C to atomize diesel fuel and finely prepare the required homogeneous mixture. Reducing the intake charge temperatures below 130

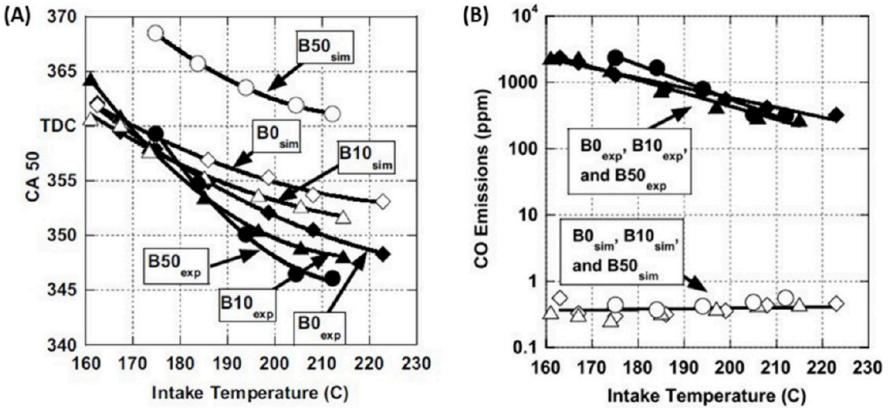

Figure 10. (A) Effect of intake temperature on combustion phasing and (B) CO emissions. Reproduced with permission from ref 163. Copyright (2007) with permission from SAE International.

https://doi.org/10.1021/acs.energyfuels.4c00705
Energy Fuels XXXX, XXX, XXX−XXX

°C results in wall-wetting, increasing HC emissions, and fuel consumption.[116]

Bunting et al.[162] successfully achieved controlled HCCI combustion with neat diesel and biodiesel-diesel blends in a diesel engine modified to operate in HCCI mode. Figure 10(A)[163] shows the effect of intake temperature on combustion phasing, crank angle at 50% cumulative heat release (CA50) of neat diesel ($B0_{exp}$ and $B0_{sim}$), and biodiesel-diesel blends ($B10_{exp}$, $B50_{exp}$, $B10_{sim}$, and $B50_{sim}$). The suffix "exp" and "sim" correspond to experimental and simulated results, respectively. The authors conclude that there is a delay in combustion phasing with reduced intake temperatures. Singh et al.[164] confirm lower in-cylinder pressures, delayed start of combustion, lower heat release rate, lower cumulative heat release, and retarded combustion phasing with reduced intake charge temperatures in the case of biodiesel-diesel HCCI. Other studies[165] also confirm the same and suggest lower intake temperatures to avoid excessive knocking in the case of HCCI combustion with biodiesel-diesel blends. Though lower intake temperatures retard the combustion phasing, HC and CO emissions increase due to relatively lower combustion temperatures. The increase in CO emissions with decreasing intake temperatures for neat diesel and biodiesel-diesel blends is shown in Figure 10(B).[163] The trade-off between combustion phasing and HC and CO emissions is confirmed by Szybist et al.[163] and Reader et al.[166]

3.5.3. Thermal Management Strategies – Charge Dilution. Charge dilution is a promising technique to delay the onset of autoignition and reduce the heat release rate in an HCCI engine. Diluting the intake charge with appropriate diluents alters its reactivity and oxygen intake concentration, facilitating load extension. Primarily, charge dilution has three effects: thermal, dilution, and chemical effects. The heat capacity of the charge increases with the inducted diluent, reducing the temperatures during compression and combustion, which is the thermal effect of charge dilution. The diluent replaces the oxygen concentration in the charge. As a result, the combustion/burn rate slows, which is considered the dilution effect. The variation in the oxygen concentration with the increasing EGR rate is shown in Figure 11. The dissociation of the inducted charge diluent affects the combustion process, which is the chemical effect.[152] Recirculated exhaust gas is the most explored charge diluent in HCCI research, while water vapor induction also has the scope to be used as a charge diluent.

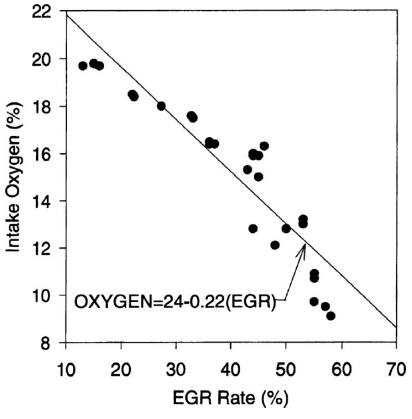

Figure 11. Variation in the intake oxygen concentration with the EGR rate. Reproduced with permission from ref 152. Copyright (1996) with permission from SAE International.

Exhaust gas recirculation is categorized into external and internal EGR. In external EGR, high levels of the exhaust are added into the intake system, whereas the exhaust is trapped inside the combustion chamber in internal EGR. The in-cylinder temperatures are higher in the case of internal EGR than externally circulated cold EGR. Thus, external cold EGR is preferred the most to control HCCI engines.[167] The EGR temperature can be reduced by using a shell and tube heat exchanger incorporated in the exhaust gas recirculation loop. Hot EGR advances autoignition, while cold EGR retards it. Increasing the EGR rate reduces the peak pressure, peak pressure rise rate, HRR, cumulative heat release, and combustion duration.[168] As discussed, this phenomenon can be attributed to the dilution and thermal effects of EGR, which help delay the start of combustion (SOC), and hence, EGR can be used to control the combustion in HCCI.[169] The potential of EGR to extend the load range in HCCI engines has been extensively studied and confirmed by many studies using fuels such as gasoline,[170] natural gas,[171] diesel,[172] biodiesel-diesel blends,[164] and neat biodiesel.[148] However, high levels of EGR affect the volumetric efficiency and increase soot emissions.[173] Ganesh et al.[174] confirm higher HC emissions with higher levels of EGR in HCCI mode due to reduced combustion temperatures. Concisely, charge dilution using EGR is an excellent strategy to achieve controlled HCCI combustion.

Ladommatos et al.[175] studied the effects of water vapor on the autoignition of diesel in CDC. Diluting intake air with water vapor increases the ignition delay.[175] Though Ladommatos et al.[175] confine the study to the effect of water vapor on ignition delay in CDC, the efficacy of thermal, dilution, and chemical effects of water vapor are established. Most recently, Gowrishankar et al.[147] could extend the achievable load from 20% of the full load to 30% using biodiesel-water emulsion instead of biodiesel. Yuan et al.[176] demonstrate the potential of water vapor in delaying the autoignition and reducing the combustion temperatures to alleviate knocking combustion in hydrogen-fuelled HCCI engines. A recent study compared the benefits of charge dilution using EGR and water vapor and concluded that water vapor is better than EGR.[148] The maximum load achieved with neat biodiesel in an HCCI engine was limited to 20%, whereas using EGR increased it to 40%. However, charge dilution using water vapor helped to achieve 46% of the rated load. Besides achieving higher maximum loads, charge dilution using water vapor exhibited better thermal efficiency, fuel economy, and lower HC emission than its counterpart, EGR.[148] Thus, although less explored, water vapor can also be a potential charge diluent to control HCCI engines.

3.5.4. Strategies for Homogeneous Mixture Preparation. In the case of early and late DI-type HCCI engines, several strategies proved successful in improving the homogeneity of the fuel-air mixture. These include employing high injection pressure and a microhole nozzle, which improves fuel atomization, avoiding spray wall-wetting inside the combustion chamber. Utilizing a high swirl ratio for air can also enhance the mixing rate in the combustion chamber. Fuel-air mixing in early DI-type HCCI engines can be improved using multistage fuel injection during the early compression stroke.[177] Mixture preparation is challenging for PFI-HCCI engines with low-volatility fuels like diesel and biodiesel. Poor fuel volatility

https://doi.org/10.1021/acs.energyfuels.4c00705
Energy Fuels XXXX, XXX, XXX−XXX

Table 3. Biodiesel-Diesel HCCI Research and Key Outcomes

Reference	Fuel	Key features	The outcome of the study
Singh et al.[300]	Diesel, B20, and B40	A dedicated vaporizer was employed.	Premix formation was easier in the case of diesel than biodiesel blends.
Bunting et al.[155]	Diesel and a variety of biodiesel-diesel blends	The influence of various blend properties on HCCI combustion was analyzed.	Among cetane number, boiling point (T50), oxygen content, lower heating value, and carbon number, the first two significantly influence HCCI combustion.
Szybist et al.[163]	Diesel, B10, and B50 of soybean biodiesel	The effect of intake temperature was studied.	The combustion phasing is delayed by reducing the intake temperatures.
Gowthaman et al.[301]	Biodiesel-diesel blend	The effect of charge temperature on HCCI engine emission characteristics was studied.	HC and CO emissions increase with decreasing charge temperatures.
Xu et al.[154]	Methyl decanoate as simulation fuel	The effect of compression ratio on formaldehyde emissions of an HCCI engine was studied.	To reduce formaldehyde emissions, best: CR: 7−13, Lambda: 1.9−2.3, Higher EGR
Singh et al.[164]	B20	The effect of charge temperature and EGR was investigated.	EGR is more effective at higher loads and higher T_{charge}.
Gowrishankar et al.[147]	B100	Biodiesel-water emulsion for load range extension	The maximum load range achieved with neat biodiesel is 20% of the rated load, whereas it could be extended to 30% using biodiesel-water emulsion.
Bukkarapu and Krishnasamy[148]	B100	The effect of charge dilution was investigated.	Water vapor is a better charge diluent than EGR.

demand using a fuel heater/vaporizer and air heaters is inevitable, reducing overall efficiency and leading to energy penalties. For better and quick vaporization of diesel and biodiesel, the fuel vaporizer temperature needs to be set to their boiling range, 190 and 380 °C, respectively.[117] As a result, the charge temperature increases significantly, resulting in an undesirable advanced autoignition. Despite high vaporizer temperatures, the high injection pressures lead to spray wall-wetting inside the vaporizer, affecting fuel consumption and thermal efficiency.[147] Therefore, mixture preparation remains a difficult task in the case of PFI-HCCI engines, especially with low-volatile fuels.

Little research has been done on improving the functionality of neat biodiesel in HCCI engines owing to the complexity involved in mixture preparation with such poor volatility and high reactivity fuels. The limited research in the literature is confined to biodiesel-diesel blends, whose key outcomes are presented in Table 3. Conclusively, conventional diesel engines cannot achieve ultralow emissions because of their combustion characteristics, resulting in higher emissions of NO_x and soot. Implementing LTC strategies decouples fuel injection timing from combustion initiation, allowing for sufficient time for fuel-air premixing. This results in forming a lean and homogeneous mixture, leading to a substantial reduction in NO_x and soot emissions. Nevertheless, there are still some obstacles to overcome in this field. These include the need to regulate combustion timing, the limited range of operating loads, high HC and CO emissions, and the challenges of preparing a homogeneous mixture, especially when using low-volatility fuels such as diesel and biodiesel. Methods to address these obstacles include changing the engine design parameters, such as the compression ratio, implementing thermal management strategies like controlling the intake charge temperature and charge dilution, and employing techniques to enhance the preparation of a homogeneous mixture. The existing state-of-the-art highlights the complexity of successful HCCI operation with diesel-like fuels and the significance of engine modifications and thermal management in achieving clean combustion in the HCCI mode.

4. CATALYTIC POSTCOMBUSTION POLLUTANT MITIGATION STRATEGIES

4.1. Advancements in Diesel Oxidation Catalyst. Catalytic oxidation has been around for several hundred years, and it was sooner than later that metal catalysts were being used to mitigate harmful components generated within our ecosystem. These catalysts were initially used in industrial processes and eventually were considered for the removal of HC and CO when it became necessary to control these emissions from automobiles. The gaseous fraction of emissions, about 98−99%, consists of nontoxic gases such as nitrogen, oxygen, and water vapor. Still, the remaining fraction accommodates highly toxic gases such as NO_x, CO, CO_2, and soluble organic fractions. The three-way catalytic convertor (TWC) was first launched in the 1980s with more focus on NO_x reduction in which CO and HC acted as NO_x reducing agents. However, this required the air-fuel stoichiometric ratio to be closest to unity and was favored for gasoline fuelled automobiles. In LTC systems, evidently the air-fuel ratio deviates toward leaner mixtures, and hence the use of a TWC is not preferable in LTC modes just as it was not favorable for diesel engine exhaust systems, considering that running these engines at 1:1 stoichiometric conditions is not mechanically and economically viable.[178] Additionally, the lean operation modes in CI diesel run engines is what contributes toward a higher fuel economy and lower CO_2 emissions compared to gasoline run SI engines. The lean burn mode also lowers combustion temperatures reducing NO_x, HC, and CO emissions compared to SI engines.

In order to convert CO and HCs to benign products, the DOC was introduced in the 1970s for industrial applications and eventually found their way into automobile exhaust treatment systems. It simultaneously catalyzes soluble organic fractions (SOFs) and volatile organic fractions (VOCs) thereby reducing the mass fraction of adsorbates on particulate matter, which in the case of vehicular exhausts is referred to as soot. Furthermore, CO and HC oxidation reactions are particularly exothermic and indirectly aid in filter regeneration due to higher temperature of exhaust gas entering the DPF.[179,180] Postpyrolysis, the remnants and products of fuel combustion, enters the DOC as it is typically the first exhaust treatment component in diesel engine run systems. It is structurally composed of a honeycomb-like monolith generally made up of cordierite ceramic and geometrically a parallel channeled flow-through rather rounded rectangle shaped structure. A material such as α-alumina, silica, titania, etc. possessing an exceptional surface area is coated on the monolith surface and is called a wash-coat within which the metal catalyst is then dispersed. These were similar to wall flow DPF systems, which aided to avoid soot plugging problems

https://doi.org/10.1021/acs.energyfuels.4c00705
Energy Fuels XXXX, XXX, XXX−XXX

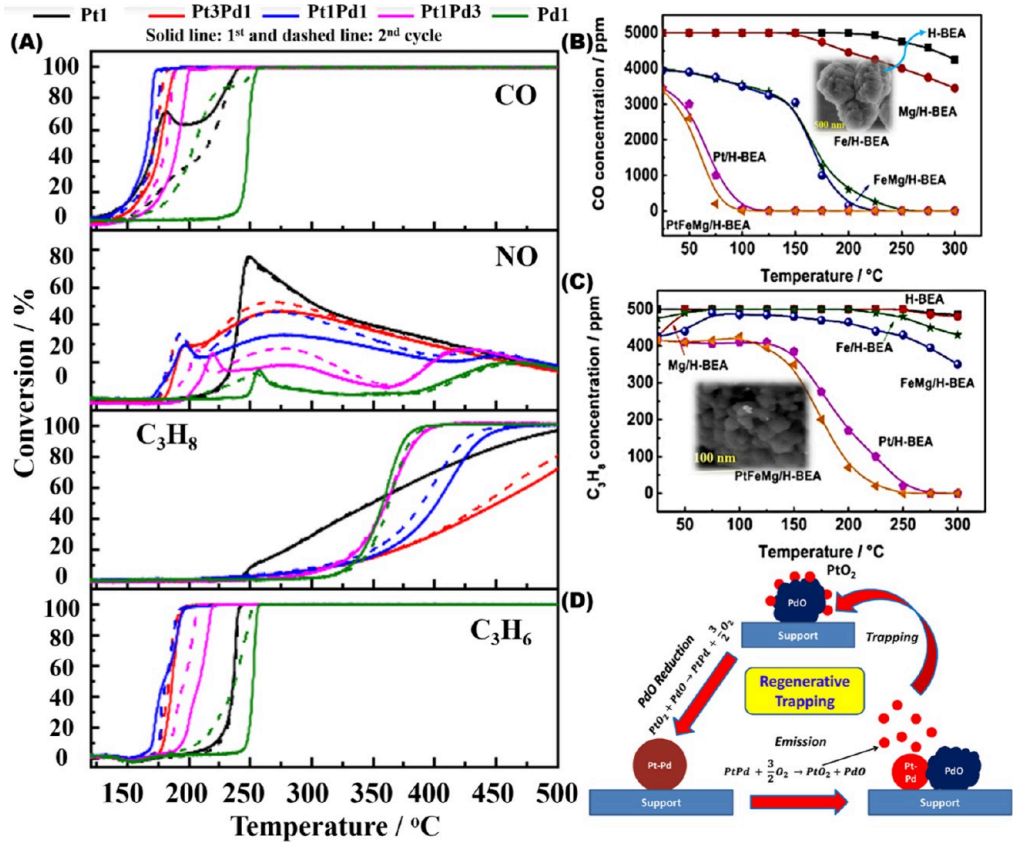

Figure 12. Pt-Pd/BEA bimetallic catalysts for DOC applications. (A) Effect of Pt/Pd variation ratios on the conversion of CO, C_3H_6, NO, and C_3H_8. Catalytical oxidation performance toward (B) CO and (C) C_3H_8 on H-BEA and metal modified H-BEA support samples. (D) Schematic showing the regenerative trapping mechanism of the Pt-Pd interaction. (A) Adapted with permission from ref 188. Copyright (2022) with permission from Elsevier, (B) and (C) ref 190. Copyright (2019) with permission from Elsevier. (D) ref 189. Copyright (2017) with permission from Elsevier.

and facilitated regeneration. These systems as a whole are designed to rapidly catalytically oxidize SOFs and VOFs and simultaneously reduce dry carbon components along with other oxidative functions.[181]

Conventionally and commercially, noble metals have been widely used for catalytic oxidation reactions. Even today, Pt/Al_2O_3 or Pt/Pd/Al_2O_3 DOCs are commercially marketed, which ironically is a reason for a number of automobile thefts due to the rising prices and scarcity of noble metals. Pd-Pt catalysts are susceptible to strong poisoning by sulfur containing components such as SO_2, hydrogen sulfide (H_2S), etc. which find their way in through lubricants, additives, or the fuel itself. However, SO_2 is also a constituent of exhaust gas which readily gets converted into sulfur trioxide (SO_3) in the presence of Pt at higher temperatures. This SO_3 further in the presence of water vapor transforms into sulfuric acid which has higher environmental toxicological effects than its precursor. Additionally, they bind and deactivate the catalyst forming species such as $PdSO_4$.[182] Hamzehlouyan et al.[183] on examining the SO_2 storage and release from Pt/γ-Al_2O_3 concluded that Pt promotes surface sulfate formation and its spill over into the alumina support. SO_2 weakly adsorbs molecularly on coordinately unsaturated Al, i.e., Lewis acid sites, whereas it gets chemisorbed on exposed electron deficient oxygen sites, i.e., Lewis base sites. Traditionally DOCs only used Pt metal, but modern systems have Pt-Pd bimetallic systems. Although Pd is less reactive toward the oxidation of HC and NO_x, it is highly effective toward CO oxidation while simultaneously exhibiting a higher resistance toward sintering and sulfur poisoning.[184] Thus, a selective, cost-effective catalyst needs to be employed so that it not only efficiently carries out oxidative catalysis but also selectively oxidizes only desirable components.

To support the claim, Ho et al.[185] discriminated the activities of Pd/Al_2O_3, Pt/Al_2O_3, Pd-Pt/Al_2O_3, and reasoned that although the Pd based catalyst shows higher CO and HC oxidative activity, the Pt catalyst has a higher efficiency toward NO oxidation. Arguably, a combination of the two, i.e. Pd-Pt/Al_2O_3 showed additionally advanced activity toward oxidation of all the exhaust components due to the formation of a Pt-Pd alloy, which maintained Pd in a reduced phase, and the alloying exhibited higher oxidation resistance than the monometallic species. The bimetallic catalyst exhibited superior activity at temperatures as low as 200 °C with a great stability toward NO oxidation. SO_2 in the reaction environment was observed to adsorb onto the alumina support and enhance the oxidation of C_3H_8 particularly. The higher storage capacity of alumina prolonged the lifetime of the catalyst but simultaneously led to a demanding regenerative process. Moden et al.[186] proposed the use of Zeolite Beta (BEA), ZSM-5, etc. for use as DOCs. Meanwhile, Ho et al.[187] in one such study concluded that beta zeolites with high silica-alumina ratios enhance performance. Further in their subsequent study, they combined Pt and Pd on a highly silicious zeolite and tested it for DOC applications. The bimetallic alloy showed significantly enhanced CO and HC

https://doi.org/10.1021/acs.energyfuels.4c00705
Energy Fuels XXXX, XXX, XXX−XXX

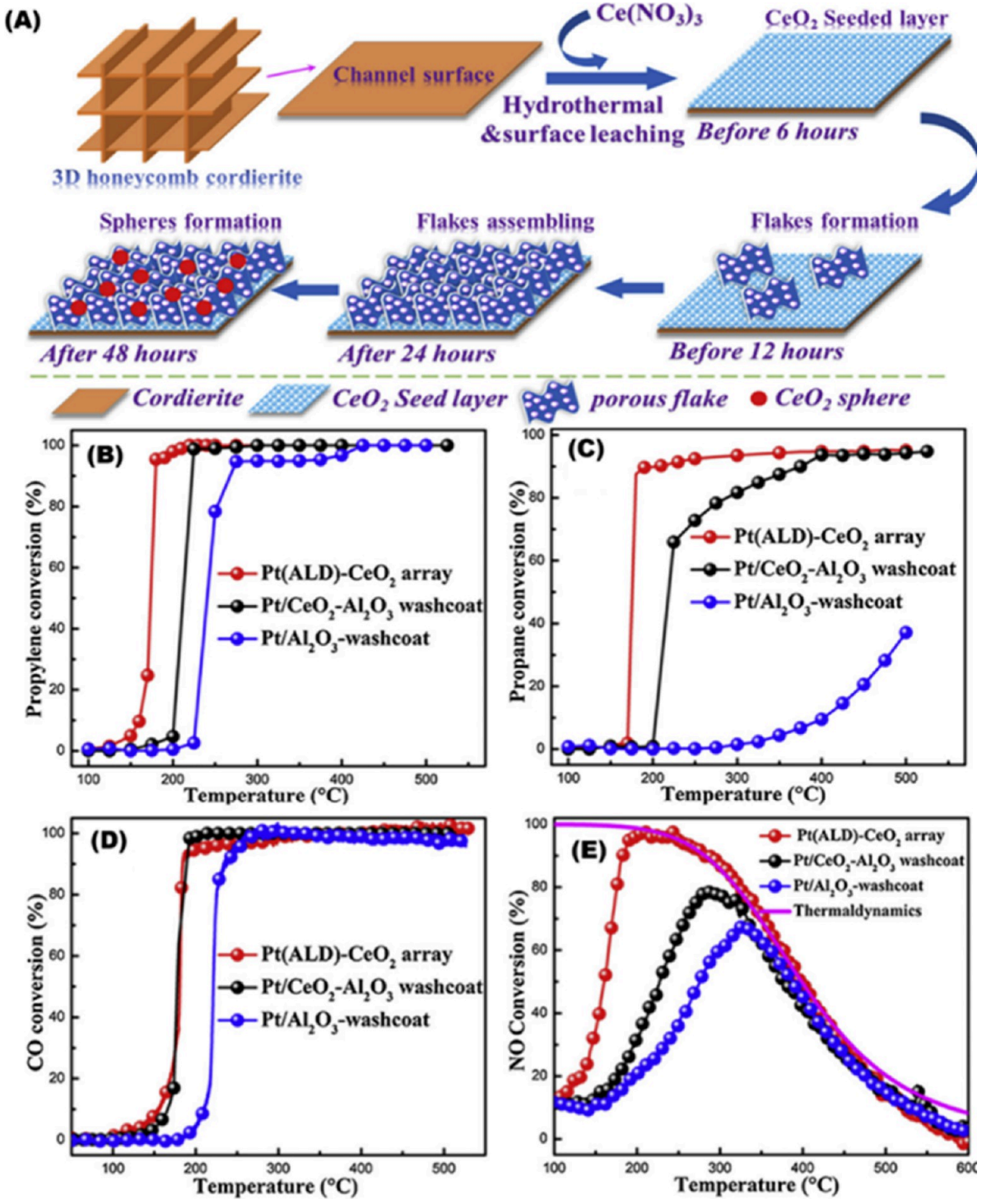

Figure 13. Pt/CeO_2 nanoarray based monolith catalysts for DOC applications (A) Schematic illustration of structural growth of Ce-Si-Al-O nanoflake arrays during the hydrothermal growth process. Temperature dependent catalytic oxidation conversions of (B) propylene, (C) propane, (D) CO, and (E) NO over Pt/CeO_2 nanoarray catalysts. (A), (B), (C), (D), and (E) Adapted with permission from ref 192. Copyright (2019) with permission from Elsevier.

oxidation along with HC assisted reduction of NO to N_2O and N_2 at lower temperatures and the unfavorable oxidation of NO to NO_2 in the presence of O_2 at higher temperatures as seen in Figure 12(A). A schematic of the regenerative trapping mechanism is depicted in Figure 12(D). This additionally delayed the deactivation time by SO_2 poisoning and also retained activity performance during the poisoning period.[188,189]

Noble metals being rare and expensive, development of noble-non-noble metal-based catalysts could be a promising, long-term, and sustainable solution for exhaust after-treatment. Zhou et al.[190] modified hierarchically porous beta zeolites (BEA) containing 0.8 wt % Pt using ion-exchange followed by a deposition-reduction process. This PtFeMg/H-BEA catalyst is highly suitable for LTC conditions showing a T_{90} as low as 95 and 225 °C in CO and C_3H_8 oxidation, along with high

https://doi.org/10.1021/acs.energyfuels.4c00705
Energy Fuels XXXX, XXX, XXX−XXX

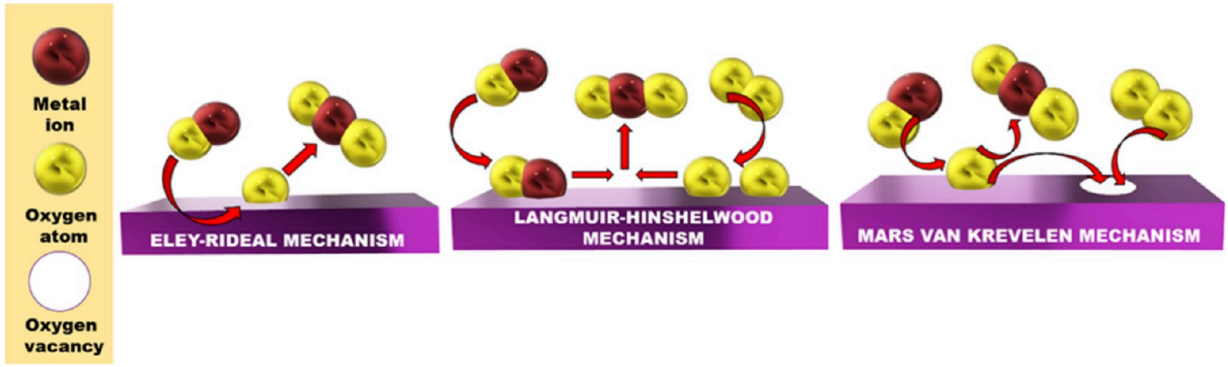

Figure 14. Diagrammatic representation of prominent mechanisms observed in catalytic after-treatment strategies.

water and sulfur resistance. This catalyst is highly cost-effective in comparison to use of noble metals alone and could be conveniently incorporated into commercial DOC cordierite monoliths, and its activity is as illustrated in Figure 12(B) and (C). In a similar study by Li et al.[191] Pt/Fe coloaded mesoporous zeolite beta (Pt/Fe-mBeta) catalysts were synthesized by an ion exchange and ethylene glycol reduction method. The catalyst has potential to practically meet the requirements of a DOC under LTC conditions, as it exhibits complete CO conversion at 90 °C and also exhibits good durability and high-water resistance. Tang et al.[192] decorated Pt nanoparticles on CeO_2-based nanoflakes forming a Pt/CeO_2 nanoarray-based monolithic catalyst. Despite the reduction in the amount of active metal, good catalytic activity was observed with an over 90% conversion rate for propylene, propane, and CO and NO oxidation below 200 °C. NO oxidation is reasoned to be essential for increase in the NO_2/NO_x ratio, which further enhances the NO_2 reduction by the SCR catalyst. The results were verified under diesel run LTC modes developed by US DRIVE, and the CO and HC oxidation temperatures were noted to be as low as 180 °C (Figure 13).

Furthermore, Shukla et al.[193] established a low cost Co_3O_4-CeO_2 mixed metal catalyst and tested it on a four-cylinder diesel engine along with comparison of the results based on the use of diesel and 20% Karanja biodiesel blended diesel. The Co-Ce-based metal catalysts were impregnated on a cylindrical cordierite ceramic substrate. It was observed that prepared DOC showed higher efficiency toward oxidation of biodiesel particulates compared to the diesel produced particulates. Overall, the organic carbon emissions decreased significantly along with the potential to be used in agricultural, on-road, and stationary engines. It is well established that catalysts require a minimum temperature to get activated, and once they attain this equivalent activation energy, they accelerate reaction kinetics toward completion of the desired reaction. Hence, it can be realized that a catalyst not only has to possess great conversion activity but also needs to show significantly great activity at lower temperatures as could be observed in LTC systems.[194]

Gu et al.[195] fabricated a novel Al_2O_3-$LaAlO_3$-ZrO_2-TiO_2 mixed oxide which exhibited exceptional low temperature catalytic activity with 90% CO, 75% NO, and total HC conversion at 196, 200, and 200 °C respectively. Use of mesoporous base catalyst materials such as γ-Al_2O_3 exhibits exceptional properties such as a well-developed pore structure, substantial number of hydroxyl groups, and high specific surface area, which are among the suitably expected properties for a catalyst support. However, these materials collapse at high temperatures due to sintering and get deactivated. $AlLaZrTiO_x$ mixed oxides enhance the thermal stability of γ-Al_2O_3 along with providing good support for DOC applications. A CeO_2-$SmMn_2O_5$ catalyst with high steam resistance and thermal stability was synthesized using a selective dissolution technique by Yang et al.[196] Characterization revealed that surface Sm cations are scarce on the surface, while Mn^{4+} and Ce^{3+} have greater surface abundance and presence of catalytically active oxygen species. The catalyst exhibits good low temperature catalytic oxidation activity with 100% CO and C_3H_6 conversion at 250 °C when compared with a Pt-based catalyst exhibiting a similar conversion at 310 °C.

In LTC modes, the exhaust temperatures fall below ∼150 °C, and although the above-discussed catalytic modes have high efficiency at the considered temperatures, which are comparatively low for normal diesel engine operation modes, these temperature ranges are still quite high for LTC operation modes.[197] CO oxidation reactions conventionally follow the Eley−Rideal (E-R), Mars−van Krevelen (MvK), and/or the Langmuir−Hinshelwood (L-H) mechanism, diagrammatically represented in Figure 14. Wang et al.[198] synthesized a Fe−Co nonoxide/hydroxide in which dual-metal single sites are atomically dispersed on N-doped carbon support. 100% CO conversion could be achieved at temperatures as low as −73 °C via the L-H mechanism with O_2 adsorption occurring at Fe sites and CO adsorption on Co sites. This reaction was reported for the very first time in the absence of supports, such as oxygen vacancies and surface hydroxyl groups. A detailed study by Cai et al.[199] outlines the synthesis of ultrathin, polycrystalline, 2-D Co_3O_4 nanoflowers which exhibited 100% CO conversion at ∼130 °C, while at 150 °C 100% conversion was maintained for more than 40 h at a stretch indicating higher stability of the material. Similarly, a number of other studies using Co_3O_4 showed excellent activity, and it was attributed mainly toward the (1 1 2) surface plane having a greater number of surface and subsurface Co^{3+} active sites with adjacent labile O^{2-} sites. This along with the strain at the grain boundaries due to oxygen vacancies makes this catalyst favorable for the given catalytic system.[200,201]

Ceria, owing to its excellent oxygen storage release properties, has been extensively used for CO oxidation applications. However, due to its ineffective thermal stability at higher temperatures, it is usually used alongside noble or rare metals. A couple of reports such as that by Kerkar and co-workers[202] highlight use of a CeO_2-CuO composite prepared via physical grinding which showed 100% conversion at ∼95 °C. It was also reported that the trend for CO conversion

https://doi.org/10.1021/acs.energyfuels.4c00705
Energy Fuels XXXX, XXX, XXX−XXX

Table 4. Comparison of Activities of Metal Oxides Suitable to Serve as DOCs along with Their Catalytic Characteristics

catalyst; synthesis method	reaction conditions	conversion efficiency (°C)	catalyst characteristics
0.125MgMnCe;[302] coprecipitation method	Tubular down flow gas reactor	CO T_{50} = 120	Concentration of oxygen vacancies, surface oxygen, and Mn^{3+} species increased after Mg doping. MgO is capable of abstracting proton facilitating oxidation of HC.
	300 ppm of CO, 300 ppm of C_3H_6, 100 ppm of $C_{10}H_{22}$, 300 ppm of NO, 5% O_2, 10% CO_2, 5% H_2O and He balance	Propene T_{50} = 218	
	GHSV = 20,000 mL g^{-1} h^{-1}	*n*-decane T_{50} = 255	
Pt-Pd-6Zr/$Ce_{0.3}Zr_{0.7}O_2$;[303] co-impregnation method	Fixed-bed quartz flow reactor	CO T_{50} = 167 (fresh sample)	ZrO_2 addition inhibited noble metal particle growth, increased their dispersion, increased active surface-oxygen species, facilitated Pt and Pd oxides reducibility, and improved surface CeO_2 reduction.
	500 ppm of NO, 180 ppm of C_3H_6, 200 ppm of CO, 10% O_2, 8% CO_2, and N_2 as balance gas, GHSV = 300,000 h^{-1}	CO T_{50} = 172 (aged sample)	
		C_3H_6 T_{50} = 192 (fresh sample)	
		C_3H_6 T_{50} = 193 (aged sample)	
Pd/0.3Ag-CeO_2;[304] coprecipitation method	Fixed-bed tubular quartz reactor	CO T_{90} = 168.7	Ag doping changes the reducibility, number of oxygen vacancies, and active Pd species.
	1% CO, 1000 ppm of C_3H_6, 10% O_2, He balance	C_3H_6 T_{90} = 172.1	
1 wt % Pd/SiO_2@Zr;[305] Stöber process, wet-impregnation method	Fixed bed U-shaped quartz reactor	CO T_{90} = 178	BET surface area (pre-hydrothermal aging: 207.2 m^2/g), (post-hydrothermal aging: 103.9 m^2/g)
	6% CO_2, 12% O_2, 6% H_2O, 400 ppm of H_2, 2000 ppm of CO, 100 ppm of NO, 1667 ppm of C_2H_4, 1000 ppm of C_3H_6, 333 ppm of C_3H_8; HCs in C1 basis and GHSV = 113,000 h^{-1} (LTC-D gas composition as defined by U.S. DRIVE)	C_3H_6 T_{90} = 372	The poor crystallinity of SiO_2@Zr contributes to a high surface area, which in turn contributes to improved hydrothermal stability.
$Ru/Sn_{0.6}Ti_{0.33}O_2$;[306] hydrothermal synthesis	Fixed-bed quartz reactor	CO T_{50} = 180	Sn^{4+} introduced into a TiO_2 lattice forming Sn^{4+}-O-Ti^{4+} species which promotes the formation of the rutile phase, which improves low-temperature activity.
	3000 ppm of CO, 600 ppm of C_3H_8, 600 ppm of NO, 50 ppm of SO_2, 7% O_2, and N_2 balance, GHSV = 60,000 mL g^{-1} h^{-1}	C_3H_6 T_{50} = 320	
Al_2O_3-$LaAlO_3$-ZrO_2-TiO_2 mixed oxide;[195] modified sol–gel method	Continuous flow reactor	CO T_{90} = 196	Wormhole-like mesoporous structure, high specific surface area (206.5 m^2/g), pore volume (0.5 mL/g), and thermal stability.
	CO (2000 ppm), C_3H_6 (1000 ppm), NO (400 ppm), CO_2 (8%), O_2 (10%), H_2O (5%) and N_2 as balance at 10 °C/min	HC (C_3H_6) T_{90} = 200	
$La_{0.9}Sr_{0.1}CoO_3$;[307] hard template method	Fixed-bed quartz tube reactor	CO T_{50} = 223	Greater surface adsorbed oxygen, higher surface area, and smaller particle size.
	0.4% CO-10% O_2 balanced with N_2/0.1% C_3H_6-10% O_2 balanced with N_2	C_3H_6 T_{50} = 338	

https://doi.org/10.1021/acs.energyfuels.4c00705
Energy Fuels XXXX, XXX, XXX−XXX

decreased in the order of CeO_2-CuO > CuO > CeO_2. Furthermore, their following study,[203] involved multidoping Ce with Mn, Cu, and Ag, and it significantly enhanced activity due to great adsorption and oxygen mobility with a conversion temperature of 95 °C.

The primary goal is now not only to enhance stable activity but also to find alternatives to noble metal catalysts. As discussed above and also tabulated in Table 4, researchers have identified a number of catalyst combinations with and without noble metals which could effectively ensure good DOC activity. However, minimal to no commercial trials have been carried out on nonprecious metals as DOCs, and at the same time most of these studies are laboratory based which lack an encounter with stumbling blocks present in a real exhaust gas scenario. Considering biodiesel combustion, the nature of the emissions is quite different from traditional petroleum fuels. The DOCs need to be evaluated under such conditions along with biodiesel compatible engine conditions and hybrid LTC engine modes. Although sulfur poisoning is often highlighted, phosphorus based deactivation is also a major drawback of existing DOCs. Although catalysts subjected to sulfation can be regenerated under reducing conditions, the S residues left behind permanently affect the active sites. Thus, an in-depth study, preferably a theoretical one, is needed to ascertain the reaction mechanism of sulfur poisoning and along with the changes it can probably cause in the nature of active sites and morphology of the catalyst.

For a DOC, the classical interaction between oxygen and the catalyst is of the utmost importance along with the dissociative adsorption and desorption kinetic processes. The cyclic formation of oxides is primarily decisive of the catalytic activity portrayed by a given catalyst, especially under lean, oxygen-rich conditions. It is also evident that along with oxygen vacancies and interaction, the uniform dispersion of active sites is imperative along with the reducibility of active materials, which also plays a vital role since these further facilitate facile oxygen exchange and transfer. A catalyst with greater thermal and hydrothermal stability, along with greater specific surface area and smaller particle size, provides greater conversion activity at lower temperatures. Additionally, catalyst supports such as alumina, silica, etc. are beneficial due to their higher surface area and pore structures; however, they are deactivated and collapse at high temperatures. Mixed-oxides such as Fe, titania, etc. provide thermal stability to these supports should they be used in conventional engines, although, for LTC applications, in lower engine exhaust temperatures, the stability of these alumina-silicates can be anticipated. As discussed earlier, replacing fossil derived petroleum diesel with biodiesel is known to drastically decrease HC and CO emissions. Hence, suitable catalysts such as the ones discussed above, incorporated into the DOC along with a switch to biodiesels, can be instrumental toward decreasing emission levels of HC and CO at lower working temperatures such as that observed in LTC modes.

4.2. NO_x Control and Conversion Tactics. NO_x emissions result in environmental shortcomings including acid rain, photochemical smog, and respiratory defects. Thus, finding cleaner, efficient methods to mitigate this pollutant is a critical issue in modern society. The TWC used in gasoline, SI engines is effective toward NO_x conversion with almost 99% efficiency and has been in use for nearly 5 decades. Here, CO and HC reduce NO_x upon a rhodium catalyst in nearly oxygen deficient environments. EGR is a common engine management strategy used moreover in LTC modes to control NO_x emissions. In this approach, a fraction of the exhaust gas consisting of CO_2, H_2O, O_2, and N_2 is recirculated back into the combustion chamber. Consequently, this results in a lower temperature increase when the energy is released after fuel combustion. This occurs due to the superior heat capacity associated with CO_2, which is ~25% higher than that of O_2 and N_2. The lower exhaust temperatures resist NO_x formation; however, this does not suffice to meet stringent NO_x emission regulations. With this perspective, several De-NO_x propositions have been scrutinized such as SCR using ammonia/urea, HC, etc., direct NO_x decomposition, and NO_x storage-reduction (NSR). Several catalysts such as noble metals, metal and mixed-metal oxides, perovskites, zeolites, etc. have been scrutinized extensively for low-temperature direct decomposition of NO_x. The typical commercially used NO_x conversion catalyst for vehicular exhaust after-treatment is V_2O_5-$WO_3(MoO_3)/TiO_2$; having a narrow effective working window of 350−400 °C, it displays low N_2 selectivity, SO_2 oxidation at higher temperatures, and biological toxicity, thus bringing about undesirability in its use. Due to the shortcomings observed in this existing catalytic method, alternative approaches have been investigated.

Catalytic reduction of NO_x has been investigated employing urea/ammonia, hydrocarbons, etc., and is known as ammonia SCR (NH_3-SCR) (Figure 15(A)) and HC-SCR respectively.

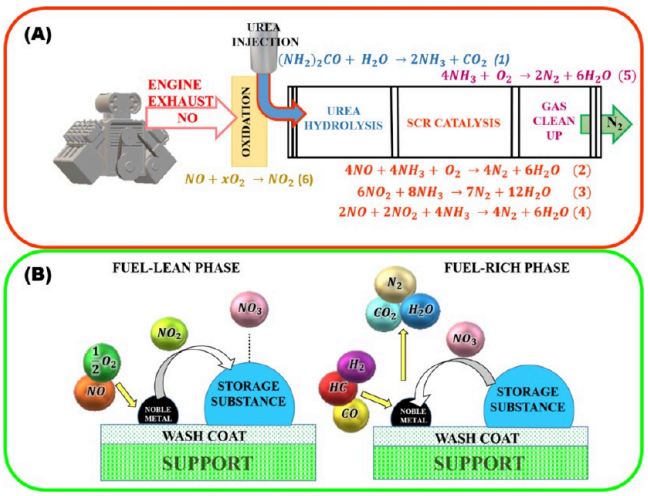

Figure 15. Working principle of (A) NH_3/urea SCR, (B) lean NO_x traps (LNT).

Another technique being used to mitigate NO_x is LNT (Figure 15(B)), also known as NO_x adsorber catalyst (NAC), De-NO_x traps (DNT), etc. These are incorporated into the catalyst wash-coat on a suitable high surface support. NO_x is hoarded onto the LNT during lean fuel conditions and is reduced to N_2 when the fuel-air mixture is rich.

4.2.1. Novel Materials for Selective Catalytic Reduction (SCR) of NO_X. 4.2.1.1. NH_3-SCR. NO_x reduction using ammonia/urea has been used not only in the automobile sector but also in power plants, boilers, and other industrial sectors. Ammonia has been commercially used as a reductant for generations, and the safest method of NH_3 storage is in the form of a solution of urea or a hydrous form of NH_3. The preference is based on the safety protocols and economic viability of the process. The overall literature suggests that

https://doi.org/10.1021/acs.energyfuels.4c00705
Energy Fuels XXXX, XXX, XXX−XXX

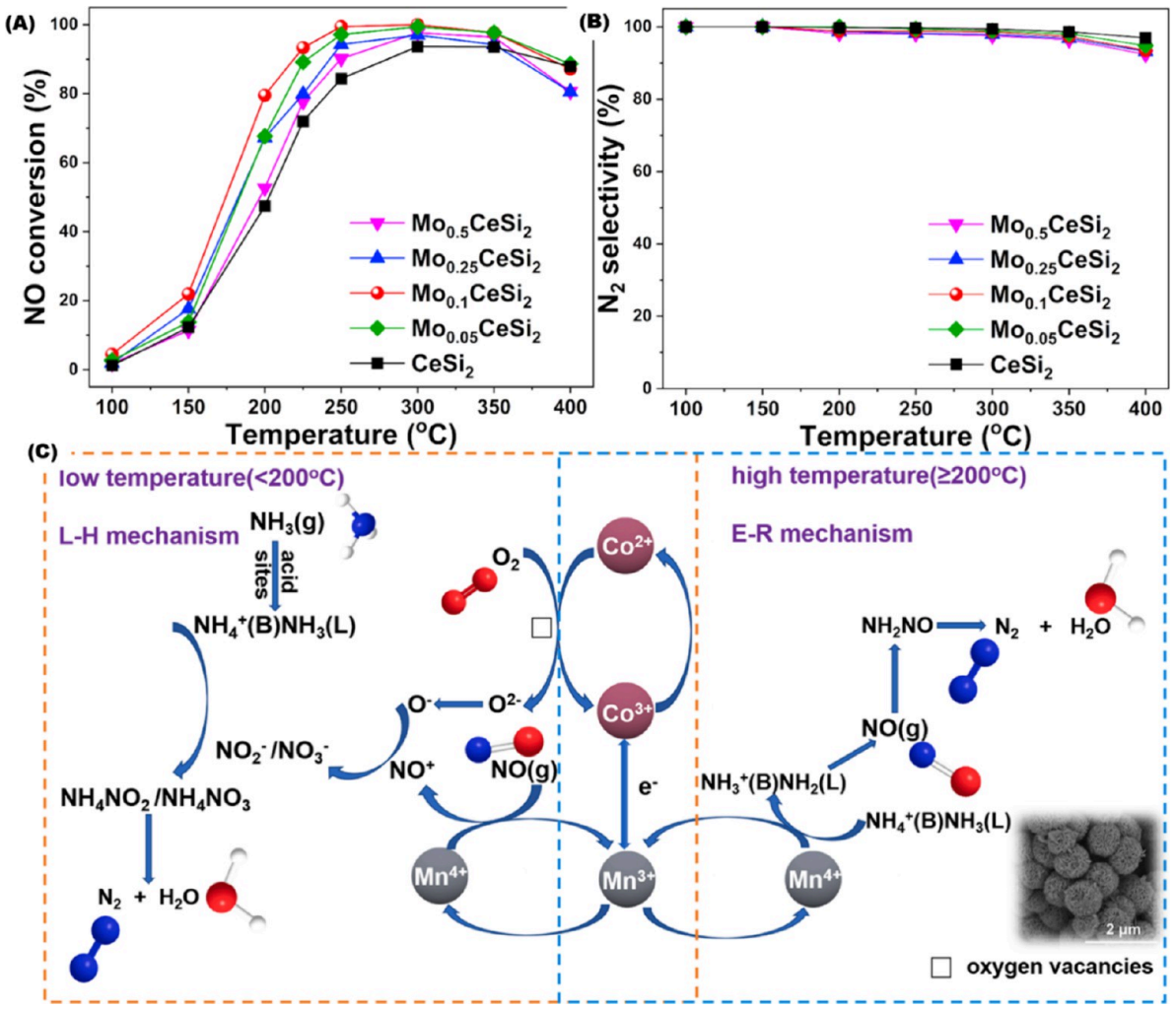

Figure 16. NO conversion (A) and N_2 selectivity (B) in NH_3-SCR conversion reactions using $CeSi_2$ and $Mo_\alpha CeSi_2$ catalysts. (C) Proposed illustration of mechanistic pathway of NH_3-SCR over Mn-Co-F catalyst. (A) and (B) Reproduced with permission from ref 213. Copyright (2022) with permission from Elsevier. (C) Reproduced with permission from ref 221. Copyright (2021) with permission from Elsevier.

NH_3-SCR displays an efficiency of 70−98%, and therefore this is one of the most preferred methods for NO_x abatement and is already being used in passenger vehicles. The SCR process involves the chemical reduction of the NO_x molecule using ammonia, and the system employs a metal-based catalyst with active sites to increase the rate of reduction reactions. The catalysts comprise an active metal or ceramic possessing highly porous structures, and within these pores lie the acidic active sites on which the reduction occurs. NO_x conversion catalysis has been revolving around V_2O_5, Fe_2O_3, and MnO_x. A number of SCR catalysts have shown good low-temperature activity due to the performance characteristics of these metal oxides.[204] Among these MnO_x has been extensively studied because of its suitable properties; however, it gets easily deactivated by SO_2.[205,206] In recent studies, metal-exchanged zeolites have also particularly displayed higher activities within a broader temperature window, along with greater thermal and chemical stability. Among the transition metals Fe, Cu, and Mn among others have been proven to be representatives of outstanding activities via metal exchange zeolites for catalytic NO_x reduction.[207]

The reactions for NH_3-SCR have been illustrated coherently in Figure 15(A). Ammonia being the reducing agent is generated onboard through urea hydrolysis, reaction E1, or in some cases is available as such. The selectivity of the reactions taking place is dependent upon the NO/NO_2 ratio flowing into the SCR catalytic converter, of which reaction E2 corresponds to standard SCR, reaction E3 and E4 to NO_2 SCR and fast SCR correspondingly. Reactions E5, i.e., ammonia oxidation, and reaction E6 being NO oxidation/NO_2 decomposition may also occur as side reactions at temperatures >400 °C. At temperatures <200 °C, ammonia nitrate formation, resulting in N_2O formation, may also take place.[208,209] Typically, this reaction occurs via an E-R or L-H mechanism in which urea gets hydrolyzed and gets adsorbed onto acidic sites on the catalyst surface. In the E-R mechanism, the gaseous NH_3 loses a proton, and e^- and gets converted into NH_2 on the acidic catalyst surface, which further reacts with NO_x from the gaseous phase and forms N_2 and H_2O, while the L-H mechanism proceeds by adsorption on NH_3 on acidic sites followed by its conversion to NH^{4+}, which further reacts with NO_2 forming NH_4NO_2. The complex then reduces itself on the catalyst surface, forming N_2 and H_2O.

AdBlue or diesel exhaust fluid is used commercially in automobiles with SCR technology to minimize the release of harmful gases, such as NO_x into the atmosphere. It comprises a clear 32.5% w/w mixture of demineralized water and highly pure synthetically manufactured urea. Joseph et al.[210]

https://doi.org/10.1021/acs.energyfuels.4c00705
Energy Fuels XXXX, XXX, XXX−XXX

experimented by replacing AdBlue injection in SCR with gaseous ammonia injection which was generated on heating solid ammonia precursors. This is preferable for low temperature exhaust systems as ruea begins to decompose into isocyanic acid and ammonia only at temperatures >200 °C.[211] They also replaced commercially available copper zeolite (CuZ) catalyst with $MnCeZrO_x$ catalyst and observed a 90% increase in NO_x conversion at exhaust temperatures of 100 °C and 80% increase at 150 °C when compared to a standard of AdBlue-CuZ SCR system for diesel fuel. When tested with biodiesel Jatropha B20 (20% by Volume Biodiesel in Diesel) fuel, more than 80% NO_x conversion was observed between 100 and 150 °C, and a maximum conversion of 93% was observed in peak loads. Present day studies focus upon the use of promoters to tailor characteristics such as thermal durability, enhanced hydrothermal stability, resistance to poisons, and better comprehension of reaction mechanisms. Rare earth modified catalysts have gained popularity in this regard. Lei et al.[212] on reviewing the performance of CeO_2 for NH_3-SCR reported high performance within a broader temperature range of 100−500 °C. They also highlighted that CeO_2 possesses higher oxygen storage capacity along with its high redox capabilities and ability to disperse and interact with various other metal atoms increasing active sites. Finally, it was also observed that ceria forms solid solutions or rather is deposited on phase boundaries improving hydrothermal stability. Tan et al.[213] in their study developed a CeO_2-SiO_2 mixed-oxide SCR catalyst with exceptional SO_2 resistibility, and they further doped this catalyst with Mo forming $Mo_{0.1}CeSi_2$ displaying 80% NO_x conversion and superior N_2 selectivity along with resistance to SO_2/H_2O all at 200 °C exemplified in Figure 16(A) and (B). In another similar study, the properties of Mn and Ce were explored by Ni et al.[214] by using citrate method to synthesize Mn-Ce bioxide on three-dimensional (3D) monolithic nickel foam, the 17 wt % $MnCeO_x$/NF catalyst showed a NO_x conversion of 98.7% at 175 °C and 90% conversion in the presence of 10 vol % water. The catalyst preparation is low-cost, with the advantage of high efficiency.

Now considering transition metal oxides, Mn-based catalysts are known to decompose NO and oxidize CO and organic volatiles, all simultaneously due to its rich metallization valences. They are known to show good low temperature activity, owing to high lattice oxygen mobility and multivalent states. Higher oxidation states of Mn show better redox properties, especially Mn in the 4+ state. Zhu et al.[215] synthesized a Fe-V-Ti oxide catalyst via coprecipitation method and observed good conversion rates. Although the temperature of conversion was as high as 250 °C, the reaction mechanism resulting from the combination of these 3 transition metal oxide composites gave a better understanding of the requirements for NH_3-SCR reactions. Studies revealed the presence of both Lewis and Bronsted acid sites on the catalyst surface, and the reaction proceeded via the E-R mechanistic pathway. Here, gaseous NO_x species could directly react with active NH_3 preadsorbed species. Since NO_x did not directly have to adsorb on the catalyst surface, it showed higher durability toward SO_2. The reaction was initiated via gaseous ammonia adsorption on acid sites followed by its activation by V^{5+} species. The gaseous NO reacts with -NH_2 forming N_2 and H_2O, while simultaneously a strong inductive effect between Fe^{3+} and V^{4+} initiates a thermodynamically feasible redox reaction, regenerating the oxidation states for the consequent reduction cycles. In order to further validate these redox systems for NO_x reductions, Shi et al.[216] prepared a series of Mn-Ce-Fe-Co-O_x/P84 (polyimide) catalytic filter materials to investigate the low-temperature catalytic activity of NO_x, under mixed atmospheric conditions with water and sulfur. Activity of Mn-Ce-Fe-Co-O_x in molar ratios of 4:5:1.25:1 achieved 81% NO_x conversion at 170 °C. Electron transfer reactions between Mn, Ce, and Fe increase the high ratio of $Mn^{4+}/(Mn^{4+} + Mn^{3+})$ and $Ce^{3+}/(Ce^{3+} + Ce^{4+})$ which may be involved in sulfur and water resistance of the catalyst material, while Xie et al.[217] synthesized a novel 0.3Mn−FeV catalyst through a one-pot synthesis method which exhibited 100% NO_x conversion rate at 225 °C. The doping of Mn was conducive to the activation of NH_3 in NH_3-SCR, and alongside $FeVO_4$ it improved the crystal size, acidity, and redox states of the catalyst system and increased its BET surface area, and it also helped maintain vanadium in its higher valence state.

Liu et al.[218] observed the change in NO_x conversion properties of MnFe/Ti and MnFeW/Ti oxides as a function of temperature. MnFe/Ti attained a maximum conversion of 90% at 200 °C and over 80% conversion at 140−250 °C. However, the conversion rate decreased significantly above 200 °C, and to overcome this the catalyst was modified with W, and the resulting MnFeW/Ti catalyst showed a 92% conversion at 150 °C and 96% at 300 °C, while Jiang et al.[219] studied the synergistic effect of codoping FeO_x and CeO_x in the low-temperature NH_3-SCR of Mn-Fe-Ce/ACN catalyst exhibiting superior catalytic activity, N_2 selectivity, and SO_2 tolerance. MnO_x catalyst loaded on modified activated carbon on which FeO_x and CeO_x were codoped by impregnation in the ratio Mn-Fe(0.4)-Ce(0.4)/CAN, exhibited NO_x conversion higher than 95% in 100−250 °C range and dropped to ∼91% after 32 h in the presence of 100 ppm of SO_2 and 10 vol % H_2O at 175 °C. The codoping enhanced redox properties and surface chemisorbed oxygen promoted NH_3-SCR, and the stronger surface acidity inhibited the adsorption of SO_2. While Bronsted acid sites dominate the catalyst surface, they simultaneously resisted adsorption of acidic SO_2 species, which impedes catalyst deactivation.[220]

A water-resistant hierarchical flower-like Mn-Co-F (1:1) synthesized by Zhu et al.[221] through solvothermal procedures showed notable 15 vol % water resistance alongside 99% NO_x conversion and >80% N_2 selectivity within 60−320 °C. The catalyst was curiously found to follow the L-H mechanism below 200 °C and E-R mechanism above 200 °C (Figure 16(C)). Tang et al.[222] combined the SCR and SO_2 resistance properties of Mn-Ce-Co using phosphotungstic acid (HPW) modification to explore enhanced catalytic effects of these metals in combination. The HPW-Mn-Ce-Co catalyst shows ∼100% conversion within 100−200 °C and N_2 selectivity >80% at 50−350 °C. The remarkable activity can be attributed to the greater number of oxygen vacancies, greater surface acidity, and redox ability of these metals in unification.

In another study, Peng et al.[223] prepared a highly crystalline novel hierarchical porous Cu-zeolite termed Cu-SSZ-13-HP with an improved mesoporous structure prepared via a dual-template method. The catalyst exhibited boosted low-temperature activity of 90% conversion in the temperature ranges of 175 and 500 °C, also displaying remarkable hydrothermal stability and SO_2 tolerance when exposed to 100 ppm of SO_2 for 4 h. In another similar study carried out by Liang et al.,[224] Cu-SSZ-13-Meso zeolite was prepared containing both small micro- and mesopores by adding carbon black as a template and showed 86% NO_x conversion at 160 °C. The catalyst also

https://doi.org/10.1021/acs.energyfuels.4c00705
Energy Fuels XXXX, XXX, XXX−XXX

exhibited hydrothermal stability and superior water and sulfur resistance. From these two studies, it was comprehended that since the molecular size of NO_x compounds is proportionate with the size of micropores in zeolites, mass transportation is limited, and this obstacle reduces catalytic performances. In order to overcome this, mesoporous compounds could be used such as in this case, which not only facilitates movement but also provides an enhanced surface for better catalytic performance.[225]

A major problem associated with catalytic systems involves deactivation by water vapor and other moisture sources. To overcome this demerit, now days, hydrophobic materials have been used in catalyst technologies such as SCRs. This hydrophobicity can be achieved by drastically reducing the surface energy of the substrate[226] or by providing a hydrophobic coating to the substrate or supporting material using hydrophobic surfactants such as montmorillonite[227] or phenyltrimethoxysilane.[228] Moving onto zeolites, which serve as great catalyst supports, they are prone to water attack through hydrogen bonding and dipole field interaction. Engineering materials with higher Si/Al ratios decreases the number of cations required to balance the surface charges which in turn increases the hydrophobicity of the material.[229,230] Small pore 3-D cage-like 8 membered zeolites with pore sizes of 0.3−0.5 nm makes it resilient to even hydrocarbons. These combinations of small pore-large cage structures have the ability to maintain their structure even after repetitive exposure to extreme hydrothermal conditions and maintain their catalytic stability.[231]

On assimilation of the discussion on selected catalysts and their properties, it can be concluded that a high surface acidity assists in NH_3 adsorption as well as inhibits adsorption of SO_2, while redox abilities such as those by metals possessing higher valence states like Mn, V, Mo, W, etc. are preferable. At the same time Cu and Fe have in recent studies exhibited good low temperature activity. Especially Cu in zeolitic frameworks has shown excellent conversion over larger temperature ranges. These also simultaneously exhibit defect sites and acid−base characteristics which can be fine-tuned to serve the requirements. The valency and homogeneous dispersion of the catalyst active sites directly correlate to the oxygen activation ability of the catalyst which corresponds to catalyst performance. The anchoring of hydroxyl groups on the catalyst supports increases or decreases the hydrothermal activity of the active catalyst along with influencing its dispersibility, valency, and particle size. From Table 5 it can also be established that catalysts with oxygen storage capabilities are desired along with a catalyst promoter which invariably boosts thermodynamically favorable redox reactions to regenerate the required oxidation states suitable for NH_3-SCR catalysts. Acid sites are of utmost importance and can be induced with the formation of lattice defects in solid solutions. W and Mo oxide addition to solid solutions are known to increase surface acidity along with the creation of defect sites which further increase oxygen vacancies. Further, in order to promote higher catalytic transformations, catalysts and their substrates with mesopores are preferential since microporous compounds would as discussed hinder the movement of NO_x molecules. Nonetheless, the active temperature ranges of most of these catalysts is still quite high for LTC operation modes, and further enhanced activity is essential toward further decrease in active temperature windows.

4.2.1.2. HC-SCR. Initially introduced by Iwamoto et al.[232] and Held et al.,[233] SCR using HC for NO_x reduction has been extensively studied for a large number of catalysts individually and in combination to achieve high stability, greater reproducibility, durability, and essentially greater activity. This technique exhibits practicability and cost-effectiveness, although the catalyst used must exhibit high sulfur tolerance, stability under exhaust conditions, a wider operation temperature range, and resistance to sintering and should decidedly be cost-effective. In this catalytic system, hydrogen gas and/or hydrocarbons such as methane, propane, butane, propylene, etc. are used as reductants, and the reaction is as follows (E1),

$$HC + NO + O_2 \rightarrow N_2 + CO_2 + H_2 \quad \text{(E1)}$$

The performance of the system varies with the nature of the catalyst and the hydrocarbon being used. Since diesel exhaust in itself contains reducing agents such as unburnt hydrocarbons, utilization of these would provide the most ideal process. But undeniably the inappropriate side-reactions limit the De-NO_x capabilities of these processes.

In a study carried out by Serhan et al.[234] using Ag/Al_2O_3 for de-NO_x treatment it was concluded that in order to enhance low-temperature NO_x conversion, injections of hydrogen (H_2) would be required. Consequently, Theinnoi et al.[235] investigated the effect of a Diesel-Biodiesel-Ethanol fuel blend on a passive mode of SCR to reduce NO_x emissions using Ag/Al_2O_3 under real engine conditions using H_2 to assist the SCR. It was found that HC and CO increased but NO_x decreased with an increase in ethanol quantity, and the hydrogen gas improved the activity of the catalyst to achieve 74% conversion at low engine load with an ethanol content of 50 vol % and 10000 ppm of H_2 added. Lee et al.[236] combined CuSn/ZSM-5 to the exiting Ag/Al_2O_3 catalyst for NO_x reduction by H_2-assisted C_3H_6. Lower Ag loading percentages are preferable owing to the reduced agglomeration of Ag onto its support material. The catalyst could reduce NO_x over a wide temperature range of 300−600 °C, where NO_x was just about completely converted into N_2 with negligible traces of N_2O, NH_3, and fulminic acid (HCNO). However, these temperature ranges are far beyond LTC operational temperatures.

Xu et al.[237] synthesized a series of rare earth metals La_yCe_z codoped Mn-based microporous zeolite ZSM-5 by the coimpregnation method. It was observed that $Mn_{0.2}La_{0.07}Ce_{0.05}$/ZSM-5 presented high activity and a broad temperature window for HC-SCR of NO_x with propene (C_3H_6) because of the strong synergistic interactions of the 3 metal ions. La and Ce enhance the low denitrification effects of Mn to display greater than 90% conversion within 180−270 °C. Xu et al.[238] has also reviewed the use of copper-based zeolites with low-temperature activity for HC-SCR based on the structure−activity relationship, design strategies, and reaction mechanisms. They concluded that an increase in Cu content and selection of appropriate reducing gas and zeolites with a superior zeolite framework with appropriate Si/Al ratios all contribute together to enhance the low-temperature de-NO_x conversion performance. Although these catalysts still reveal greater performance at higher temperatures, it was inferred that active catalysts should have acidic sites, an active phase, and basically have elements such as Ag or mixed metals. In order to avoid deactivation of the catalyst and to enhance recyclability, noble metals such as Pt, Rh, etc. could be incorporated. Catalyst supports such as zeolites are highly

https://doi.org/10.1021/acs.energyfuels.4c00705
Energy Fuels XXXX, XXX, XXX−XXX

Table 5. Comparison of Activities and Catalytic Characteristics of Metal Oxides Suitable for NH_3-SCR

catalyst; synthesis method	reaction conditions	conversion efficiency (° C)	catalyst characteristics
Nanoflakes 0.5 V_2O_5-3% WO_3/TiO_2;[308] wet bead milling	Fixed bed quartz reactor	T_{100} = 221	Reduction of V_2O_5 species plays a low temperature role.
	300 ppm of NO, 300 ppm of NH_3, 5% O_2, (300 mL/min), and N_2 balance		
	GHSV = 600,000 mL g^{-1} h^{-1}		
Hollow structure WO_3@CeO_2;[309] templating method	Fixed bed quartz reactor	T_{88} = 200	SO_2 and H_2O tolerance at 300 °C, high specific surface area, reducible W species, increased specific amount of chemisorbed oxygen species and acid sites.
	500 ppm of NO, 500 ppm of NH_3, 5% H_2O, 3% O_2, and N_2 balance		
	GHSV = 400,000 mL g^{-1} h^{-1}		
Porous $Ce_{0.4}Nb_{0.6}$ nanospheres;[310] modified seed-mediated growth approach	-	T_{98} = 250−450	Interaction between both metal oxides affects oxygen defects, valence, reducibility, and more no. of acid sites.
Ce/Fe (1:0.35) oxide;[311] microwave hydrothermal method	Vertical tubular furnace	T_{90} = 200	Fe^{3+} replaces Ce^{4+} changing its crustal structure, facilitating homogeneous distribution of active sites, and increasing acid sites and specific surface area.
	0.05% NH_3, 0.05% NO, 3% O_2, and N_2 balance.	T_{80} = 150−300	
	GHSV = 6000 h^{-1}		
Fe-Mn/1Ce2Al oxide;[312] coprecipitation method	Reactions carried out under steady state	T_{90} = 75−250	Addition of Al increases surface area, higher concentrations of Mn^{4+} and Ce^{3+} and surface oxygen species. Added surface acid sites facilitating NH_3 activation.
	500 ppm of NO, 500 ppm of NH_3, 5 vol % O_2, and N_2 as balance		
	GHSV = 30000 mL g^{-1} h^{-1}		
MnFeW/Ti oxide;[218] ultrasonic-assisted impregnation method	Fixed bed plug flow quartz reactor	T_{90} = 200	Transfer of e^-'s from SO_2 to Mn^{4+} and Fe^{3+} inhibited by facile e^- transport among Mn, Fe, and W reducing metal sulfates and enhancing SO_2 tolerance.
	500 ppm of NO, 500 ppm of NH_3, 5 vol % O_2, and N_2 as balance	T_{80} = 140−250	
	GHSV = 80000 mL g^{-1} h^{-1}		
4Ce-10Mn/TiO_2;[313] reverse coprecipitation	Quartz tube furnace	T_{90} = 119−332	Uniform dispersion of active components; good synergistic effect of MnO_x and CeO_2.
	500 ppm of NO, 500 ppm of NH_3, 3% O_2, and N_2 as balance		
	GHSV = 75,000 mL g^{-1} h^{-1}		
Ce(1.0)Mn/TiO_2;[314] in-situ deposition method	Vertical quartz atmospheric fixed-bed reactor	T_{90} = 150−300	Large number of Mn^{4+} species and adsorbed oxygen species and enhanced transport characteristics.
	1000 mg m^3 NO, 1000 mg m^3 NH_3, 3% O_2, N_2 as balance (350 mL/min)		
	GSHV = 10,500 h^{-1}		
$WO_3/CeZrO_x$[315]	Fixed-bed quartz tube flow reactor	T_{90} = 222−454	Stronger interaction between Mo and Ce compared to W and Ce leads to fewer Lewis acid sites and oxygen vacancies in addition to strong oxidation properties inhibiting NO_x adsorption and causing peroxidation of NH_3.
$MoO_3/CeZrO_x$[315]	500 ppm of NO/NH_3, 5 vol % O_2 and N_2 reaction gases	T_{90} = 254−410	
	GHSV = 30,000 h^{-1}		
$Mo_{0.4}Ce_{0.3}FeO_x$;[316] two-step solid interface reaction	Quartz tube at atmospheric pressure	T_{85} = 250−300	Mo inhibits the formation of NH_4^+-NO_3^-, and it produces a greater number of Bronsted acid sites while reducing the number of basic sites.
	2000 ppm of NH_3, 2000 ppm of NO, 8 vol % O_2 and N_2 as balance		

https://doi.org/10.1021/acs.energyfuels.4c00705
Energy Fuels XXXX, XXX, XXX−XXX

Table 5. continued

catalyst; synthesis method	reaction conditions	conversion efficiency (°C)	catalyst characteristics
CeW/Ti;[317] wet impregnation	Fixed-bed reactor	T_{80} = 200−550	Formation of solid solutions increases lattice defects, unsaturated cations and Ce(Ti)−O−W bonds serve as Lewis and Bronsted acid sites.
CeW/Ti;[317] mechanical mixing	500 ppm of NO, 500 ppm of NH_3, 5% O_2, 5% H_2O, and N_2 balance GHSV = 50,000 h^{-1}	T_{75} = 275 T_{85} = 550	

favored in this mode. Nevertheless, in real-engine applications, addition of HCs may further increase the complexity of side-reactions and contribute to higher degree pollutants, and also the HCs could promote simultaneous soot formation.

4.2.1.3. H_2/CO-SCR. Urea SCR technologies have been profoundly explored and are being implemented in passenger vehicles. However, leakage of ammoniated solutions or gases cause grave concerns, and in recent years the SCR of NO_x with H_2 in the presence of O_2, i.e., H_2-SCR, is in the spotlight attributable to the cascading decrease in noxious byproducts.[239] In a study by Patel et al.,[240] a Pd/ZrO_2-CeO_2 mixed oxide synthesized by coprecipitation followed by impregnation of palladium displayed a 92% NO reduction within a wide temperature window of 150−400 °C when examined for SCR of NO with H_2 in the presence of excess oxygen (6% O_2).

Another interesting category of SCR is CO-SCR in which a contaminant arising from the combustion process has a practical application. In this technique, NO_x and CO can simultaneously be reduced and oxidized to N_2 and CO_2 respectively. Additionally, CO being cheaper and easily available is very ideal for such an application. After many examinations of CO-SCR in the presence and absence of O_2, it was concluded that O_2 acts as an inhibitor in this process due to the competition reaction of CO between O_2 and NO_x.[241,242] Formerly, Ir was known to be the only active metal catalyst for this system, but its activity was gravely affected by the nature of its support and other additives.[243] You et al.[244] showed the synergistic effect between Ir and Ru showing excellent catalytic activity and properties suitable for NO_x reduction by CO under lean conditions such as those in LTC modes. Ir-Ru/Al_2O_3 showed an excellent NO_x conversion of 91% at 175 °C along with superb N_2 selectivity. Sun et al.[245] showed that the synergy between Cu and Ce led to a greater number Cu-Ce interfaces, and a Cu:Ce-1:3 catalyst showed superior NO conversion with over 90% N_2 selectivity and no amount of N_2O byproduct in the temperature range of 50−200 °C. The catalyst also exhibited water and sulfur resistance. Wang et al.[246] studied a Cu-Ni-Ce/activated carbon low-temperature denitrification, in which the catalyst was prepared using an ultrasonic equal volume coimpregnation method. The oxide catalyst 6Cu-4Ni-5Ce/activated carbon was conceived to be a superb catalyst reaching 99.8% at a denitration temperature of 150 °C in the presence of 5% O_2.

The acidity or basicity of the support material is crucial toward the determination of the activity for NO reduction to N_2 and N_2O. Highly acidic surfaces are known to enhance selectivity toward N_2 formation as these provide an additional route toward NH_3 formation via reduction of NO by hydrogen on the catalyst surfaces. This is also accompanied by NH_4^+ storage on acidic sites and may proceed with NH_3-SCR catalysis. H_2-SCR seems like a promising approach toward NO_x mitigation in lean-burn systems and at lower temperatures. It can be easily produced from hydrocarbon fuel reformations and could be recognized as an efficient technique in next generation hydrogen fuelled vehicles. CO on the other hand is more practical as its already present in the vehicular exhaust; however, these reactions require relatively oxygen deficient conditions to function. Also, CO produced during combustion may not be available or sufficient to carry out quantitative de-NO_x reactions in conventional engines. However, in LTC modes, since CO emissions are found to be higher than normal diesel engine operations, this emitted CO can be effectively channelled toward the CO-SCR of NO_x.

https://doi.org/10.1021/acs.energyfuels.4c00705
Energy Fuels XXXX, XXX, XXX−XXX

4.2.2. Direct Catalytic Decomposition of NO_x. Ammonia selective catalytic reduction intermittently suffers from concerns such as high operating temperatures and urea or NH_3 leakages. In order to surmount these drawbacks, direct catalytic decomposition of NO_x using novel metal-SCR catalysts are desirable. Such catalysts displaying low-temperature catalytic performance in the absence of NH_3 are crucially required. Among the metal oxide catalysts, Mn-based catalysts have displayed magnificent low-temperature SCR activity due to their variable valence states, bountiful surface reactive oxygen species, enhanced number of surface Lewis sites, and strong redox property. However, due to low N_2 selectivity and sulfur poisoning, Mn catalysts need to be fine-tuned to enhance the surface area, oxidative capacities, surface morphologies, and crystal structures to develop better novel Mn-based SCR catalysts that can selectively carry out NO_x conversion at lower temperatures.

Cheng et al.[247] proposed an ammonia-free SCR of NO_x at low operating temperatures on melamine impregnated MnO_x-CeO_2/carbon aerogels. The aerogels displayed rich surface chemistry and pore structure that not only facilitate homogeneous dispersion of the metal oxide but also accelerate the diffusion of gas molecules. Using impregnated melamine instead of NH_3 reduces the formation of byproducts such as NH_3, N_2O, etc., and a 15 wt % melamine loading exhibits optimal activity of 100% steady conversion for 7 h at 185 °C. NO_x can be selectively catalyzed to N_2 using chabazite structured Cu-zeolites (CHA, Cu-SSZ-13); however, diffusion limits and micropore blocking at low temperatures inhibits their use in practical applications.

The N−O bond has a sufficiently high binding energy, and breaking this bond involves a reaction involving a very high activation energy. Thus, it is essential to develop a catalytic composite material that can reversibly absorb and desorb oxygen and readily regenerate catalytic sites. NO is acidic, and its adsorption is significantly dependent upon the basicity of the catalyst, while at the same time for NH_3-SCR, the reactivity is dependent upon the Bronsted acidity of the catalyst for adsorption of NH_3. Fine-tuning catalytic pathways is thus dependent on the mechanistic pathway that the reaction follows. The adsorption of acidic or basic reactants determines the nature of the required adsorption sites. Concurrently, the pore structure and diffusion limits of these pores are distinctly dependent upon the size, shape, and reactivity of the starting reactants. For direct NO_x conversion, the catalyst should possess higher solid basicity along with a mesoporous surface, considering the size of NO molecules which will face some cutbacks in the case of microporous compounds. This property is likely to be found in alkali and alkaline earth metals, typically in Ba which is extensively used in LNT as will be subsequently discussed. On the other hand, the basicity of catalyst also facilitates CO adsorption which can further poison the catalyst surface. Hence, the difficulty lies not only with synthesis of a catalyst with the appropriate morphology, pore structure, and surface sites but also in overcoming the hurdle involving resistance to certain other species which could poison the catalyst.

4.2.3. Lean NO_x Traps. The increase in NO_x emissions as a result of the gradual transition to renewable biofuels has been now substantiated in a motor bench.[248,249] Although SCR technologies considerably lower NO_x emissions, coupling of NO_x storage and reduction (NSR) with SCR technologies is arguably the most effective technique to reduce NO_x emissions from vehicles in recent years. This NSR technology is implemented using LNT, wherein NO_x reduction occurs via a cyclic process, which is discussed subsequently. Since SCR processes are based on the mineralization of NO_x to N_2 and H_2O in the presence of urea or HC, this process requires an external reducing agent. The oxidizing atmosphere of lean burn engines calls for specialized after-treatment catalysts for NO_x removal from the exhaust gas, and LNT provides such leverage. When both the systems, i.e., LNT and SCR, are coupled such that the SCR system is placed downstream in the catalytic treatment process, it was observed that the NO_x conversion values increased, and there was a decrease in the ammonia-slip, enhanced catalyst durability, and a wider operating temperature window was recognized. It could also be noted that a decrease in HC production could be expected in LNT-SCR processes as expressed in Figure 15(B).[250,251]

Customarily, the LNT catalyst contains a storage material such as $BaO(CO_3)$, CeO_2, etc., a support material such as Al_2O_3, and a platinum group metal (PGM), i.e., Pt/Pd and Rh to oxidize and reduce NO_x respectively. These storage and redox sites are placed in close proximity to increase the efficiency. The reaction mechanism of LNT technology is fundamentally dependent on the oxygen concentration, i.e., lean phase and rich phase. During the lean phase which extends to a few minutes and O_2 is in excess, NO_x is adsorbed on the storage sites in the form of nitrates and nitrites. The rich phase is prompted once these sites are saturated and is now in operation where the fuel is in excess, and this lasts for a couple of seconds. The stored NO_x is now released, bulk of which is converted to N_2 with traces of N_2O and NH_3 being left behind. The catalyst is now regenerated to store more NO_x, and the cycle thus repeats itself.[252,253]

The following reactions (E2−E5) occur when Ba is used as a storage catalyst:

$$BaO + 3NO_2 \rightarrow Ba(NO_3)_2 + NO \quad \text{(E2)}$$

$$Ba(NO_3)_2 + 8H_2 \rightarrow 2NH_3 + BaO + 5H_2 \quad \text{(E3)}$$

$$Ba(NO_3)_2 + 5H_2 \rightarrow N_2 + BaO + 5H_2O \quad \text{(E4)}$$

$$Ba(NO_3)_2 + 10NH_3 \rightarrow 8N_2 + 3BaO + 15H_2O \quad \text{(E5)}$$

$$NO + 1/2O_2 \rightarrow NO_2 \quad \text{(E6)}$$

The NSR capacity of the catalyst is dependent on the concentration of Ba around the Pt atoms. Since PGMs are not cost-effective and due to the competing HC-SCR at the Pt sites, undesirable formation of N_2O is observed in the lean operation mode. A number of alternatives have been proposed, such as perovskites. Ecker et al.[254,255] synthesized a platinized perovskite-based infiltration composite Pt/$La_{0.5}Sr_{0.5}Fe_{0.5}Ti_{0.5}O_3/Al_2O_3$, but it was observed that at lower temperatures the competing reactions with C_3H_6-SCR resulted in a dramatic increase in N_2O. This catalyst was further coated with Rh, and this led to an increase in NO_x storage capacity (NSC), although no decrease in N_2O emissions was observed within a temperature range of 300−450 °C. They further replaced 20% of the LNT with an oxidation catalyst, i.e., 2 wt % Pd/20 wt % CeO_2/Al_2O_3, and a 13−60% N_2O emission reduction was observed along with NSC up to 176 μmol/g at 200 °C inferring that oxidation of propylene is one of the most effective ways to reduce N_2O formation.

https://doi.org/10.1021/acs.energyfuels.4c00705
Energy Fuels XXXX, XXX, XXX−XXX

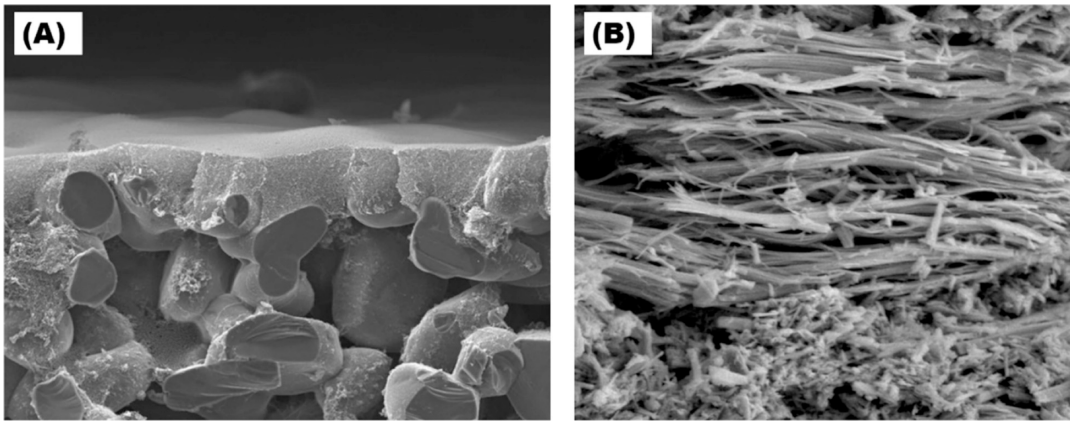

Figure 17. (A) Soot-cake build-up on bare DPF channel surface. (B) CeO_2 fibers deposited on alumina wash-coat and calcined in situ on the DPF channel surface. (A) and (B) ref 280. Copyright (2012) with permission from Elsevier.

Albaladejo-Fuentes et al.[256] studied the $BaTi_{0.8}Cu_{0.2}O_3$ catalyst and observed that BaO generated on the catalyst by decomposition of Ba_2TiO_4 is essential in the NO_x storage process. At temperatures <350 °C, NO adsorption leads to formation of nitrites on the catalyst, and at temperatures >350 °C, NO oxidation occurs and promotes NO_2 generation and nitrate formation. The characterization affirmed that the introduction of Cu into the perovskite lattice initiates a pseudodistortion of the structure which segregates the Ba_2TiO_4 and $BaCO_3$ phases aiding in NO_x storage capacities. Chen et al.[257] observed the crystal size effect on the NO_x adsorption and desorption over Pd/SSZ-13 passive NO_x adsorbers and concluded that 0.4 μm Pd/SSZ-13 showed highest NO_x storage capacity and hydrothermal stability. They also noted that variation in distribution of acidic sites varies the intrinsic nature of the catalyst, and the availability of surface acidic sites determines the difficulty of Pd^{n+} ion diffusion. Higher NO_x storage is observed for smaller crystal-sized SSZ-13 as these render more valid Pd^{n+} adsorption sites. LNTs are known to have restricted performance at low temperatures and are customarily deactivated upon hydrothermal aging. Kim et al.[258] employed a reduced γ-Al_2O_3 support with unsaturated penta-coordinated Al^{3+} sites which can hasten the catalytic process. Pt-BaO-CeO_2 and Cu-CeO_2 were tested by deposition on the reduced support and meagrely any degradation was observed after hydrothermal treatment at 750 °C. This was also concluded by Kim et al.[259] in their study based on Cu-Ba/γ Al_2O_3. Although LNTs facilitate NO_x reduction and assist the SCR process, HCs interfere with the catalysts and result in HC-SCR conditions which further result in the formation of undesirable products. In such instances, it is only appropriate to treat HCs prior to subjecting the exhaust mixture into the LNT. Furthermore, they have relatively higher working temperatures and require lean and rich engine operation modes for their smooth functioning. Such conditions are not quite feasible in diesel engine modes let alone be used in LTC systems. A potential solution to this could be an electrified NSR technological strategy conceptualized by Mei et al.,[260] wherein Pt and K cosupported Sb doped Sn oxides were employed using C_3H_6 as a reductant. The lattice oxygen release assists in NO adsorption−desorption and finally reduction for improvement in NSR activity at temperatures almost 100 °C lower than those of temperature dependent methods. The catalysts used in LNT modes can also be tested for their activity in SCR modes, which are already well developed and direct decomposition reactions in order to enhance presently reported activities.

4.3. Catalytically Augmented High-Performance Diesel Particulate Filters. Diesel exhaust gas, being a major anthropogenic pollutant, has been thoroughly investigated unveiling that it is made up of gaseous and solid fractions. Solid fraction mainly consists of PM responsible for the blackish appearance of unfiltered diesel exhaust. These are primarily formed due to pyrolyzation of unburnt fuel, lubrication oil, etc. followed by polymerization reactions and ring cleavage. Further, stacking results in the formation of PAH binding together to form primary soot particles.[261] DPFs are designed to trap particulate matter and soot before they could be released into the atmosphere. The exhaust gases are allowed to pass through the permeable wall of the DPF, trapping the solid fraction into the channels (Figure 17(A) and (B)), and this particle accumulation further increases the pressure drop consequently decreasing the efficiency of the engine. In order to avoid this sort of filter blocking, the DPF is wash coated with a catalyst which is an advanced and effective regeneration system, out of which the prevalent commercially available technology encompasses a Pt-based catalyst. However, due to the extravagant pricing and limited availability of this noble metal, there is a need to look into cheaper active phase substitutes that would provide good results within the low-temperature regime.[262]

Catalytic soot oxidation is predominantly dependent on the structure and superficial characteristics of the catalyst. While a number of favorable catalysts have been proposed since the 1950s for soot elimination, it is indispensable to develop catalysts with a greater number of contact areas and enhanced reactivity to show impressive catalytic soot oxidation features. The combination of a DPF with an oxidation catalyst known as continuously regenerating trap (CRT) is one of the best abatement systems, and hence, catalysts such as spinels, perovskites, alkali doped catalysts, ceria-based compounds, and single and mixed metal catalysts have been proposed. However, they are still in need of further advancement to be commercially viable particularly at lower exhaust temperatures.[263,264]

As highlighted previously, Pt is used commercially, and this is due to its high activity and durability; however, due to its high cost, cheaper alternatives such as ceria are used. Although it shows good activity and is sufficiently durable to a considerable extent, its use is not favorable at higher

https://doi.org/10.1021/acs.energyfuels.4c00705
Energy Fuels XXXX, XXX, XXX−XXX

temperatures and is easily attacked by catalyst poisons. Thus, ceria has to be modified, and the key refinements need to be explored.[265] A rundown of selected perovskites, alkali-doped catalysts, ceria-based catalysts, and single and mixed metal catalysts has been encapsulated in Table 6. On scrutinizing the catalysts, it can be comprehended that the presence of NO shows lower oxidation temperatures in comparison to oxidation in the absence of NO. Additionally, it is also observed that the addition of dopants in differing compositions varies the activities of the catalysts in accordance with the number of defects or oxygen vacancies which can be formed correspondingly. Higher surface areas with 0-D or 1-D morphologies and macro- or mesopores are preferable as these typically provide a higher number of surface-active sites and allow easy mass transfer and heat dissipation. Thus, the particle size, porosity, and surface-active metallic oxide species contribute toward an increase or decrease in catalytic activity. Overall, exploring various normalities and abnormalities in catalyst properties is highly influential toward mitigation of a certain pollutant.[266]

In a recent study on spinels, by Fedyna et al.[267] cryptomelane catalysts comprising transition metals (M/K-OMS-2, M = Cu, Ni, Co, Cr and Fe) were synthesized and tested for soot oxidation under various conditions such as O_2, O_2 + NO, O_2 + SO_2, and O_2 + NO + SO_2. It was observed that doping with transition metal cations with varied electronic configurations enhanced the comprehension of the complex mechanistic nature of soot oxidation studies. The fundamental performance of the cryptomelane catalysts depends upon the average oxidation state of the ion, potassium release from the surface, and in situ NO_2 formation ability. A cobalt-manganese spinel-based catalyst was noted to be the most efficient of the lot, and increased doping of the cryptomelane matrix is known to enhance sulfur resistance.

In a path breaking work by Xiong et al.[268] a 3D ordered meso-macroporous (3DOMM) $Ce_{0.2}Zr_{0.8}O_2$ was synthesized by a combination of evaporation-induced interfacial self-assembly and colloidal crystal templates, followed by supporting spinel-type $Pd_xCo_{3-x}O_4$ nanoparticles on this 3DOMM by gas bubbling assisted coprecipitation. This novel catalyst displayed admirable catalytic performance of (temperature of 10% conversion) T_{10}, (temperature of 50% conversion) T_{50}, and (temperature of 90% conversion) T_{90} at 313, 367, and 404 °C under loose contact mode, the mechanism of which is illustrated in Figure 18(A). Zhou and co-workers[269] synthesized a TiO_2 and spinel $Cu_{1.5}Mn_{1.5}O_4$ comodified hierarchically porous beta zeolite, i.e., Ti/$Cu_{1.5}Mn_{1.5}O_4$-HBeta with a 3D interpenetrating micromeso-porosity. The catalyst showed great soot oxidation activity of T_{50} = 390 °C and T_{90} = 450 °C, even in the presence of O_2/NO/N_2 owing to the rich moderate intensity acidic sites and chemisorbed oxygen species. It also exhibited substantial sulfur-resistance as sulfates easily decomposed after surface adsorption.[270] Zhao et al.[271] prepared a ceria modified $MgAl_2O_3$ spinel and used it as a support for Ag nanoparticles. The initial reaction temperature and temperature of the maximum reaction rate were 236 and 359 °C respectively. It was established that the presence of ceria significantly enriched peroxide and superoxide formation and also established strong interactions with Ag, thereby allowing high Ag metal dispersion with distinguished thermal stability, promoting catalytic performance in soot oxidation.

A toxic pollutant such as NO_x can also be utilized in the soot oxidation process due to its admirable oxidative properties. NO oxidization to NO_2 gets accelerated in the vicinity of Pt containing catalysts present on the surface of the CRT. Since Ag/CeO_2 has been widely used in scrutinizing soot oxidation properties, Lee et al.[272] introduced Mn into this catalyst and performed NO_x assisted soot oxidation studies. The Ag/$2MnO_{x-1}CeO_2$ catalyst improved the T_{50} to 391 °C in comparison to Ag/CeO_2 having a T_{50} of 400 °C. The catalyst exhibited not only low-temperature NO oxidation but also NO desorption at a fair temperature. Thus, we conclude that not only NO oxidation but also NO_x adsorption characteristics are essential in NO_x assisted soot oxidation. A model NO_x assisted reaction pathway has been diagrammatically shown in Figure 18(C).[273] Zhao and co-workers[274] synthesized a 3D ordered macroporous nickel−cobalt based spinel catalyst for NO_x assisted soot oxidation, and under a loose contact mode its T_{50} and TOF values corresponded to 379 °C and 1.36×10^{-3} s^{-1} respectively. The doping of Ni into Co_3O_4 induces structural distortion, thus increasing oxygen vacancies and enhancing lattice oxygen mobility. The catalyst also encouraged a vacancy-mediated NO oxidation strategy.

Liu et al.[275] adopted a nonthermal plasma (NTP) strategy using $La_{1-x}Ag_xMn_{1-y}Co_yO_{3-\delta}$ perovskites under diesel exhaust gas conditions. The catalyst hardly showed any effect on soot oxidation at 200 °C in the absence of NTP, but the synergy between the NTP-$La_{0.5}Ag_{0.5}Mn_{0.8}Co_{0.2}O_{3-\delta}$ hybrid showed soot conversion and CO_2 selectivity of 86% and 94% respectively at 200 °C. In yet another study by Fu et al.[276] $MnO_{(0.4)}$-CeO_2 was researched for soot oxidation with a pulse dielectric barrier discharge (DBD), and it was found that the initial light-off temperature (T_i) decreased from 240.8 to 216.4 °C on increasing the pulse of the DBD frequencies from 50 to 400 Hz. Surface species formed such as O^{2-}, O^-, and Mn^{4+} were responsible for the enhanced soot oxidation. Recently the focus has turned to electrically powered programmed oxidation of soot, wherein an electrified catalytic strategy drastically decreases soot ignition temperatures much more than expected in traditional thermal catalytic soot combustion. This technology facilitates the rapid release of lattice oxygen from a conductive catalyst, thereby reducing the soot ignition temperature. Simultaneously the soot-catalyst contact efficiency improves due to electrostatic fluidization of the catalyst-soot interfaces.[277] Mei et al.[278] reported such an electrification strategy aiming for a T_{50} of <75 °C using conductive oxide catalysts such as K supported Sb−Sn oxides. The implementation of this technology into LTC engine modes could reduce soot emissions to a great extent. However, such a study is not yet realized.

From the above literature evidence, it can be deduced that mesoporous ordered frameworks coupled with metal oxides having pronounced redox properties accelerate soot oxidation kinetics. Surface irregularities time and again substantiate an increase in reactivity by increases in vacancies and oxygen mobility. At the same time, in NO_x-assisted catalytic reaction conditions, it is paramount to consider the pore sizes of the catalyst to achieve maximum utilization of the catalyst exposed areas, due to the relatively bulky size of NO_x molecules. Composites of metal oxides along with spinels or perovskites, in most cases decorated with noble metals, exhibit very good activity. In recent studies, it was observed that certain p-block elements especially in the later periods show considerable redox activity supporting a MvK mechanism for CO_2 selective

https://doi.org/10.1021/acs.energyfuels.4c00705
Energy Fuels XXXX, XXX, XXX−XXX

Table 6. Comparison of Activities of Metal Oxides as Soot Mitigation Catalysts along with Their Catalytic Characteristics

catalyst; synthesis method	soot oxidation conditions	T_{max}/°C	catalyst characteristics
1%Pt/Al_2O_3[318] (commercial)	Tubular quartz reactor	475	Small particle size facilitates efficient active oxygen transfer.
	Catalyst + soot (4:1), loose contact; 500 ppm of NO_x/5% O_2/N_2 (500 mL/min) at 10 °C/min		
$Ce_{0.5}Pr_{0.5}O_2$		444	
Nanoparticles;[318] reversed microemulsion			
Porous CeO_2 nanobars;[319] hydrothermal synthesis	Fixed-bed tubular reactor	456	Porous, hollow structures with more oxygen vacancies
	Catalyst + soot (9:1), loose contact; 79.5 vol % N_2/20.5 vol % O_2 (100 mL/min) at 5 °C/min		
5% Ag/$Ce_{0.8}Pr_{0.2}O_2$	Thermogravimetric analyzer	387	Higher surface concentrations of Ce^{3+}, Ag^+, O_2^{2-}, and O^- enhance surface reducibility, oxygen vacancies, and good sot-catalyst contact
Nanoflakes;[320] microwave assisted coprecipitation, wetness impregnation	Catalyst + soot (10:1), tight contact; 79% N_2, 21% O_2 (100 mL/min) at 10 K/min		
Ce-Hf-Ru[321] nanoparticle clusters; PVP assisted sol−gel	Thermogravimetric analyzer	390	Hf^{4+} and Mg^{2+} doped into ceria lattice exhibited higher oxygen vacancies
	Catalyst + soot (10:1), tight contact; 5% O_2/N_2 (60 mL/min) at 10 °C/min		Exhibited secondary tetragonal and orthorhombic phases deposited into the cubic fluorite phase
Na/CeO_2;[322] saturated impregnation	Continuous flow fixed-bed reactor	413	Superior redox activity and lattice ion mobility
	Catalyst + soot (10:1), loose contact; 600 ppm of NO + 10% O_2 + N_2 (500 mL/min) at 5 °C/min		
K/CeO_2;[322] saturated impregnation		415	
Ca/CeO_2;[271] saturated impregnation		445	Inferior redox activity and lattice ion mobility with slightly strong NO_x storage capacity
P/CeO_2;[322] saturated impregnation		448	Greater amount of surface-active oxygen species, enhanced ignition of soot particles
10% Cs/3% Co/$Ce_{0.5}Sn_{0.5}O_2$;[323] coprecipitation, impregnation method	Fixed-bed reactor	393	-
	Catalyst + soot (10:1), tight contact;		Alkali oxides such as Cs favor soot-catalyst contact due to low melting points or eutectics improving surface mobility of active species
	1000 ppm of NO, 50 ppm of SO_2, 5% H_2O and 10% O_2, N_2 (500 mL/min) at 10 °C/min		
Bi doped CeO_2 ($Bi_{0.2}Ce_{0.8}$);[282] coprecipitation method	O_2-TPD; theoretical studies	472	Enhanced oxygen mobility, oxygen vacancies, and weakened metal−oxygen bond (Figure 18(D))
$Ce_{0.8}Eu_{0.2}O_{2-\delta}$;[324] deposition coprecipitation method	Thermogravimetric analyzer	500 (Al_2O_3 support)	Formation of more oxygen defects in supported materials generating more active oxygen
	Catalyst + soot (4:1), tight contact; air flow (50 mL/min) at 5 K/min	477 (SiO_2 support)	
		458 (TiO_2 support)	
Ag-$CeZrO_4$;[325] hydrothermal reduction method	Thermogravimetric analysis	387	Increase in active oxygen at contact points with carbon particles
	Catalyst + soot (20:1), tight contact; 5% O_2/Ar 95% gas mixture (50 mL/min) at 10 °C/min		
Ce/Mn-Ni foam[326] (2.0 Mn wt %, 1.1 Ce wt %, Ce/Mn = 0.22); hydrothermal, wet impregnation	Fixed-bed tubular quartz reactor	385	Macroporous nanostructure facilitates mass and heat transfer along with an increase in tangible sites for soot combustion
	Catalyst + soot (10:1), loose contact; 10% O_2 and 600 ppm of NO/N_2 at 2 °C/min		
$SrMn_{0.98}Cu_{0.02}O_3$;[281] sol−gel method	Thermogravimetric analyzer	431	$Mn^{4+}/Mn^{3+}/Mn^{2+}$, Co^{3+}/Co^{2+} cations with stable Sr^{2+}, Cu^{2+} on the surface exhibit good catalytic activity toward soot oxidation (Figure 18(B))
	Catalyst + soot (10:1), tight contact; (60 mL/min) at 10 °C/min		

https://doi.org/10.1021/acs.energyfuels.4c00705
Energy Fuels XXXX, XXX, XXX−XXX

Table 6. continued

catalyst; synthesis method	soot oxidation conditions	T_{max}/°C	catalyst characteristics
$La_{0.6}Sr_{0.4}CoO_{3-\delta}$ nanotubes;[327] sol−gel, electrospinning	Tubular quartz fixed-bed reactor Catalyst + soot (9:1), loose contact; 5% O_2, 500 ppm of NO/N_2 (100 mL/min) at 5 °C/min	415	Higher specific surface areas contribute to larger O* and better dispersion of active oxygen species
$GdFe_{0.90}Cu_{0.1}O_3$;[328] EDTA-citrate method	Thermogravimetric analyzer Catalyst + soot (20:1), tight contact; N_2 medium (60 mL/min) at 10 °C/min	427	Introduction of Cu improves redox properties by increasing oxygen-deficient sites

oxidation of soot. Moderately acidic sites can prevent the adsorption of sulfur compounds and assist in avoiding sulfur poisoning and consequent catalyst deactivation. A catalyst providing the possibility of producing peroxides and superoxide species or even the presence of oxygen radicals in the reaction atmosphere could hasten reaction kinetics. Moreover, addition of value-added impurity ions into the lattice of solid solutions creates additional oxygen vacancies which is the fundamental catalytic requirement for soot oxidation.[279] Complete soot oxidation is not feasible at temperatures suited for the LTC combustion modes. However, the amount of soot produced in LTC is already negligible; hence, existing methods with some refinements could suffice.

5. CHALLENGES AND PERSPECTIVES

After review of the three main subdivisions in developing vehicular exhaust pollutant mitigation systems, the first impression suggests that none can single-handedly bring down emissions below the expected levels. It is, therefore, significant that a sustainable combination of varied methods can progressively lower pollutant emissions. Further enhancing existing technologies to reduce pollutants to near-zero levels is a pressing priority. Despite the complexities of the system, the modification of single pieces of technology, bit by bit, can, as a whole, have a transformative effect on the emissions.

- Vehicular emission norms laid down by government organizations are getting stringent as we speak, and since transportation is largely dependent on the automobile industry with its roots into fossil fuels a potential solution to curb emissions is a pressing priority.
- FBCs are effective in enhancing passive regeneration of DPFs and have a nearly positive effect on engine performance. However, postcombustion these metal nanoparticles may travel along with the exhaust gas and result in nanoparticle build-up, thereby clogging the honeycomb structure of the DPF. The soot will combust catalytically and escape in the form of CO/CO_2. But metallic particle build-up over a long period of time will urge a replacement of the exhaust treatment system. With prolonged use these may even settle down at the bottom of the fuel tank and result in clogging of the fuel injection system. A good compatible surfactant or emulsifier is required to avoid this issue along with smaller particles with a higher surface area to increase the number of active sites.
- A greener revolutionary fuel additive includes using biodiesels, which are beneficial for reducing pollutants and providing a solution to recycling certain waste products. The BTE and BSFC rise with increasing % blending of biodiesels, a consequential limitation of increased density and viscosity in biodiesels. These, on a whole reduce CO, HC, and soot, increasing the amount of NO_x and CO_2. The viscosity and density could be balanced out by employing hybrid biodiesel formulations, blending small percentages of alcohols or lower viscosity solvents with appropriate cetane numbers and calorific values.
- Another dilemma associated with potential solutions to biodiesel related issues involves nonstandard testing protocols followed by researchers. With the emergence of LTC engine operational modes, the effect of varied biodiesel compositions and blending modes along with

https://doi.org/10.1021/acs.energyfuels.4c00705
Energy Fuels XXXX, XXX, XXX−XXX

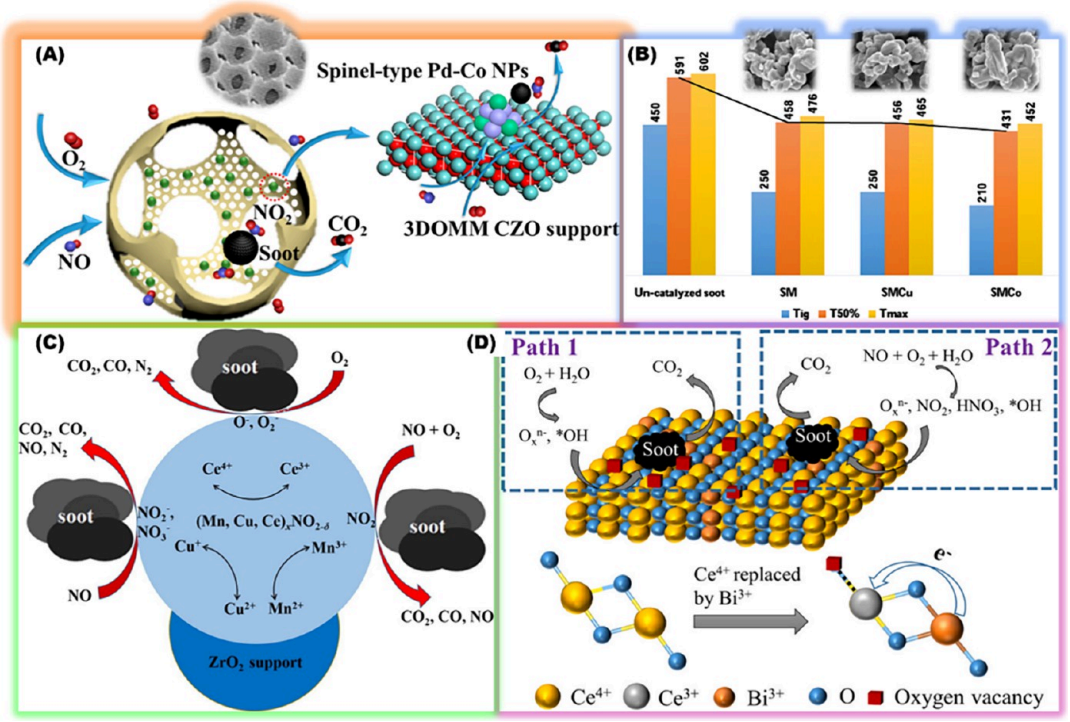

Figure 18. (A) Mechanistical illustration of 3DOMM Pd-Co bimetallic oxide catalysts for soot combustion. (B) The soot conversion temperatures of catalyzed and uncatalyzed soot of $SrMnO_3$(SM), $SrMn_{0.98}Cu_{0.02}O_3$(SMCu), and $SrMn_{0.98}Co_{0.02}O_3$(SMCo), with insets of the corresponding EDS analysis. (C) Probable mechanism for soot combustion over $MnCuCeZrO_{2-\delta}$ mixed oxides, (D) soot oxidation scheme over Bidoped CeO_2. (A) Adapted with permission from ref 268. Copyright (2018) with permission from American Chemical Society. (B) ref 281. Copyright (2020) with permission from Elsevier. (C) ref 273. Copyright (2018) with permission from Elsevier. (D) ref 282. Copyright (2021) with permission from Elsevier.

their resultant pollutant forming mechanistic pathways needs to be defined. Theoretical or computational model fitting studies prior to laboratory experiments have a wide scope in this area to facilitate the development and design of industrial scale prototypes.

- HCCI combustion of neat biodiesel has not been explored sufficiently due to its low volatility, which presents challenges in homogeneous mixture preparation. Thus, novel approaches must be explored to vaporize the neat biodiesel fuel with a reduced energy input. Another major shortcoming of biodiesel in HCCI operation is its high reactivity, which does not allow for the extension of the load range. Charge dilution using EGR helps in extending the load range but not remarkably. Also, mixture preparation is challenging for PFI-HCCI engines with low-volatile fuels like diesel and biodiesel, which need immediate attention.
- An optimal VVT and charge dilution combination can help achieve higher loads with biodiesel-fuelled HCCI engines. Monitoring and managing engine parameters in real-time using closed-loop control systems to gauge engine conditions and tune engine calibration settings could improve the performance of biodiesel-fuelled HCCI engines.
- Commercial DOCs practically depend on noble metals such as Pd and Pt, and the use of these in the present and future is impractical. Although various laboratory models exist for transition and rare earth metals, no commercial development has progressed for these. Current DOCs research is on the lines of current diesel engine setups but have insufficient insight into futuristic biodiesel-based hybrid engines. At the same time with hybrid fuels and engines, the nature of the pollutants may vary, and a catalyst that can take-up and convert such pollutants to benign products needs to be explored.
- Addition of metal ions displaying higher valence states such as W, Mo, Mn, etc. due to their size induces defects in solid solution catalysts, thus increasing oxygen vacancies and simultaneously increasing surface acidity. This feature could greatly benefit NH_3-SCR, as acid sites would readily adsorb NH_3 and oxygen vacancies could facilitate NO_x reduction. A simultaneous exchange of the picked-up oxygen species with the carbonaceous soot present in the exhaust gas could simultaneously accelerate soot oxidation, thus forming a codependent catalytic cycle eliminating two pollutants simultaneously.
- For direct NO_x conversions, catalysts with basic sites are favored. This is to allow direct adsorption of acidic NO_x species on the catalyst surface. Addition of rare earth metals, alkali, and alkaline earth metals is known to increase surface alkalinity, and considering the molecular size of NO, microporous compounds do not suffice, and mesoporous catalysts are preferred.
- Soot oxidation has shown better activity with mixed oxide catalysts and even spinels and perovskites. Lower dimension morphologies are preferred as they have a higher number of exposed surface-active sites. The oxidative catalysts used in HC and CO oxidation also usually have a narrow operating window, and to overcome this, there is a need to develop a catalyst that not only activates O_2 but can also activate NO_x, since it is an even better oxidizer. This would allow

https://doi.org/10.1021/acs.energyfuels.4c00705
Energy Fuels XXXX, XXX, XXX−XXX

simultaneous NO_x reduction along with HC, CO, and PM oxidation. Activation of NO_x would also enhance its reactivity with the SCR system present thereby allowing nearly zero emissions of this malignant pollutant. The perspective basically involves enhancing activities by performing assisted oxidations or reductions with NO_x or H_2 respectively.

- Present research into electrically driven pollutant mitigation is progressing. However, these systems need to be incorporated into existing and futuristic engines to understand their outcomes. These systems would require upgrading of existing after-treatment system setups rather than mere replacement by higher efficiency catalysts.
- The excellent redox properties of metal oxide catalysts are quite favorable for DOC, SCR, and DPF applications although each has a certain stumbling block which in some cases could be overcome by forming composites, spinels or other hybrid structures. In low temperature combustion systems, although the metal oxide catalysts would not gravely have to face the effects of sintering as the combustion occurs at relatively lower temperature ranges, the catalysts are still attacked by catalyst poisons such as sulfur, phosphorus, moisture, and other lubricant and fuel derived deactivating substances.
- With the emergence of hydrophobic materials, a coating or association of these on the catalyst substrate could protect the catalyst from moisture attack. Additionally, small-pore zeolites now emerge with their resilience to deactivation even after exposure to extreme hydrothermal conditions. PtFeMg, $AlLaZrTiO_2$, etc. have been proven to show great sulfur and moisture resistance along with these mixtures of metals complementing each other further providing thermal stability to the catalyst support. NO_x conversion can be achieved via varied routes, and since the LTC mode primarily ensures a reduction in NO_x conversions, an active catalyst can completely eliminate its release into the atmosphere from automobiles.
- In order to enhance the productivity of catalysts in the sustainable direction, it is essential to further replace the existing noble catalysts with non-noble metals which itself act as highly active catalysts. In the case of HC and CO treatment, noble metals combined with transition elements on zeolite supports show activity favorable in LTC temperature ranges. The catalyst necessarily should have structural stability as well as the ability to undergo cyclic regeneration of its active sites under hydrothermal exhaust gas conditions.
- Another essential requirement in these catalysts is the turnover number or the number of catalytic cycles the catalyst can endure before it is rendered ineffectual. The combined use of essentially the DOC and DPF combined with the HCCI fuelled biodiesel engine in the discussed mitigation systems have tremendous advantages such as greater conversion levels, optimized management of catalyst supporters etc., and improved fuel-saving and management with better combustion, and in the long run can also prove to be cost-effective.

6. CONCLUSION

Existent automobile pollution mitigation strategies do not meet the stringent pollution control norms laid down by government bodies. In order to satisfy the needs of the present and future, hybrid modernist catalytic systems and engines need to be evaluated for practical large-scale commercial implementation. In this review, clean combustion via fuel and engine modifications has been discussed. Evaluating fuel borne catalysts and biodiesels concluded a decrease in pollutant emissions; however, while certain engine properties seemed to improve under set conditions, these alterations of the fuel have been tested either in laboratory scale models or engine conditions preferential to the research team. These results thus have contradictory conclusions when compared and lack a basis for commercialization. Primarily a lot of ambiguities are noticed with respect to NO_x emissions, where some studies showed an increasing trend, while others showed a downward one. Addition of FBCs preferentially modify the BTE, BSFC, cetane number, and calorific values of fuel under combustion. These properties undergo alterations when biodiesels are used and, to some extent, can be balanced out by the use of FBCs, while HCCI combustion control is primarily influenced by fuel molecular composition and associated chemical kinetics. Ultralow NO_x and soot emissions can be achieved in HCCI combustion without a significant penalty on the thermal efficiency compared to conventional diesel combustion. The significant limitations associated with HCCI engines include no direct control over the combustion phasing, a narrow load range of operation, high HC and CO emissions, and difficulty in homogeneous mixture preparation. Lowering the compression ratio of a diesel engine delays the start of combustion and reduces the peak pressure rise rate, which helps extend the load range. By preventing the cylinder charge from igniting too early, the EGR can effectively delay the onset of combustion, leading to better thermal efficiency windows. Controlled intake charge temperature, in combination with compression ratio modifications and charge dilution, can help attain delayed autoignition and smooth combustion, thereby extending the load range. Further to achieve near zero emissions, catalytic after-treatment strategies such as DOC, NH_3, CO, and H_2-SCR, direct NO_x conversions, LNTs and DPFs were discussed. A HCCI-biodiesel blended diesel system as discussed largely reduces soot and NO_x and their emission control requires a combination preferably of a DOC (Pt/Pd with Ce or Cu) and DPF (3DOMM with metal oxides having high OSR) to take care of the populating CO and HC produced during biodiesel combustion.

AUTHOR INFORMATION

Corresponding Authors

Pranay P. Morajkar − *School of Chemical Sciences, Goa University, Taleigao Plateau 403206 Goa, India;* orcid.org/0000-0002-2602-6183; Email: pranay@unigoa.ac.in

Anand Krishnasamy − *Internal Combustion Engines Laboratory, Department of Mechanical Engineering, Indian Institute of Technology Madras, Chennai 600036 Tamil Nadu, India;* orcid.org/0000-0001-7848-6213; Email: anand_k@iitm.ac.in

Authors

Samantha Da Costa − *School of Chemical Sciences, Goa University, Taleigao Plateau 403206 Goa, India*

https://doi.org/10.1021/acs.energyfuels.4c00705
Energy Fuels XXXX, XXX, XXX−XXX

Kiran Raj Bukkarapu − *Internal Combustion Engines Laboratory, Department of Mechanical Engineering, Indian Institute of Technology Madras, Chennai 600036 Tamil Nadu, India*

Ravi Fernandes − *Department 3.3, Department of Physical Chemistry, Physikalisch-Technische Bundesanstalt, 38116 Braunschweig, Germany*

Complete contact information is available at: https://pubs.acs.org/10.1021/acs.energyfuels.4c00705

Notes

The authors declare no competing financial interest.

Biographies

Ms. Samantha Da Costa has received a Bachelor of Science degree with a Chemistry major in 2018 and a Master of Science degree in Physical Chemistry in 2020 from Goa University, Goa, India. She is presently enrolled as a research scholar and is pursuing her Ph.D. degree under the guidance of Dr. Pranay P. Morajkar at the School of Chemical Sciences, Goa University. Her research focuses on designing clean combustion technologies.

Mr. Kiran Raj Bukkarapu completed his Masters in Thermal Engineering in the Department of Mechanical Engineering, Indian Institute of Technology Madras. He served as an Assistant Professor at Vignan University, India. He is pursuing a Ph.D. at the Indian Institute of Technology Madras on optimizing biodiesel composition using machine learning tools to improve fuel properties and engine characteristics in advanced combustion mode to achieve high efficiency and clean combustion.

Dr. Ravi Fernandes is a professor at the Institute of Internal Combustion Engines of the Technical University of Brunswick and head of Department, Physical Chemistry at the National Metrology Institute PTB-Germany. He obtained his Ph.D. at the Karlsruhe Institute of Technology, Germany. He was a researcher at Max-Planck Institute, Germany, Sandia National Laboratories, U.S.A., and Assistant Professor at RWTH Aachen University in Germany. His research expertise includes reaction kinetics, renewable energy carriers, and advanced combustion.

Dr. Anand Krishnasamy is a professor at the Department of Mechanical Engineering, Indian Institute of Technology Madras, India. He has been working there for the past ten years. Before that, he completed postdoctoral research at the Engine Research Centre, University of Wisconsin-Madison, USA. His research interests are in developing high-efficiency and clean-combustion diesel engines. He has published his research work in 84 International Journals, 61 Conference Proceedings, and 8 Patents.

Dr. Pranay P. Morajkar is a Sr. Assistant Professor at the School of Chemical Sciences, Goa University. He received his Ph.D. from the University of Lille in collaboration with University of Bordeaux (France, 2012). He served as a CNRS postdoctoral researcher at the LRGP-ENSIC-University of Lorraine, (France) and as a Research Scientist at the Khalifa University of Science and Technology, (U.A.E). His research focuses on designing nanostructured materials for clean energy and environmental applications.

■ ACKNOWLEDGMENTS

The authors thank DST India for financial support via DST/INNO-INDIGO (DST/IMRCD/INNO-INDIGO/BIOCFD/2017(G)). The authors also acknowledge UGC, New Delhi, at the level of DSA-I under the Special Assistance Program (SAP) (F. No. 540/14/DSA-I/2015/(SAP-I)). Additionally, the authors recognize DST & WM, Government of Goa and DST-FIST-II for financial assistance. S.D.C. would like to acknowledge Goa University for providing financial aid through a Research Studentship (2022-23) and the Goa State Research Foundation (GSRF) through a doctoral fellowship (2024).

■ DEDICATION

Pranay Morajkar would like to dedicate this paper to Prof. J. S. Budkuley on the occasion of his 76th Birthday celebration.

■ REFERENCES

(1) Jin, H.; Ishida, M. A Novel Gas Turbine Cycle with Hydrogen-Fueled Chemical-Looping Combustion. *Int. J. Hydrogen Energy* **2000**, *25* (12), 1209−1215.

(2) Zhang, Z.; Wang, S.; Pan, M.; Lv, J.; Lu, K.; Ye, Y.; Tan, D. Utilization of Hydrogen-Diesel Blends for the Improvements of a Dual-Fuel Engine Based on the Improved Taguchi Methodology. *Energy* **2024**, *292*, 130474.

(3) Zhang, Z.; Liu, H.; Li, Y.; Ye, Y.; Tian, J.; Li, J.; Xu, Y.; Lv, J. Research and Optimization of Hydrogen Addition and EGR on the Combustion, Performance, and Emission of the Biodiesel-Hydrogen Dual-Fuel Engine with Different Loads Based on the RSM. *Heliyon* **2024**, *10* (1), No. e23389.

(4) Steiner, S.; Bisig, C.; Petri-Fink, A.; Rothen-Rutishauser, B. Diesel Exhaust: Current Knowledge of Adverse Effects and Underlying Cellular Mechanisms. *Arch. Toxicol.* **2016**, *90*, 1541−1553.

(5) de Melo, J. O.; Soto, S. F.; Katayama, I. A.; Wenceslau, C. F.; Pires, A. G.; Veras, M. M.; Furukawa, L. N. S.; de Castro, I.; Saldiva, P. H. N.; Heimann, J. C. Inhalation of Fine Particulate Matter during Pregnancy Increased IL-4 Cytokine Levels in the Fetal Portion of the Placenta. *Toxicol. Lett.* **2015**, *232* (2), 475−480.

(6) Watanabe, N. Decreased Number of Sperms and Sertoli Cells in Mature Rats Exposed to Diesel Exhaust as Fetuses. *Toxicol. Lett.* **2005**, *155* (1), 51−58.

(7) Bendtsen, K. M.; Gren, L.; Malmborg, V. B.; Shukla, P. C.; Tuner, M.; Essig, Y. J.; Krais, A. M.; Clausen, P. A.; Berthing, T.; Loeschner, K.; Jacobsen, N. R.; Wolff, H.; Pagels, J.; Vogel, U. B. Particle Characterization and Toxicity in C57BL/6 Mice Following Instillation of Five Different Diesel Exhaust Particles Designed to Differ in Physicochemical Properties. *Part. Fibre Toxicol.* **2020**, *17*, 38.

(8) Panigrahi, T. H.; Sahoo, S. R.; Murmu, G.; Maity, D.; Saha, S. Current Challenges and Developments of Inorganic/Organic Materials for the Abatement of Toxic Nitrogen Oxides (NOx)-A Critical Review. *Prog. Solid State Chem.* **2022**, *68*, 100380.

(9) Xue, W.; Warshawsky, D. Metabolic Activation of Polycyclic and Heterocyclic Aromatic Hydrocarbons and DNA Damage: A Review. *Toxicol. Appl. Pharmacol.* **2005**, *206* (1), 73−93.

(10) Martins, J.; Brito, F. P. Alternative Fuels for Internal Combustion Engines. *Energies* **2020**, *13* (16), 4086.

(11) Leach, F.; Kalghatgi, G.; Stone, R.; Miles, P. The Scope for Improving the Efficiency and Environmental Impact of Internal Combustion Engines. *Transp. Eng.* **2020**, *1*, 100005.

(12) Krishnasamy, A.; Bukkarapu, K. R. A Comprehensive Review of Biodiesel Property Prediction Models for Combustion Modeling Studies. *Fuel* **2021**, *302* (May), 121085.

(13) A Alotaibi, M.; Naeem, A.; Wali Khan, I.; Farooq, M.; Ud Din, I.; Saharun, M. S. Optimization and Cost Analysis Evaluation Studies of the Biodiesel Production from Waste Cooking Oil Using Na-Si/Ce-500 Heterogeneous Catalyst. *Biomass and Bioenergy* **2024**, *182*, 107078.

(14) Bukkarapu, K. R.; Krishnasamy, A. A Critical Review on Available Models to Predict Engine Fuel Properties of Biodiesel. *Renew. Sustain. Energy Rev.* **2022**, *155*, 111925.

(15) Nguyen, V. G.; Sharma, P.; Dzida, M.; Bui, V. H.; Le, H. S.; El-Shafay, A. S.; Le, H. C.; Le, D. T. N.; Tran, V. D. A Review on Metal-Organic Framework as a Promising Catalyst for Biodiesel Production. *Energy Fuels* **2024**, *38* (4), 2654−2689.

(16) Krishnasamy, A.; Gupta, S. K.; Reitz, R. D. Prospective Fuels for Diesel Low Temperature Combustion Engine Applications: A Critical Review. *Int. J. Engine Res.* **2021**, *22* (7), 2071−2106.
(17) Verma, S. K.; Gaur, S.; Akram, T.; Gautam, S.; Kumar, A. Emissions from Homogeneous Charge Compression Ignition (HCCI) Engine Using Different Fuels: A Review. *Environ. Sci. Pollut. Res.* **2022**, *29* (34), 50960−50969.
(18) Bindra, M.; Vashist, D. Particulate Matter and NOx Reduction Techniques for Internal Combustion Engine: A Review. *J. Inst. Eng. Ser. C* **2020**, *101* (6), 1073−1082.
(19) Garcia, A.; Gil, A.; Monsalve-Serrano, J.; Sari, R. L. OMEx-Diesel Blends as High Reactivity Fuel for Ultra-Low NOx and Soot Emissions in the Dual-Mode Dual-Fuel Combustion Strategy. *Fuel* **2020**, *275*, 117898.
(20) Reusser, C. A.; Hernández, R. H.; Lie, T. T. Hybrid Vehicle CO_2 Emissions Reduction Strategy Based on Model Predictive Control. *Electronics* **2023**, *12* (6), 1474.
(21) Sher, F.; Chen, S.; Raza, A.; Rasheed, T.; Razmkhah, O.; Rashid, T.; Rafi-ul-Shan, P. M.; Erten, B. Novel Strategies to Reduce Engine Emissions and Improve Energy Efficiency in Hybrid Vehicles. *Clean. Eng. Technol.* **2021**, *2* (March), 100074.
(22) Beccari, S. On the Use of a Hydrogen-Fueled Engine in a Hybrid Electric Vehicle. *Appl. Sci.* **2022**, *12* (24), 12749.
(23) Simsek, S.; Uslu, S. Comparative Evaluation of the Influence of Waste Vegetable Oil and Waste Animal Oil-Based Biodiesel on Diesel Engine Performance and Emissions. *Fuel* **2020**, *280*, 118613.
(24) Devarajan, Y.; Jayabal, R. K.; Ragupathy, D.; Venu, H. Emissions Analysis on Second Generation Biodiesel. *Front. Environ. Sci. Eng.* **2017**, *11*, 3.
(25) Muraza, O. Highlighting the Greener Shift in Transportation Energy and Fuels Based on Novel Catalytic Materials. *Energy Fuels* **2021**, *35* (1), 25−44.
(26) Zhu, M.; Ma, Y.; Zhang, D. Effect of a Homogeneous Combustion Catalyst on the Combustion Characteristics and Fuel Efficiency in a Diesel Engine. *Appl. Energy* **2012**, *91* (1), 166−172.
(27) Stepień, Z.; Ziemiański, L.; Żak, G.; Wojtasik, M.; Jeczmionek, Ł.; Burnus, Z. The Evaluation of Fuel Borne Catalyst (FBC's) for DPF Regeneration. *Fuel* **2015**, *161*, 278−286.
(28) Munuswamy, D. B.; Devarajan, Y.; Ramalingam, S.; Subramani, S.; Munuswamy, N. B. Critical Review on Effects of Alcohols and Nanoadditives on Performance and Emission in Low-Temperature Combustion Engines: Advances and Perspectives. *Energy Fuels* **2022**, *36* (14), 7245−7268.
(29) Nash, D. G.; Swanson, N. B.; Preston, W. T.; Yelverton, T. L. B.; Roberts, W. L.; Wendt, J. O. L.; Linak, W. P. Environmental Implications of Iron Fuel Borne Catalysts and Their Effects on Diesel Particulate Formation Andcomposition. *J. Aerosol Sci.* **2013**, *58*, 50−61.
(30) Miller, A.; Ahlstrand, G.; Kittelson, D.; Zachariah, M. The Fate of Metal (Fe) during Diesel Combustion: Morphology, Chemistry, and Formation Pathways of Nanoparticles. *Combust. Flame* **2007**, *149* (1−2), 129−143.
(31) Zhang, Z.-H.; Balasubramanian, R. Effects of Cerium Oxide and Ferrocene Nanoparticles Addition as Fuel-Borne Catalysts on Diesel Engine Particulate Emissions: Environmental and Health Implications. *Environ. Sci. Technol.* **2017**, *51* (8), 4248−4258.
(32) Liu, J.; Wang, L.; Sun, P.; Wang, P.; Li, Y.; Ma, H.; Wu, P.; Liu, Z. Effects of Iron-Based Fuel Borne Catalyst Addition on Microstructure, Element Composition and Oxidation Activity of Diesel Exhaust Particles. *Fuel* **2020**, *270*, 117597.
(33) Fennell, P. S.; Hayhurst, A. N. The Kinetics of the Reduction of NO to N_2 by Reaction with Particles of Fe. *Proc. Combust. Inst.* **2002**, *29* (2), 2179−2185.
(34) Zhang, Z.-H.; Balasubramanian, R. Influence of an Iron-Based Fuel-Borne Catalyst on Physicochemical and Toxicological Characteristics of Particulate Emissions from a Diesel Engine. *Appl. Energy* **2015**, *146*, 270−278.
(35) Liu, J.; Wu, P.; Sun, P.; Ji, Q.; Zhang, Q.; Wang, P. Effects of Iron-Based Fuel Borne Catalyst Addition on Combustion, in-Cylinder Soot Distribution and Exhaust Emission Characteristics in a Common-Rail Diesel Engine. *Fuel* **2021**, *290*, 120096.
(36) Krishna, K.; Makkee, M. Pt-Ce-Soot Generated from Fuel-Borne Catalysts: Soot Oxidation Mechanism. *Top. Catal.* **2007**, *42*, 229−236.
(37) Okuda, T.; Schauer, J. J.; Olson, M. R.; Shafer, M. M.; Rutter, A. P.; Walz, K. A.; Morschauser, P. A. Effects of a Platinum- Cerium Bimetallic Fuel Additive on the Chemical Composition of Diesel Engine Exhaust Particles. *Energy Fuels* **2009**, *23* (10), 4974−4980.
(38) Shukla, M. K.; Tripathi, G.; Farooqui, S. A.; Sinha, A. K.; Dhar, A. Effect of Au/CeO2 as Fuel Borne Catalysts on Performance, Combustion and Emissions Characteristics of CI Engine. *Clean. Eng. Technol.* **2021**, *5*, 100335.
(39) Bazooyar, B.; Hosseini, S. Y.; Begloo, S. M. G.; Shariati, A.; Hashemabadi, S. H.; Shaahmadi, F. Mixed Modified Fe2O3-WO3 as New Fuel Borne Catalyst (FBC) for Biodiesel Fuel. *Energy* **2018**, *149*, 438−453.
(40) Zhao, H.; Ge, Y.; Zhang, T.; Zhang, J.; Tan, J.; Zhang, H. Unregulated Emissions from Diesel Engine with Particulate Filter Using Fe-Based Fuel Borne Catalyst. *J. Environ. Sci.* **2014**, *26* (10), 2027−2033.
(41) Hassan, T.; Rahman, M. M. A.; Rabbi, M. S.; Rahman, M. M. A.; Meraz, R. M. Recent Advancement in the Application of Metal Based Nanoadditive in Diesel/Biodiesel Fueled Compression Ignition Engine: A Comprehensive Review on Nanofluid Preparation and Stability, Fuel Property, Combustion, Performance, and Emission Characteristics. *Environ. Prog. Sustain. Energy* **2023**, *42* (2), No. e13976.
(42) Celik, M.; Yucesu, H. S.; Guru, M. Investigation of the Effects of Organic Based Manganese Addition to Biodiesel on Combustion and Exhaust Emissions. *Fuel Process. Technol.* **2016**, *152*, 83−92.
(43) Rajesh Kana, S.; Shaija, A. Performance, Combustion and Emission Characteristics of a Diesel Engine Using Waste Avocado Biodiesel with Manganese-Doped Alumina Nanoparticles. *Int. J. Ambient Energy* **2022**, *43* (1), 1437−1444.
(44) Hassan, T.; Rahman, M. M.; Adib, A. R.; Meraz, R. M.; Rahman, M. A.; Tushar, M. S. H. K. Effect of Ni and Al Nanoadditives on the Performance and Emission Characteristics of a Diesel Engine Fueled with Diesel-Castor Oil Biodiesel-n-Butanol Blends. *Case Stud. Chem. Environ. Eng.* **2023**, *8*, 100531.
(45) Steiner, S.; Czerwinski, J.; Comte, P.; Heeb, N. V.; Mayer, A.; Petri-Fink, A.; Rothen-Rutishauser, B. Effects of an Iron-Based Fuel-Borne Catalyst and a Diesel Particle Filter on Exhaust Toxicity in Lung Cells in Vitro. *Anal. Bioanal. Chem.* **2015**, *407*, 5977−5986.
(46) Stančin, H.; Mikulčić, H.; Wang, X.; Duić, N. A Review on Alternative Fuels in Future Energy System. *Renew. Sustain. energy Rev.* **2020**, *128*, 109927.
(47) Lapuerta, M.; Hernández, J. J.; Rodríguez-Fernández, J.; Calle-Asensio, A. Vehicle Emissions from a Glycerol-Derived Biofuel under Cold and Warm Conditions. *Energy Fuels* **2020**, *34* (5), 6020−6029.
(48) Khujamberdiev, R.; Cho, H. M.; Mahmud, M. I. Experimental Investigation of Single-Cylinder Engine Performance Using Biodiesel Made from Waste Swine Oil. *Energies* **2023**, *16* (23), 7891.
(49) Zheng, F.; Cho, H. Combustion and Emission of Castor Biofuel Blends in a Single-Cylinder Diesel Engine. *Energies* **2023**, *16* (14), 5427.
(50) Ayetor, G. K.; Sunnu, A.; Parbey, J. Effect of Biodiesel Production Parameters on Viscosity and Yield of Methyl Esters: Jatropha Curcas, Elaeis Guineensis and Cocos Nucifera. *Alexandria Eng. J.* **2015**, *54* (4), 1285−1290.
(51) Zhang, Y.; Cao, G.; Yang, X. Advances in De-NO x Methods and Catalysts for Direct Catalytic Decomposition of NO: A Review. *Energy Fuels* **2021**, *35* (8), 6443−6464.
(52) Zheng, F.; Cho, H. M. The Effect of Different Mixing Proportions and Different Operating Conditions of Biodiesel Blended Fuel on Emissions and Performance of Compression Ignition Engines. *Energies* **2024**, *17* (2), 344.

https://doi.org/10.1021/acs.energyfuels.4c00705
Energy Fuels XXXX, XXX, XXX−XXX

(53) Zheng, F.; Cho, H. M. Investigation of the Impact of Castor Biofuel on the Performance and Emissions of Diesel Engines. *Energies* **2023**, *16* (22), 7665.
(54) Bukkarapu, K. R.; Krishnasamy, A. Fourier-Transform-Infrared-Spectroscopy-Based Approach to Predict Engine Fuel Properties of Biodiesel. *Energy Fuels* **2021**, *35* (9), 7993−8005.
(55) Kumbhar, V.; Pandey, A.; Sonawane, C. R.; El-Shafay, A. S.; Panchal, H.; Chamkha, A. J. Statistical Analysis on Prediction of Biodiesel Properties from Its Fatty Acid Composition. *Case Stud. Therm. Eng.* **2022**, *30*, 101775.
(56) Gaur, A.; Dwivedi, G.; Baredar, P.; Jain, S. Influence of Blending Additives in Biodiesel on Physiochemical Properties, Engine Performance, and Emission Characteristics. *Fuel* **2022**, *321*, 124072.
(57) Khujamberdiev, R.; Cho, H. Impact of Biodiesel Blending on Emission Characteristics of One-Cylinder Engine Using Waste Swine Oil. *Energies* **2023**, *16* (14), 5489.
(58) Wu, G.; Wang, X.; Abubakar, S.; Li, Y.; Liu, Z. A Realistic Skeletal Mechanism for the Oxidation of Biodiesel Surrogate Composed of Long Carbon Chain and Polyunsaturated Compounds. *Fuel* **2021**, *289*, 119934.
(59) Abboud, J.; Schobing, J.; Legros, G.; Matynia, A.; Bonnety, J.; Tschamber, V.; Brillard, A.; Leyssens, G.; Da Costa, P. Impacts of Ester's Carbon Chain Length and Concentration on Sooting Propensities and Soot Oxidative Reactivity: Application to Diesel and Biodiesel Surrogates. *Fuel* **2018**, *222*, 586−598.
(60) Yu, J.; Ju, Y.; Gou, X. Surrogate Fuel Formulation for Oxygenated and Hydrocarbon Fuels by Using the Molecular Structures and Functional Groups. *Fuel* **2016**, *166*, 211−218.
(61) Hotard, C.; Tekawade, A.; Oehlschlaeger, M. A. Constant Volume Spray Ignition of C9-C10 Biodiesel Surrogates: Methyl Decanoate, Ethyl Nonanoate, and Methyl Decenoates. *Fuel* **2018**, *224*, 219−225.
(62) Le, X. T.; Mai, T. V. T.; Ratkiewicz, A.; Huynh, L. K. Mechanism and Kinetics of Low-Temperature Oxidation of a Biodiesel Surrogate: Methyl Propanoate Radicals with Oxygen Molecule. *J. Phys. Chem. A* **2015**, *119* (16), 3689−3703.
(63) Jiang, B.; Liu, D.; Lin, Z. Soot Particles Diagnostics in Ethylene Inverse Diffusion Flame Blending with Biodiesel Surrogates of Saturated Methyl Butyrate and Unsaturated Methyl Crotonate. *Fuel Process. Technol.* **2020**, *202*, 106379.
(64) Bai, Y.; Wang, Y.; Wang, X. Development of a Skeletal Mechanism for Four-Component Biodiesel Surrogate Fuel with PAH. *Renew. Energy* **2021**, *171*, 266−274.
(65) Wang, W.; Gowdagiri, S.; Oehlschlaeger, M. A. Comparative Study of the Autoignition of Methyl Decenoates, Unsaturated Biodiesel Fuel Surrogates. *Energy Fuels* **2013**, *27* (9), 5527−5532.
(66) Liu, S.; Wu, X.; Weng, D.; Ran, R. NOX-Assisted Soot Oxidation on Pt-Mg/Al_2O_3 Catalysts: Magnesium Precursor, Pt Particle Size, and Pt-Mg Interaction. *Ind. Eng. Chem. Res.* **2012**, *51* (5), 2271−2279.
(67) Das, D. D.; McEnally, C. S.; Pfefferle, L. D. Sooting Tendencies of Unsaturated Esters in Nonpremixed Flames. *Combust. Flame* **2015**, *162* (4), 1489−1497.
(68) Lai, J. Y. W.; Lin, K. C.; Violi, A. Biodiesel Combustion: Advances in Chemical Kinetic Modeling. *Prog. Energy Combust. Sci.* **2011**, *37* (1), 1−14.
(69) Lin, K. C.; Dahiya, A.; Tao, H.; Kao, F.-H. Combustion Mechanism and CFD Investigation of Methyl Isobutanoate as a Component of Biodiesel Surrogate. *Energy* **2022**, *249*, 123589.
(70) Wang, Z.; Li, L.; Wang, J.; Reitz, R. D. Effect of Biodiesel Saturation on Soot Formation in Diesel Engines. *Fuel* **2016**, *175*, 240−248.
(71) Da Costa, S.; Salkar, A.; Krishnasamy, A.; Fernandes, R.; Morajkar, P. Investigating the Oxidative Reactivity and Nano-structural Characteristics of Diffusion Flame Generated Soot Using Methyl Crotonate and Methyl Butyrate Blended Diesel Fuels. *Fuel* **2022**, *309*, 122141.
(72) Morajkar, P. P.; Abdrabou, M. K.; Salkar, A. V.; Raj, A.; Elkadi, M.; Anjum, D. H. Nanostructural Disorder and Reactivity Comparison of Flame Soot and Engine Soot Using Diesel and Jatropha Biodiesel/Diesel Blend as Fuels. *Energy Fuels* **2020**, *34* (10), 12960−12971.
(73) Zhang, Y.; Zhong, Y.; Lu, S.; Zhang, Z.; Tan, D. A Comprehensive Review of the Properties, Performance, Combustion, and Emissions of the Diesel Engine Fueled with Different Generations of Biodiesel. *Processes* **2022**, *10* (6), 1178.
(74) Liu, J.; Huang, Q.; Ulishney, C.; Dumitrescu, C. E. Machine Learning Assisted Prediction of Exhaust Gas Temperature of a Heavy-Duty Natural Gas Spark Ignition Engine. *Appl. Energy* **2021**, *300*, 117413.
(75) Rahman, M. A.; Aziz, M. A. Biodiesel from Water Hyacinth Biomass and Its Influence on CI Engine Performance, Emission, Combustion and Heat Loss Characteristics with the Induction of Hydroxy. *Energy* **2021**, *224*, 120151.
(76) Rajak, U.; Nashine, P.; Verma, T. N. Effect of Spirulina Microalgae Biodiesel Enriched with Diesel Fuel on Performance and Emission Characteristics of CI Engine. *Fuel* **2020**, *268*, 117305.
(77) Emiroğlu, A. O.; Keskin, A.; Sen, M. Experimental Investigation of the Effects of Turkey Rendering Fat Biodiesel on Combustion, Performance and Exhaust Emissions of a Diesel Engine. *Fuel* **2018**, *216*, 266−273.
(78) Dhamodaran, G.; Krishnan, R.; Pochareddy, Y. K.; Pyarelal, H. M.; Sivasubramanian, H.; Ganeshram, A. K. A Comparative Study of Combustion, Emission, and Performance Characteristics of Rice-Bran-, Neem-, and Cottonseed-Oil Biodiesels with Varying Degree of Unsaturation. *Fuel* **2017**, *187*, 296−305.
(79) Resitoglu, I. A. The Effect of Biodiesel on Activity of Diesel Oxidation Catalyst and Selective Catalytic Reduction Catalysts in Diesel Engine. *Renew. Sustain. Energy Rev.* **2021**, *148*, 111286.
(80) Jamshaid, M.; Masjuki, H. H.; Kalam, M. A.; Zulkifli, N. W. M.; Arslan, A.; Qureshi, A. A. Experimental Investigation of Performance, Emissions and Tribological Characteristics of B20 Blend from Cottonseed and Palm Oil Biodiesels. *Energy* **2022**, *239*, 121894.
(81) Ellappan, S.; Rajendran, S. A Comparative Review of Performance and Emission Characteristics of Diesel Engine Using Eucalyptus-Biodiesel Blend. *Fuel* **2021**, *284*, 118925.
(82) Shrivastava, P.; Verma, T. N. Effect of Fuel Injection Pressure on the Characteristics of CI Engine Fuelled with Biodiesel from Roselle Oil. *Fuel* **2020**, *265*, 117005.
(83) Valente, O. S.; Pasa, V. M. D.; Belchior, C. R. P.; Sodré, J. R. Exhaust Emissions from a Diesel Power Generator Fuelled by Waste Cooking Oil Biodiesel. *Sci. Total Environ.* **2012**, *431*, 57−61.
(84) Hoang, A. T. Experimental Study on Spray and Emission Characteristics of a Diesel Engine Fueled with Preheated Bio-Oils and Diesel Fuel. *Energy* **2019**, *171*, 795−808.
(85) Krishania, N.; Rajak, U.; Chaurasiya, P. K.; Singh, T. S.; Birru, A. K.; Verma, T. N. Investigations of Spirulina, Waste Cooking and Animal Fats Blended Biodiesel Fuel on Auto-Ignition Diesel Engine Performance, Emission Characteristics. *Fuel* **2020**, *276*, 118123.
(86) Ogunkunle, O.; Ahmed, N. A. Exhaust Emissions and Engine Performance Analysis of a Marine Diesel Engine Fuelledwith Parinari Polyandra Biodiesel-Diesel Blends. *Energy Reports* **2020**, *6*, 2999−3007.
(87) Nguyen, T.; Pham, M.; Le Anh, T. Spray, Combustion, Performance and Emission Characteristics of a Common Rail Diesel Engine Fueled by Fish-Oil Biodiesel Blends. *Fuel* **2020**, *269*, 117108.
(88) Simsek, S. Effects of Biodiesel Obtained from Canola, Sefflower Oils and Waste Oils on the Engine Performance and Exhaust Emissions. *Fuel* **2020**, *265*, 117026.
(89) Rajesh, K.; Natarajan, M. P.; Devan, P. K.; Ponnuvel, S. Coconut Fatty Acid Distillate as Novel Feedstock for Biodiesel Production and Its Characterization as a Fuel for Diesel Engine. *Renew. Energy* **2021**, *164*, 1424−1435.
(90) Mirhashemi, F. S.; Sadrnia, H. NOX Emissions of Compression Ignition Engines Fueled with Various Biodiesel Blends: A Review. *J. Energy Inst.* **2020**, *93* (1), 129−151.
(91) Jonson, J. E.; Borken-Kleefeld, J.; Simpson, D.; Nyíri, A.; Posch, M.; Heyes, C. Impact of Excess NOx Emissions from Diesel Cars on

https://doi.org/10.1021/acs.energyfuels.4c00705
Energy Fuels XXXX, XXX, XXX−XXX

Air Quality, Public Health and Eutrophication in Europe. *Environ. Res. Lett.* **2017**, *12* (9), 094017.
(92) Sun, J.; Caton, J. A.; Jacobs, T. J. Oxides of Nitrogen Emissions from Biodiesel-Fuelled Diesel Engines. *Prog. Energy Combust. Sci.* **2010**, *36* (6), 677−695.
(93) Sayyed, S.; Das, R. K.; Kulkarni, K. Experimental Investigation for Evaluating the Performance and Emission Characteristics of DICI Engine Fueled with Dual Biodiesel-Diesel Blends of Jatropha, Karanja, Mahua, and Neem. *Energy* **2022**, *238*, 121787.
(94) Rajendran, S. Effect of Antioxidant Additives on Oxides of Nitrogen (NOx) Emission Reduction from Annona Biodiesel Operated Diesel Engine. *Renew. energy* **2020**, *148*, 1321−1326.
(95) Baweja, S.; Trehan, A.; Kumar, R. Combustion, Performance, and Emission Analysis of a CI Engine Fueled with Mustard Oil Biodiesel Blended in Diesel Fuel. *Fuel* **2021**, *292*, 120346.
(96) Sathiyamoorthi, R.; Sankaranarayanan, G. Experimental Investigation of Performance, Combustion and Emission Characteristics of Neat Lemongrass Oil in DI Diesel Engine. *Int. J. Curr. Eng. Technol.* **2014**, *3*, 25.
(97) How, H. G.; Masjuki, H. H.; Kalam, M. A.; Teoh, Y. H. An Investigation of the Engine Performance, Emissions and Combustion Characteristics of Coconut Biodiesel in a High-Pressure Common-Rail Diesel Engine. *Energy* **2014**, *69*, 749−759.
(98) Mourad, M.; Mahmoud, K. R. M.; NourEldeen, E.-S. H. Improving Diesel Engine Performance and Emissions Characteristics Fuelled with Biodiesel. *Fuel* **2021**, *302*, 121097.
(99) Mubarak, M.; Shaija, A.; Suchithra, T. V. Experimental Evaluation of Salvinia Molesta Oil Biodiesel/Diesel Blends Fuel on Combustion, Performance and Emission Analysis of Diesel Engine. *Fuel* **2021**, *287*, 119526.
(100) Tizvir, A.; Shojaeefard, M. H.; Zahedi, A.; Molaeimanesh, G. R. Performance and Emission Characteristics of Biodiesel Fuel from Dunaliella Tertiolecta Microalgae. *Renew. Energy* **2022**, *182*, 552−561.
(101) Mohamed, E. A.; Betiha, M. A.; Negm, N. A. Insight into the Recent Advances in Sustainable Biodiesel Production by Catalytic Conversion of Vegetable Oils: Current Trends, Challenges, and Prospects. *Energy Fuels* **2023**, *37* (4), 2631−2647.
(102) Ethiraj, J.; Wagh, D.; Manyar, H. Advances in Upgrading Biomass to Biofuels and Oxygenated Fuel Additives Using Metal Oxide Catalysts. *Energy Fuels* **2022**, *36* (3), 1189−1204.
(103) Tangy, A.; Pulidindi, I. N.; Dutta, A.; Borenstein, A. Strontium Oxide Nanoparticles for Biodiesel Production: Fundamental Insights and Recent Progress. *Energy Fuels* **2021**, *35* (1), 187−200.
(104) Riyadi, T. W. B.; Spraggon, M.; Herawan, S. G.; Idris, M.; Paristiawan, P. A.; Putra, N. R.; Silambarasan R, M.; Veza, I. Biodiesel for HCCI Engine: Prospects and Challenges of Sustainability Biodiesel for Energy Transition. *Results Eng.* **2023**, *17*, 100916.
(105) Dwivedi, G.; Jain, S.; Sharma, M. P. Impact Analysis of Biodiesel on Engine Performance—A Review. *Renew. Sustain. Energy Rev.* **2011**, *15* (9), 4633−4641.
(106) Fazal, M. A.; Haseeb, A.; Masjuki, H. H. Biodiesel Feasibility Study: An Evaluation of Material Compatibility; Performance; Emission and Engine Durability. *Renew. Sustain. energy Rev.* **2011**, *15* (2), 1314−1324.
(107) Kokabi, H.; Najafi, M.; Jazayeri, S. A.; Jahanian, O. Performance Optimization of RCCI Engines Running on Landfill Gas, Propane and Hydrogen through the Deep Neural Network and Genetic Algorithm. *Sustain. Energy Technol. Assessments* **2023**, *56*, 103045.
(108) Agarwal, A. K.; Singh, A. P.; Garcia, A.; Monsalve-Serrano, J. Challenges and Opportunities for Application of Reactivity-Controlled Compression Ignition Combustion in Commercially Viable Transport Engines. *Prog. Energy Combust. Sci.* **2022**, *93*, 101028.
(109) Dahham, R. Y.; Wei, H.; Pan, J. Improving Thermal Efficiency of Internal Combustion Engines: Recent Progress and Remaining Challenges. *Energies* **2022**, *15* (17), 6222.
(110) Ashwin, J.; Ashok, B.; Vignesh, R.; Sarvanan, B.; Avinash, A. Chapter 3 - NOx and PM Trade-off in IC Engines. *NOx Emission Control Technologies in Stationary and Automotive Internal Combustion Engines: Approaches Toward NOx Free Automob.*; Elsevier, 2022; pp 69−93.
(111) Pachiannan, T.; Zhong, W.; Rajkumar, S.; He, Z.; Leng, X.; Wang, Q. A Literature Review of Fuel Effects on Performance and Emission Characteristics of Low-Temperature Combustion Strategies. *Appl. Energy* **2019**, *251*, 113380.
(112) Narayanan, A. M.; Jacobs, T. J. Observed Differences in Low-Temperature Heat Release and Their Possible Effect on Efficiency between Petroleum Diesel and Soybean Biodiesel Operating in Low-Temperature Combustion Mode. *Energy Fuels* **2015**, *29* (7), 4510−4521.
(113) Chaurasiya, R.; Krishnasamy, A. A Single Fuel Port and Direct Injected Low Temperature Combustion Strategy to Reduce Regulated Pollutants from a Light-Duty Diesel Engine. *Fuel* **2023**, *335*, 127114.
(114) Chauhan, B. V. S.; Sayyed, I.; Vedrantam, A.; Garg, A.; Bharti, S.; Shukla, M. State of the Art in Low-Temperature Combustion Technologies: HCCI, PCCI, and RCCI. *Part Energy, Environ. Sustain.* **2022**, 95−139.
(115) Krishnamoorthi, M.; Malayalamurthi, R.; He, Z.; Kandasamy, S. A Review on Low Temperature Combustion Engines: Performance, Combustion and Emission Characteristics. *Renew. Sustain. Energy Rev.* **2019**, *116*, 109404.
(116) Gray, A. W.; Ryan, T. W.; Gray, I. I. I.; A, W.; Ryan, I. I. I.; T, W. Homogeneous Charge Compression Ignition (HCCI) of Diesel Fuel. *SAE Trans.* **1997**, No. 412, 1927−1935.
(117) Pandian, M. M.; Anand, K. Comparison of Different Low Temperature Combustion Strategies in a Light Duty Air Cooled Diesel Engine. *Appl. Therm. Eng.* **2018**, *142*, 380−390.
(118) Hasan, M. M.; Rahman, M. M.; Kadirgama, K.; Ramasamy, D. Numerical Study of Engine Parameters on Combustion and Performance Characteristics in an N-Heptane Fueled HCCI Engine. *Appl. Therm. Eng.* **2018**, *128*, 1464−1475.
(119) Khandal, S. V.; Banapurmath, N. R.; Gaitonde, V. N.; Hiremath, S. S. Paradigm Shift from Mechanical Direct Injection Diesel Engines to Advanced Injection Strategies of Diesel Homogeneous Charge Compression Ignition (HCCI) Engines-A Comprehensive Review. *Renew. Sustain. Energy Rev.* **2017**, *70*, 369−384.
(120) Ilango, T.; Natarajan, S. Effect of Compression Ratio on Partially Premixed Charge Compression Ignition Engine Fuelled with Methanol Diesel Blends-an Experimental Investigation. *Int. J. Mech. Prod. Eng.* **2014**, *2*, 41−45.
(121) Hwang, J.; Jung, Y.; Bae, C. Biodiesel PCI Combustion for Performance and Emission Improvement in a Compression Ignition Engine. *Energy Fuels* **2021**, *35* (2), 1523−1534.
(122) Elkelawy, M.; Bastawissi, H. A.; Shenawy, E. A. El; El-gamal, M. A. M. A Critical Review of the Performance, Combustion, and Emissions Characteristics of PCCI Engine Controlled by Injection Strategy and Fuel Properties. *J. Eng. Res.* **2022**, *6* (3). DOI: 10.21608/erjeng.2022.168050.1108
(123) Bobi, S.; Kashif, M.; Laoonual, Y. Combustion and Emission Control Strategies for Partially-Premixed Charge Compression Ignition Engines: A Review. *Fuel* **2022**, *310*, 122272.
(124) Bhurat, S.; Pandey, S.; Chintala, V.; Jaiswal, M.; Kurien, C. Effect of Novel Fuel Vaporiser Technology on Engine Characteristics of Partially Premixed Charge Compression Ignition (PCCI) Engine with Toroidal Combustion Chamber. *Fuel* **2022**, *315*, 123197.
(125) Han, J.; Wang, S.; Somers, B. Comparative Study on the Effects of Inlet Heating, Inlet Boosting, and Double-Injection Strategy on Partially Premixed Combustion. *SAE Technical Pap.* **2019**, No. April, 2019-01-1149.
(126) Natarajan, S.; Shankar, S. A.; Sundareswaran, A. U. M. Early Injected PCCI Engine Fuelled with Bio Ethanol and Diesel Blends-an Experimental Investigation. *Energy Procedia* **2017**, *105*, 358−366.
(127) Kiplimo, R.; Tomita, E.; Kawahara, N.; Yokobe, S. Effects of Spray Impingement, Injection Parameters, and EGR on the Combustion and Emission Characteristics of a PCCI Diesel Engine. *Appl. Therm. Eng.* **2012**, *37*, 165−175.

(128) Loeper, P.; Ra, Y.; Adams, C.; Foster, D. E.; Ghandhi, J.; Andrie, M.; Krieger, R.; Durrett, R. Experimental Investigation of Light-Medium Load Operating Sensitivity in a Gasoline Compression Ignition (GCI) Light-Duty Diesel Engine. *SAE Technical Pap.* **2013**, 2013-01-0896.
(129) Dempsey, A. B.; Walker, N. R.; Gingrich, E.; Reitz, R. D. Comparison of Low Temperature Combustion Strategies for Advanced Compression Ignition Engines with a Focus on Controllability. *Combust. Sci. Technol.* **2014**, *186* (2), 210−241.
(130) Dec, J. E.; Yang, Y.; Dronniou, N. Boosted HCCI-Controlling Pressure-Rise Rates for Performance Improvements Using Partial Fuel Stratification with Conventional Gasoline. *SAE Int. J. Engines* **2011**, *4* (1), 1169−1189.
(131) Splitter, D. A.; Reitz, R. D. Fuel Reactivity Effects on the Efficiency and Operational Window of Dual-Fuel Compression Ignition Engines. *Fuel* **2014**, *118*, 163−175.
(132) Singh, A. P.; Jain, A.; Agarwal, A. K. Fuel-Injection Strategy for PCCI Engine Fueled by Mineral Diesel and Biodiesel Blends. *Energy Fuels* **2017**, *31* (8), 8594−8607.
(133) Pradeep, V.; Anand, K. Novel Strategies to Extend the Operating Load Range of a Premixed Charge Compression Ignited Light-Duty Diesel Engine. *Fuel* **2022**, *317*, 123520.
(134) Chen, L.; Zhang, R.; Wei, H. Auto-Ignition and Flame Characteristics of Ammonia Reactivity-Controlled Compression Ignition Combustion in Comparison with Methane. *Energy Fuels* **2023**, *37* (16), 12503−12513.
(135) Zhang, R.; Chen, L.; Li, J.; Wang, W.; Wei, H.; Pan, J. Effects of Injection Timings and Energy Ratios on the Combustion and Emission Characteristics of N-Heptane/Ammonia RCCI Mode. *Energy Fuels* **2024**, *38* (4), 3491−3502.
(136) Kokjohn, S. L.; Hanson, R. M.; Splitter, D. A.; Reitz, R. D. Fuel Reactivity Controlled Compression Ignition (RCCI): A Pathway to Controlled High-Efficiency Clean Combustion. *Int. J. Engine Res.* **2011**, *12* (3), 209−226.
(137) Fırat, M.; Altun, S.; Okcu, M.; Varol, Y. Comparison of Ethanol/Diesel Fuel Dual Direct Injection (DI2) Strategy with Reactivity Controlled Compression Ignition (RCCI) in a Diesel Research Engine. *Energy* **2022**, *255*, 124556.
(138) Benajes, J.; García, A.; Monsalve-Serrano, J.; Boronat, V. Achieving Clean and Efficient Engine Operation up to Full Load by Combining Optimized RCCI and Dual-Fuel Diesel-Gasoline Combustion Strategies. *Energy Convers. Manag.* **2017**, *136*, 142−151.
(139) Benajes, J.; Pastor, J. V.; García, A.; Monsalve-Serrano, J. The Potential of RCCI Concept to Meet EURO VI NOx Limitation and Ultra-Low Soot Emissions in a Heavy-Duty Engine over the Whole Engine Map. *Fuel* **2015**, *159*, 952−961.
(140) Elkelawy, M.; El Shenawy, E. A.; Mohamed, S. A.; Elarabi, M. M.; Bastawissi, H. A.-E. Impacts of Using EGR and Different DI-Fuels on RCCI Engine Emissions, Performance, and Combustion Characteristics. *Energy Convers. Manag. X* **2022**, *15*, 100236.
(141) Kaddatz, J.; Andrie, M.; Reitz, R. D.; Kokjohn, S. Light-Duty Reactivity Controlled Compression Ignition Combustion Using a Cetane Improver. *SAE Technol. Pap.* **2012**, 2012-01-1110.
(142) Duan, H.; Jia, M.; Chang, Y.; Liu, H. Experimental Study on the Influence of Low-Temperature Combustion (LTC) Mode and Fuel Properties on Cyclic Variations in a Compression-Ignition Engine. *Fuel* **2019**, *256*, 115907.
(143) Singh, A. P.; Kumar, V.; Agarwal, A. K. Evaluation of Comparative Engine Combustion, Performance and Emission Characteristics of Low Temperature Combustion (PCCI and RCCI) Modes. *Appl. Energy* **2020**, *278*, 115644.
(144) Gan, S.; Ng, H. K.; Pang, K. M. Homogeneous Charge Compression Ignition (HCCI) Combustion: Implementation and Effects on Pollutants in Direct Injection Diesel Engines. *Appl. Energy* **2011**, *88* (3), 559−567.
(145) Helmantel, A.; Denbratt, I. HCCI Operation of a Passenger Car Common Rail DI Diesel Engine with Early Injection of Conventional Diesel Fuel. *SAE Technical Pap.* **2004**, 2004-01-0935.
(146) Peng, X. Homogeneous Charge Compression Ignition (HCCI) Engine Control Strategies and Fuel-Air Mixture Preparation Research. *2022 IEEE 2nd Int. Conf. Power, Electron. Comput. Appl.* **2022**, 1146−1150.
(147) Gowrishankar, S.; Krishnasamy, A.; Pradeep Bhasker, J. Investigations on a Homogenous Charge Compression Ignition Engine Operated with Biodiesel and Its Emulsions with Water. *SAE Technol. Pap.* **2022**, 2022-01-0515.
(148) Bukkarapu, K. R.; Krishnasamy, A. Charge Dilution Strategy to Extend the Stable Combustion Regime of a Homogenous Charge Compression Ignited Engine Operated With Biodiesel. *SAE Technical Pap.* **2023**, 2023-32-0132.
(149) Shrivastava, P.; Salam, S.; Verma, T. N.; Samuel, O. D. Experimental and Empirical Analysis of an IC Engine Operating with Ternary Blends of Diesel, Karanja and Roselle Biodiesel. *Fuel* **2020**, *262*, 116608.
(150) Christensen, M.; Johansson, B. Influence of Mixture Quality on Homogeneous Charge Compression Ignition. *SAE Trans.* **1998**, 982454.
(151) Singh, A. K.; Pundir, B. P.; Singh, A. Fuel System for Dual-Fuel Operation of an Automotive Diesel. *International Symposium on Alcohol Fuels Technology*, Sao Paulo, Brazil, 5 Oct 1980; Vol. *2*, pp 507−511.
(152) Ryan, T. W.; Callahan, T. J. Homogeneous Charge Compression Ignition of Diesel Fuel. *SAE Trans.* **1996**, 928−937.
(153) Imtenan, S.; Varman, M.; Masjuki, H. H.; Kalam, M. A.; Sajjad, H.; Arbab, M. I.; Fattah, I. M. R. Impact of Low Temperature Combustion Attaining Strategies on Diesel Engine Emissions for Diesel and Biodiesels: A Review. *Energy Convers. Manag.* **2014**, *80*, 329−356.
(154) Xu, G.; Zhong, W.; Lin, C.; Mingdi, L.; Lilin, L.; Shuai, L. The Study on Formaldehyde Emissions of Biodiesel in the HCCI Combustion Mode. *2011 Int. Conf. Electr. Inf. Control Eng.* **2011**, 5555−5558.
(155) Bunting, B.; Bunce, M.; Joyce, B.; Crawford, R. Investigation and Optimization of Biodiesel Chemistry for HCCI Combustion. *Sustain. Automot. Technol. 2011* **2011**, 51−58.
(156) Christensen, M.; Hultqvist, A.; Johansson, B. Demonstrating the Multi Fuel Capability of a Homogeneous Charge Compression Ignition Engine with Variable Compression Ratio. *SAE Trans.* **1999**, 2099−2113.
(157) Olsson, J.-O.; Tunestål, P.; Johansson, B.; Fiveland, S.; Agama, R.; Willi, M.; Assanis, D. Compression Ratio Influence on Maximum Load of a Natural Gas Fueled HCCI Engine. *SAE Trans.* **2002**, 442−458.
(158) Hyvönen, J.; Haraldsson, G.; Johansson, B. Supercharging HCCI to Extend the Operating Range in a Multi-Cylinder VCR-HCCI Engine. *SAE Trans.* **2003**, 2456−2468.
(159) Yamaoka, S.; Kakuya, H.; Nakagawa, S.; Okada, T.; Shimada, A.; Kihara, Y. HCCI Operation Control in a Multi-Cylinder Gasoline Engine. *SAE Technical Pap.* **2005**, 2005-01-0120.
(160) Babagiray, M.; Kocakulak, T.; Ardebili, S. M. S.; Calam, A.; Solmaz, H. Optimization of Operating Conditions in a Homogeneous Charge Compression Ignition Engine with Variable Compression Ratio. *Int. J. Environ. Sci. Technol.* **2023**, *20* (5), 5311−5332.
(161) Shere, A.; Subramanian, K. A. Experimental Investigation on Effects of Equivalence Ratio on Combustion with Knock, Performance, and Emission Characteristics of Dimethyl Ether Fueled CRDI Compression Ignition Engine under Homogeneous Charge Compression Ignition Mode. *Fuel* **2022**, *322*, 124048.
(162) Bunting, B. G.; Eaton, S. J.; Crawford, R. W.; Xu, Y.; Wolf, L. R.; Kumar, S.; Stanton, D.; Fang, H. Performance of Biodiesel Blends of Different FAME Distributions in HCCI Combustion. *SAE Technical Pap.* **2009**, 2009-01-1342.
(163) Szybist, J. P.; McFarlane, J.; Bunting, B. G. Comparison of Simulated and Experimental Combustion of Biodiesel Blends in a Single Cylinder Diesel HCCI Engine. *SAE Trans.* **2007**, 1250−1260.

https://doi.org/10.1021/acs.energyfuels.4c00705
Energy Fuels XXXX, XXX, XXX−XXX

(164) Singh, A. P.; Agarwal, A. K. Effect of Intake Charge Temperature and EGR on Biodiesel Fuelled HCCI Engine. *SAE Technical Pap.* **2016**, 2016-28-0257.
(165) Moulali, P.; Tarigonda, H.; Prasad, B. D. Optimization of Performance Characteristics of Homogeneous Charge Compression Ignition Engine with Biodiesel Using Artificial Neural Network (ANN) and Response Surface Methodology (RSM). *J. Inst. Eng. Ser. C* **2022**, *103* (4), 875−888.
(166) Reader, G. T.; Asad, U.; Zheng, M. Energy Efficiency Trade-off with Phasing of HCCI Combustion. *Int. J. Energy Res.* **2013**, *37* (3), 200−210.
(167) Shi, L.; Cui, Y.; Deng, K.; Peng, H.; Chen, Y. Study of Low Emission Homogeneous Charge Compression Ignition (HCCI) Engine Using Combined Internal and External Exhaust Gas Recirculation (EGR). *Energy* **2006**, *31* (14), 2665−2676.
(168) Kawasaki, K.; Takegoshi, A.; Yamane, K.; Ohtsubo, H.; Nakazono, T.; Yamauchi, K. Combustion Improvement and Control for a Natural Gas HCCI Engine by the Internal EGR by Means of Intake-Valve Pilot-Opening. *SAE Technical Pap.* **2006**, 2006-01-0208.
(169) Cairns, A.; Blaxill, H. The Effects of Combined Internal and External Exhaust Gas Recirculation on Gasoline Controlled Auto-Ignition. *SAE Technical Pap.* **2005**, 2005-01-0133.
(170) Xu, F.; Wang, Z.; Yang, D.; Wang, J. Potential of High Load Extension for Gasoline HCCI Engine Using Boosting and Exhaust Gas Recirculation. *Energy Fuels* **2009**, *23* (5), 2444−2452.
(171) Handford, D. I.; Checkel, M. D. Extending the Load Range of a Natural Gas HCCI Engine Using Direct Injected Pilot Charge and External EGR. *SAE Technical Pap.* **2009**, 2009-01-1884.
(172) Yao, M.; Zheng, Z.; Liu, H. Progress and Recent Trends in Homogeneous Charge Compression Ignition (HCCI) Engines. *Prog. energy Combust. Sci.* **2009**, *35* (5), 398−437.
(173) Valentino, G.; Corcione, F. E.; Iannuzzi, S. E.; Serra, S. Experimental Study on Performance and Emissions of a High Speed Diesel Engine Fuelled with N-Butanol Diesel Blends under Premixed Low Temperature Combustion. *Fuel* **2012**, *92* (1), 295−307.
(174) Ganesh, D.; Nagarajan, G.; Ibrahim, M. M. Study of Performance, Combustion and Emission Characteristics of Diesel Homogeneous Charge Compression Ignition (HCCI) Combustion with External Mixture Formation. *Fuel* **2008**, *87* (17−18), 3497−3503.
(175) Ladommatos, N.; Abdelhalim, S. M.; Zhao, H.; Hu, Z. The Dilution, Chemical, and Thermal Effects of Exhaust Gas Recirculation on Diesel Engine Emissions-Part 3: Effects of Water Vapour. *SAE Technical Pap.* **1997**, No. 971659, DOI: 10.4271/971659.
(176) Yuan, W.; Huang, X.; Fu, J.; Ma, Y.; Li, G.; Huang, Q. Water Vapor Blending Ratio Effects on Combustion Thermal Performance and Emission of Hydrogen Homogeneous Charge Compression Ignition. *Energies* **2022**, *15* (23), 9055.
(177) Bendu, H.; Murugan, S. Homogeneous Charge Compression Ignition (HCCI) Combustion: Mixture Preparation and Control Strategies in Diesel Engines. *Renew. Sustain. Energy Rev.* **2014**, *38*, 732−746.
(178) Lee, S.; Gonzalez, D.; M, A.; Reitz, R. D. Effects of Engine Operating Parameters on near Stoichiometric Diesel Combustion Characteristics. *SAE Trans.* **2007**, 103−119.
(179) Russell, A.; Epling, W. S. Diesel Oxidation Catalysts. *Catal. Rev.* **2011**, *53* (4), 337−423.
(180) Resitoğlu, İ. A.; Altinisik, K.; Keskin, A. The Pollutant Emissions from Diesel-Engine Vehicles and Exhaust Aftertreatment Systems. *Clean Technol. Environ. Policy* **2015**, *17*, 15−27.
(181) Votsmeier, M.; Kreuzer, T.; Gieshoff, J.; Lepperhoff, G.; Elvers, B. Catalytic Exhaust Aftertreatment, General Concepts. *Handb. Fuels Energy Sources Transp.* **2021**, 475−481.
(182) Farrauto, R. J.; Voss, K. E. Monolithic Diesel Oxidation Catalysts. *Appl. Catal. B Environ.* **1996**, *10* (1−3), 29−51.
(183) Hamzehlouyan, T.; Sampara, C. S.; Li, J.; Kumar, A.; Epling, W. S. Kinetic Study of Adsorption and Desorption of SO_2 over γ-Al_2O_3 and Pt/γ-Al_2O_3. *Appl. Catal. B Environ.* **2016**, *181*, 587−598.
(184) Yang, W.; Gong, J.; Wang, X.; Bao, Z.; Guo, Y.; Wu, Z. A Review on the Impact of SO_2 on the Oxidation of NO, Hydrocarbons, and CO in Diesel Emission Control Catalysis. *ACS Catal.* **2021**, *11* (20), 12446−12468.
(185) Ho, P. H.; Woo, J.-W.; Feizie Ilmasani, R.; Han, J.; Olsson, L. The Role of Pd-Pt Interactions in the Oxidation and Sulfur Resistance of Bimetallic Pd-Pt/γ-Al2O3 Diesel Oxidation Catalysts. *Ind. Eng. Chem. Res.* **2021**, *60* (18), 6596−6612.
(186) Moden, B.; Donohue, J. M.; Cormier, W. E.; Li, H.-X. The Uses and Challenges of Zeolites in Automotive Applications. *Top. Catal.* **2010**, *53* (19), 1367−1373.
(187) Ho, P. H.; Woo, J.; Ilmasani, R. F.; Salam, M. A.; Creaser, D.; Olsson, L. The Effect of Si/Al Ratio on the Oxidation and Sulfur Resistance of Beta Zeolite-Supported Pt and Pd as Diesel Oxidation Catalysts. *ACS Eng. Au* **2022**, *2* (1), 27−45.
(188) Ho, P. H.; Shao, J.; Yao, D.; Ilmasani, R. F.; Salam, M. A.; Creaser, D.; Olsson, L. The Effect of Pt/Pd Ratio on the Oxidation Activity and Resistance to Sulfur Poisoning for Pt-Pd/BEA Diesel Oxidation Catalysts with High Siliceous Content. *J. Environ. Chem. Eng.* **2022**, *10* (4), 108217.
(189) Carrillo, C.; DeLaRiva, A.; Xiong, H.; Peterson, E. J.; Spilde, M. N.; Kunwar, D.; Goeke, R. S.; Wiebenga, M.; Oh, S. H.; Qi, G.; Challa, S. R.; Datye, A. K. Regenerative Trapping: How Pd Improves the Durability of Pt Diesel Oxidation Catalysts. *Appl. Catal. B Environ.* **2017**, *218*, 581−590.
(190) Zhou, X.; Wang, M.; Yan, D.; Li, Q.; Chen, H. Synthesis and Performance of High Efficient Diesel Oxidation Catalyst Based on Active Metal Species-Modified Porous Zeolite BEA. *J. Catal.* **2019**, *379*, 138−146.
(191) Li, Q.; Zhou, X.; Zhao, W.; Peng, C.; Wu, H.; Chen, H. Pt/Fe Co-Loaded Mesoporous Zeolite Beta for CO Oxidation with High Catalytic Activity and Water Resistance. *RSC Adv.* **2019**, *9* (48), 28089−28094.
(192) Tang, W.; Lu, X.; Liu, F.; Du, S.; Weng, J.; Hoang, S.; Wang, S.; Nam, C.-Y.; Gao, P.-X. Ceria-Based Nanoflake Arrays Integrated on 3D Cordierite Honeycombs for Efficient Low-Temperature Diesel Oxidation Catalyst. *Appl. Catal. B Environ.* **2019**, *245*, 623−634.
(193) Shukla, P. C.; Gupta, T.; Labhsetwar, N. K.; Agarwal, A. K. Development of Low Cost Mixed Metal Oxide Based Diesel Oxidation Catalysts and Their Comparative Performance Evaluation. *RSC Adv.* **2016**, *6* (61), 55884−55893.
(194) Waikar, J.; More, P. Low Temperature Oxidation of CO Using Alkali-and Alkaline-Earth Metal-Modified Ceria-Supported Metal Catalysts: A Review. *Bull. Mater. Sci.* **2021**, *44*, 263.
(195) Gu, Y.; Pan, Z.; Zhang, H.; Zhu, J.; Yuan, B.; Pan, D.; Wu, C.; Dong, B.; Guo, Z. Synthesis of High Performance Diesel Oxidation Catalyst Using Novel Mesoporous AlLaZrTiOx Mixed Oxides by a Modified Sol-Gel Method. *Adv. Compos. Hybrid Mater.* **2020**, *3*, 583−593.
(196) Yang, Q.; Li, Q.; Wang, X.; Wang, X.; Li, L.; Chu, X.; Wang, D.; Men, J.; Li, X.; Si, W.; Peng, Y.; Ma, Y.; Li, J. Synergistic Effects of a CeO2/SmMn2O5-H Diesel Oxidation Catalyst Induced by Acid-Selective Dissolution Drive the Catalytic Oxidation Reaction. *ACS Appl. Mater. Interfaces* **2022**, *14* (2), 2860−2870.
(197) Parks II, J. E.; Prikhodko, V.; Storey, J. M. E.; Barone, T. L.; Lewis Sr, S. A.; Kass, M. D.; Huff, S. P. Emissions from Premixed Charge Compression Ignition (PCCI) Combustion and Affect on Emission Control Devices. *Catal. Today* **2010**, *151* (3−4), 278−284.
(198) Wang, J.; You, R.; Zhao, C.; Zhang, W.; Liu, W.; Fu, X.-P.; Li, Y.; Zhou, F.; Zheng, X.; Xu, Q.; Yao, T.; Jia, C.-J.; Wang, Y.-G.; Huang, W.; Wu, Y. N-Coordinated Dual-Metal Single-Site Catalyst for Low-Temperature CO Oxidation. *ACS Catal.* **2020**, *10* (4), 2754−2761.
(199) Cai, Y.; Xu, J.; Guo, Y.; Liu, J. Ultrathin, Polycrystalline, Two-Dimensional Co3O4 for Low-Temperature CO Oxidation. *ACS Catal.* **2019**, *9* (3), 2558−2567.
(200) Zhao, S.; Li, T.; Lin, J.; Wu, P.; Li, Y.; Li, A.; Chen, T.; Zhao, Y.; Chen, G.; Yang, L.; Meng, Y.; Jin, X.; Qiu, Y.; Ye, D. Engineering Co3+-Rich Crystal Planes on Co3O4 Hexagonal Nanosheets for CO

https://doi.org/10.1021/acs.energyfuels.4c00705
Energy Fuels XXXX, XXX, XXX−XXX

and Hydrocarbons Oxidation with Enhanced Catalytic Activity and Water Resistance. *Chem. Eng. J.* **2021**, *420*, 130448.
(201) Tang, X.; Wang, J.; Ma, Y.; Li, J.; Zhang, X.; La, P.; Liu, B. Flexible Co_3O_4/TiO_2 Monolithic Catalysts for Low-temperature and Long-term Stable CO Oxidation. *Nano Sel.* **2021**, *2* (1), 72−82.
(202) Kerkar, R. D.; Salker, A. V. A Route to Develop the Synergy Between CeO_2 and CuO for Low Temperature CO Oxidation. *Catal. Lett.* **2020**, *150*, 2774−2783.
(203) Kerkar, R. D.; Salker, A. V. Significant Effect of Multi-Doped Cerium Oxide for Carbon Monoxide Oxidation Studies. *Mater. Chem. Phys.* **2020**, *253*, 123326.
(204) Zhu, L.; Wang, X.; Shen, D. Review and Perspectives of Novel Flue-Gas Internal Recirculation Combustion Technology for Low Nitrogen Emission: Fundamentals, Performance, Method, and Applications for Conventional Fossil Fuels and Sustainable e-Fuels. *Energy Fuels* **2023**, *37* (13), 8765−8780.
(205) Zeng, Y.; Haw, K.; Wang, Y.; Zhang, S.; Wang, Z.; Zhong, Q.; Kawi, S. Recent Progress of CeO2- TiO2 Based Catalysts for Selective Catalytic Reduction of NOx by NH3. *ChemCatChem.* **2021**, *13* (2), 491−505.
(206) Zhou, J.; Guo, R.; Zhang, X.; Liu, Y.; Duan, C.; Wu, G.; Pan, W. Cerium Oxide-Based Catalysts for Low-Temperature Selective Catalytic Reduction of NO x with NH3: A Review. *Energy Fuels* **2021**, *35* (4), 2981−2998.
(207) Wang, X.; Xu, Y.; Zhao, Z.; Liao, J.; Chen, C.; Li, Q. Recent Progress of Metal-Exchanged Zeolites for Selective Catalytic Reduction of NOx with NH3 in Diesel Exhaust. *Fuel* **2021**, *305*, 121482.
(208) Chen, L.; Janssens, T. V. W.; Vennestrøm, P. N. R.; Jansson, J.; Skoglundh, M.; Gronbeck, H. A Complete Multisite Reaction Mechanism for Low-Temperature NH3-SCR over Cu-CHA. *ACS Catal.* **2020**, *10* (10), 5646−5656.
(209) Bendrich, M.; Scheuer, A.; Hayes, R. E.; Votsmeier, M. Unified Mechanistic Model for Standard SCR; Fast, SCR, and NO2 SCR over a Copper Chabazite Catalyst. *Appl. Catal. B Environ.* **2018**, *222*, 76−87.
(210) Joseph, J.; Pachamuthu, S.; Solomon, J. M.; Sathyamurthy, R. Experimental Investigation to Enhance the Low-temperature Nitrogen Oxide Emission Reduction in Biodiesel Exhaust Using Selective Catalytic Reduction with Direct Ammonia Injection and Manganese Cerium Zirconia Catalyst. *Environ. Prog. Sustain. Energy* **2021**, *40* (4), No. e13622.
(211) Koebel, M.; Strutz, E. O. Thermal and Hydrolytic Decomposition of Urea for Automotive Selective Catalytic Reduction Systems: Thermochemical and Practical Aspects. *Ind. Eng. Chem. Res.* **2003**, *42* (10), 2093−2100.
(212) Chen, L.; Si, Z.; Wu, X.; Weng, D.; Ran, R.; Yu, J. Rare Earth Containing Catalysts for Selective Catalytic Reduction of NOx with Ammonia: A Review. *J. Rare Earths* **2014**, *32* (10), 907−917.
(213) Tan, W.; Wang, J.; Cai, Y.; Li, L.; Xie, S.; Gao, F.; Liu, F.; Dong, L. Molybdenum Oxide as an Efficient Promoter to Enhance the NH3-SCR Performance of CeO2-SiO2 Catalyst for NOx Removal. *Catal. Today* **2022**, *397*, 475−483.
(214) Ni, S.; Tang, X.; Yi, H.; Gao, F.; Wang, C.; Shi, Y.; Zhang, R.; Zhu, W. Novel Mn-Ce Bi-Oxides Loaded on 3D Monolithic Nickel Foam for Low-Temperature NH3-SCR de-NOx: Preparation Optimization and Reaction Mechanism. *J. Rare Earths* **2022**, *40* (2), 268−278.
(215) Zhu, N.; Shan, W.; Lian, Z.; Zhang, Y.; Liu, K.; He, H. A Superior Fe-V-Ti Catalyst with High Activity and SO2 Resistance for the Selective Catalytic Reduction of NOx with NH3. *J. Hazard. Mater.* **2020**, *382*, 120970.
(216) Shi, G.; Liu, M.; Li, Y.; Li, T.; Duan, Y. Influence of Fe-modified Mn-Ce-Fe-Co-Ox/P84 Catalytic Filter Materials for Low-temperature NO Removal Synergistic Hg0 Oxidation. *Asia-Pacific J. Chem. Eng.* **2021**, *16* (5), No. e2677.
(217) Xie, H.; Shu, D.; Chen, T.; Liu, H.; Zou, X.; Wang, C.; Han, Z.; Chen, D. An In-Situ DRIFTs Study of Mn Doped FeVO4 Catalyst by One-Pot Synthesis for Low-Temperature NH3-SCR. *Fuel* **2022**, *309*, 122108.
(218) Liu, L.; Su, S.; Chen, D.; Shu, T.; Zheng, X.; Yu, J.; Feng, Y.; Wang, Y.; Hu, S.; Xiang, J. Highly Efficient NH3-SCR of NOx over MnFeW/Ti Catalyst at Low Temperature: SO2 Tolerance and Reaction Mechanism. *Fuel* **2022**, *307*, 121805.
(219) Jiang, L.; Liang, Y.; Liu, W.; Wu, H.; Aldahri, T.; Carrero, D. S.; Liu, Q. Synergistic Effect and Mechanism of FeOx and CeOx Co-Doping on the Superior Catalytic Performance and SO2 Tolerance of Mn-Fe-Ce/ACN Catalyst in Low-Temperature NH3-SCR of NOx. *J. Environ. Chem. Eng.* **2021**, *9* (6), 106360.
(220) Hu, C.; Wei, L.; Wu, T.; Yue, C.; Guo, R. Minireview and Perspective of One-Dimensional Manganese Oxide Nanostructures for the Removal of Air Pollutants. *Energy Fuels* **2023**, *37* (15), 10886−10896.
(221) Zhu, Y.; Xiao, X.; Wang, J.; Ma, C.; Jia, X.; Qiao, W.; Ling, L. Enhanced Activity and Water Resistance of Hierarchical Flower-like Mn-Co Binary Oxides for Ammonia-SCR Reaction at Low Temperature. *Appl. Surf. Sci.* **2021**, *569*, 150989.
(222) Tang, X.; Wang, C.; Gao, F.; Zhang, R.; Shi, Y.; Yi, H. Acid Modification Enhances Selective Catalytic Reduction Activity and Sulfur Dioxide Resistance of Manganese-Cerium-Cobalt Catalysts: Insight into the Role of Phosphotungstic Acid. *J. Colloid Interface Sci.* **2021**, *603*, 291−306.
(223) Peng, C.; Yan, R.; Mi, Y.; Li, G.; Zheng, Y.; Luo, Y.; Liang, J.; Liu, W.; Li, Z.; Wu, D.; Wang, X.; Peng, H. Toward Rational Design of a Novel Hierarchical Porous Cu-SSZ-13 Catalyst with Boosted Low-Temperature NOx Reduction Performance. *J. Catal.* **2021**, *401*, 309−320.
(224) Liang, J.; Tao, J.; Mi, Y.; Liu, W.; Wang, Z.; Li, Z.; Wu, D.; Wu, P.; Peng, H. Unraveling the Boosting Low-Temperature Performance of Ordered Mesoporous Cu-SSZ-13 Catalyst for NOx Reduction. *Chem. Eng. J.* **2021**, *409*, 128238.
(225) Ye, Z.; Zhao, P.; Tang, X.; Hagio, T.; Sato, K.; Nagaoka, K.; Li, X. Effects of the Topological Structure of Different Cu-Zeolites on the Relationship between Soot and NOx Removal on NH3-SCRF. *Energy Fuels* **2024**, *38*, 2212.
(226) Xiong, T.; Gao, F.; Wang, J.; Wen, J.; Zhou, Y.; Yi, H.; Zhao, S.; Tang, X. Enhancing Strategies for the Activity and H_2O Resistance of MnCo-CMS Flexible SCR Catalysts and Hydrophobic Modification by Modulating the Surface Energy. *Sep. Purif. Technol.* **2024**, *333*, 125949.
(227) Li, T.-Y.; Li, W.-J.; Wey, M.-Y. Strategies for Designing Hydrophobic MnCe-Montmorillonite Catalysts against Water Vapor for Low-Temperature NH_3-SCR. *Fuel* **2023**, *350*, 128857.
(228) Fu, Z.; Zhang, G.; Han, W.; Tang, Z. The Water Resistance Enhanced Strategy of Mn Based SCR Catalyst by Construction of TiO_2 Shell and Superhydrophobic Coating. *Chem. Eng. J.* **2021**, *426*, 131334.
(229) Du, T.; Qu, H.; Liu, Q.; Zhong, Q.; Ma, W. Synthesis, Activity and Hydrophobicity of Fe-ZSM-5@ Silicalite-1 for NH3-SCR. *Chem. Eng. J.* **2015**, *262*, 1199−1207.
(230) Liu, L.; Singh, R.; Li, G.; Xiao, G.; Webley, P. A.; Zhai, Y. Synthesis of Hydrophobic Zeolite X@ SiO2 Core-Shell Composites. *Mater. Chem. Phys.* **2012**, *133* (2−3), 1144−1151.
(231) Zhang, J.; Li, Z.; Yi, H.; Tang, X.; Cheng, H.; Yu, Q. Synthesis and Application Prospect of Small-Pore Zeolites in Vehicle Exhaust Purification. *Fuel* **2023**, *348*, 128577.
(232) Iwamoto, M.; Yahiro, H.; Shundo, S.; Yu-u, Y.; Mizuno, N. Influence of Sulfur Dioxide on Catalytic Removal of Nitric Oxide over Copper Ion-Exchanged ZSM-5 Zeolite. *Appl. Catal.* **1991**, *69* (1), L15−L19.
(233) Held, W.; Koenig, A.; Richter, T.; Puppe, L. Catalytic NOx Reduction in Net Oxidizing Exhaust Gas. *SAE Trans.* **1990**, 209−216.
(234) Serhan, N.; Tsolakis, A.; Wahbi, A.; Martos, F. J.; Golunski, S. Modifying Catalytically the Soot Morphology and Nanostructure in Diesel Exhaust: Influence of Silver De-NOx Catalyst (Ag/Al2O3). *Appl. Catal. B Environ.* **2019**, *241*, 471−482.

https://doi.org/10.1021/acs.energyfuels.4c00705
Energy Fuels XXXX, XXX, XXX−XXX

(235) Theinnoi, K.; Sawatmongkhon, B.; Wongchang, T.; Haoharn, C.; Wongkhorsub, C.; Sukjit, E. Effects of Diesel-Biodiesel-Ethanol Fuel Blend on a Passive Mode of Selective Catalytic Reduction to Reduce NO x Emission from Real Diesel Engine Exhaust Gas. *ACS omega* **2021**, *6* (41), 27443−27453.
(236) Lee, K.; Choi, B.; Kim, C.; Lee, C.; Oh, K. De-NOx Characteristics of HC-SCR System Employing Combined Ag/Al2O3 and CuSn/ZSM-5 Catalyst. *J. Ind. Eng. Chem.* **2021**, *93*, 461−475.
(237) Xu, J.; Tang, T.; Zhang, Q.; Zhang, C.; Guo, F. Remarkable Low Temperature Catalytic Activity for SCR of NO with Propylene under Oxygen-Rich Conditions over Mn0. 2La0. 07Ce0. 05Ox/ZSM-5 Catalyst. *Vacuum* **2021**, *188*, 110174.
(238) Xu, J.; Qin, Y.; Wang, H.; Guo, F.; Xie, J. Recent Advances in Copper-Based Zeolite Catalysts with Low-Temperature Activity for the Selective Catalytic Reduction of NO x with Hydrocarbons. *New J. Chem.* **2020**, *44* (3), 817−831.
(239) Hu, Z.; Yong, X.; Li, D.; Yang, R. T. Synergism between Palladium and Nickel on Pd-Ni/TiO2 for H2-SCR: A Transient DRIFTS Study. *J. Catal.* **2020**, *381*, 204−214.
(240) Patel, V. K.; Sharma, S. Effect of Oxide Supports on Palladium Based Catalysts for NO Reduction by H2-SCR. *Catal. Today* **2021**, *375*, 591−600.
(241) Zhang, Y.; Zhao, L.; Duan, J.; Bi, S. Insights into DeNOx Processing over Ce-Modified Cu-BTC Catalysts for the CO-SCR Reaction at Low Temperature by in Situ DRIFTS. *Sep. Purif. Technol.* **2020**, *234*, 116081.
(242) Choi, B.; Lee, K.; Son, G. Review of Recent After-Treatment Technologies for de-NOx Process in Diesel Engines. *Int. J. Automot. Technol.* **2020**, *21*, 1597−1618.
(243) Hamada, H.; Haneda, M. A Review of Selective Catalytic Reduction of Nitrogen Oxides with Hydrogen and Carbon Monoxide. *Appl. Catal. A Gen.* **2012**, *421*, 1−13.
(244) You, Y.-W.; Kim, Y. J.; Lee, J. H.; Arshad, M. W.; Kim, S. K. S. M.; Kim, S. K. S. M.; Lee, H.; Thompson, L. T.; Heo, I. Unraveling the Origin of Extraordinary Lean NOx Reduction by CO over Ir-Ru Bimetallic Catalyst at Low Temperature. *Appl. Catal. B Environ.* **2021**, *280*, 119374.
(245) Sun, R.; Yu, F.; Wan, Y.; Pan, K.; Li, W.; Zhao, H.; Dan, J.; Dai, B. Reducing N_2O Formation over CO-SCR Systems with CuCe Mixed Metal Oxides. *ChemCatChem.* **2021**, *13* (11), 2709−2718.
(246) Wang, D.; Huang, B.; Shi, Z.; Long, H.; Li, L.; Yang, Z.; Dai, M. Influence of Cerium Doping on Cu-Ni/Activated Carbon Low-Temperature CO-SCR Denitration Catalysts. *RSC Adv.* **2021**, *11* (30), 18458−18467.
(247) Cheng, X.; Xiao, X.; Yin, Y.; Wang, J.; Qiao, W.; Ling, L. Ammonia-Free Selective Catalytic Reduction of NO at Low Temperature on Melamine Impregnated MnO x-CeO_2/Carbon Aerogels. *Ind. Eng. Chem. Res.* **2021**, *60* (36), 13233−13242.
(248) Sayed, M.; Elhemaly, M. Review on NOx Emissions from Using Biodiesel Blends in Diesel Engines. *Int. J. Heavy Veh. Syst.* **2021**, *28* (1), 125−136.
(249) Kumar, P.; Sandhu, S. S. Impact Analysis of Partially Premixed Combustion Strategy on the Emissions of a Compression Ignition Engine Fueled with Higher Octane Number Fuels: A Review. *Mater. Today Proc.* **2021**, *45*, 5772−5777.
(250) Pereda-Ayo, B.; Duraiswami, D.; González-Velasco, J. R. Control of NOx Storage and Reduction in NSR Bed for Designing Combined NSR-SCR Systems. *Catal. today* **2011**, *172* (1), 66−72.
(251) Cortes-Reyes, M.; Herrera, C.; Larrubia, M. A.; Alemany, L. J. Hybrid Technology for DeNOxing by LNT-SCR System for Efficient Diesel Emission Control: Influence of Operation Parameters in H2O + CO2 atm. *Catalysts* **2020**, *10* (2), 228.
(252) Pereda-Ayo, B.; González-Velasco, J. R.; Burch, R.; Hardacre, C.; Chansai, S. Regeneration Mechanism of a Lean NOx Trap (LNT) Catalyst in the Presence of NO Investigated Using Isotope Labelling Techniques. *J. Catal.* **2012**, *285* (1), 177−186.
(253) Roy, S.; Baiker, A. NO x Storage- Reduction Catalysis: From Mechanism and Materials Properties to Storage- Reduction Performance. *Chem. Rev.* **2009**, *109* (9), 4054−4091.
(254) Ecker, S. I.; Dornseiffer, J.; Baumann, S.; Guillon, O.; Bouwmeester, H. J. M.; Meulenberg, W. A. Measures to Reduce the N2O Formation at Perovskite-Based Lean NOx Trap Catalysts under Lean Conditions. *Catalysts* **2021**, *11* (8), 917.
(255) Ecker, S.I.; Dornseiffer, J.; Werner, J.; Schlenz, H.; Sohn, Y.J.; Sauerwein, F.S.; Baumann, S.; Bouwmeester, H.J.M.; Guillon, O.; Weirich, T.E.; Meulenberg, W.A. Novel Low-Temperature Lean NOx Storage Materials Based on La0.5Sr0.5Fe1-XMxO3-δ/Al_2O_3 Infiltration Composites (M = Ti, Zr, Nb). *Appl. Catal. B Environ.* **2021**, *286*, 119919.
(256) Albaladejo-Fuentes, V.; Sánchez-Adsuar, M.-S.; Anderson, J. A.; Illán-Gómez, M.-J. NOx Storage on BaTi0.8Cu0.2O3 Perovskite Catalysts: Addressing a Feasible Mechanism. *Nanomaterials* **2021**, *11* (8), 2133.
(257) Chen, Z.; Wang, M.; Wang, J. J.; Wang, C.; Wang, J. J.; Li, W.; Shen, M. Investigation of Crystal Size Effect on the NOx Storage Performance of Pd/SSZ-13 Passive NOx Adsorbers. *Appl. Catal. B Environ.* **2021**, *291*, 120026.
(258) Kim, B.-S.; Jeong, H.; Bae, J.; Kim, P. S.; Kim, C. H.; Lee, H. Lean NOx Trap Catalysts with High Low-Temperature Activity and Hydrothermal Stability. *Appl. Catal. B Environ.* **2020**, *270*, 118871.
(259) Kim, H.; Jung, H.; Han, J. W.; Lee, K. B. Experimental and Density Functional Theory Studies on Cu/Ba-Coimpregnated γ-Al2O3 for Low-Temperature NOx Storage and Adsorbent Regeneration. *Chem. Eng. J.* **2022**, *429*, 132112.
(260) Mei, X.; Xin, Y.; Zhang, Y.; Nie, W.; Zhang, Z.; Lu, P.; Zhang, Z.; Chen, G.; Zhang, J. Electrification-Enhanced Low-Temperature NO x Storage-Reduction on Pt and K Co-Supported Antimony-Doped Tin Oxides. *Environ. Sci. Technol.* **2023**, *57* (49), 20905−20914.
(261) Da Costa, S.; Salkar, A. V.; Morajkar, P. P. Advanced Methodologies for Remediation of Combustion-Generated Particulate Matter (Soot) from the Environment. *Adv. Nano Biochem.* **2023**, 199−231.
(262) Tan, D.; Dong, R.; Zhang, Z.; Zhang, B.; Jiang, F.; Ye, Y.; Li, D.; Liu, H. Multi-Objective Impact Mechanism on the Performance Characteristic for a Diesel Particulate Filter by RF-NSGA III-TOPSIS during Soot Loading. *Energy* **2024**, *286*, 129582.
(263) Neha; Prasad, R.; Singh, S. V. A Review on Catalytic Oxidation of Soot Emitted from Diesel Fuelled Engines. *J. Environ. Chem. Eng.* **2020**, *8* (4), 103945.
(264) Matarrese, R. Catalytic Materials for Gasoline Particulate Filters Soot Oxidation. *Catalysts* **2021**, *11* (8), 890.
(265) Liu, S.; Wu, X.; Weng, D.; Ran, R. Ceria-Based Catalysts for Soot Oxidation: A Review. *J. Rare Earths* **2015**, *33* (6), 567−590.
(266) Cui, B.; Li, Y.; Li, S.; Xia, Y.; Zheng, Z.; Liu, Y.-Q. Bi-Doped Ceria as a Highly Efficient Catalyst for Soot Combustion: Improved Mobility of Lattice Oxygen in Ce x Bi1-x O y Catalysts. *Energy Fuels* **2020**, *34* (8), 9932−9939.
(267) Fedyna, M.; Legutko, P.; Gryboś, J.; Janas, J.; Yu, X.; Zhao, Z.; Kotarba, A.; Sojka, Z. Screening Investigations into the Effect of Cryptomelane Doping with 3d Transition Metal Cations on the Catalytic Activity in Soot Oxidation, NO_2 Formation and SO_2 Resistance. *Appl. Catal. A Gen.* **2021**, *624*, 118302.
(268) Xiong, J.; Wu, Q.; Mei, X.; Liu, J.; Wei, Y.; Zhao, Z.; Wu, D.; Li, J. Fabrication of Spinel-Type Pd x Co3-xO4 Binary Active Sites on 3D Ordered Meso-Macroporous Ce-Zr-O2 with Enhanced Activity for Catalytic Soot Oxidation. *ACS Catal.* **2018**, *8* (9), 7915−7930.
(269) Zhou, X. X.; Zhao, H.; Huang, W. M.; Chen, H. R.; Shi, J. L. TiO 2 and Cu 1.5 Mn 1.5 O 4 Co-Modified Hierarchically Porous Zeolite Beta for Soot Oxidation with Excellent Sulfur-Resistance and Stability. *Dalt. Trans.* **2017**, *46* (18), 6111−6116.
(270) Zhao, H.; Zhou, X. X.; Pan, L. Y.; Wang, M.; Chen, H. R.; Shi, J. L. Facile Synthesis of Spinel Cu 1.5 Mn 1.5 O 4 Microspheres with High Activity for the Catalytic Combustion of Diesel Soot. *RSC Adv.* **2017**, *7* (33), 20451−20459.
(271) Zhao, Y.; Wen, Z.; Huang, Y.; Duan, X.; Cao, Y.; Ye, L.; Jiang, L.; Yuan, Y. Low-Temperature Soot Combustion over Ceria Modified

https://doi.org/10.1021/acs.energyfuels.4c00705
Energy Fuels XXXX, XXX, XXX−XXX

MgAl2O4-Supported Ag Nanoparticles. *Catal. Commun.* **2018**, *111*, 26−30.
(272) Lee, E. J.; Kim, M. J.; Choung, J. W.; Kim, C. H.; Lee, K.-Y. NOx-Assisted Soot Oxidation Based on Ag/MnOx-CeO2Mixed Oxides. *Appl. Catal. A Gen.* **2021**, *627*, 118396.
(273) Guan, B.; Lin, H.; Zhan, R.; Huang, Z. Catalytic Combustion of Soot over Cu, Mn Substitution CeZrO2-δ Nanocomposites Catalysts Prepared by Self-Propagating High-Temperature Synthesis Method. *Chem. Eng. Sci.* **2018**, *189*, 320−339.
(274) Zhao, M.; Deng, J.; Liu, J.; Li, Y.; Liu, J.; Duan, Z.; Xiong, J.; Zhao, Z.; Wei, Y.; Song, W.; Sun, Y. Roles of Surface-Active Oxygen Species on 3DOM Cobalt-Based Spinel Catalysts Mx Co3-x O4 (M = Zn and Ni) for NO x-Assisted Soot Oxidation. *ACS Catal.* **2019**, *9* (8), 7548−7567.
(275) Liu, S.; Liu, Y.; Tang, D.; Miao, Y.; Cao, Z.; Zhao, Z. Synergy of NTP-La 1-x Ag x Mn 1-y Co y O 3-δ Hybrid for Soot Catalytic Combustion at Low Temperature. *Plasma Chem. Plasma Process.* **2021**, *41*, 1009−1019.
(276) Fu, M.; Lin, J.; Zhu, W.; Wu, J.; Chen, L.; Huang, B.; Ye, D. Surface Reactive Species on MnOx (0.4)-CeO2 Catalysts towards Soot Oxidation Assisted with Pulse Dielectric Barrier Discharge. *J. Rare Earths* **2014**, *32* (2), 153−158.
(277) Weng, R.; Mei, X.; Zhang, Z.; Xin, Y.; Xu, J.; Zhang, Y.; Zhang, J. Affecting Factors of Electrified Soot Combustion on Potassium-Supported Antimony Tin Oxides. *Chem. Eng. J.* **2023**, *465*, 143046.
(278) Mei, X.; Zhu, X.; Zhang, Y.; Zhang, Z.; Zhong, Z.; Xin, Y.; Zhang, J. Decreasing the Catalytic Ignition Temperature of Diesel Soot Using Electrified Conductive Oxide Catalysts. *Nat. Catal.* **2021**, *4* (12), 1002−1011.
(279) Khaskheli, A. A.; Xu, L.; Liu, D. Manganese Oxide-Based Catalysts for Soot Oxidation: A Review on the Recent Advances and Future Directions. *Energy Fuels* **2022**, *36* (14), 7362−7381.
(280) Kumar, P. A.; Tanwar, M. D.; Bensaid, S.; Russo, N.; Fino, D. Soot Combustion Improvement in Diesel Particulate Filters Catalyzed with Ceria Nanofibers. *Chem. Eng. J.* **2012**, *207*, 258−266.
(281) Uppara, H. P.; Pasuparthy, J. S.; Pradhan, S.; Singh, S. K.; Labhsetwar, N. K.; Dasari, H. The Comparative Experimental Investigations of SrMn (Co3+/Co2+) O3±δ and SrMn (Cu2+) O3±δ Perovskites towards Soot Oxidation Activity. *Mol. Catal.* **2020**, *482*, 110665.
(282) Wang, Y.; Xie, Y.; Zhang, C.; Chen, W.; Wang, J.; Zhang, R.; Yang, H. Tuning the Oxygen Mobility of CeO2 via Bi-Doping for Diesel Soot Oxidation: Experimental and DFT Studies. *J. Environ. Chem. Eng.* **2021**, *9* (1), 105049.
(283) ul Haq, M.; Turab Jafry, A.; Ali, M.; Ajab, H.; Abbas, N.; Sajjad, U.; Hamid, K. Influence of Nano Additives on Diesel-Biodiesel Fuel Blends in Diesel Engine: A Spray, Performance, and Emissions Study. *Energy Convers. Manag. X* **2024**, *23*, 100574.
(284) Gad, M. S.; Ağbulut, Ü.; Afzal, A.; Panchal, H.; Jayaraj, S.; Qasem, N. A. A.; El-Shafay, A. S. A Comprehensive Review on the Usage of the Nano-Sized Particles along with Diesel/Biofuel Blends and Their Impacts on Engine Behaviors. *Fuel* **2023**, *339*, 127364.
(285) Azad, A. K.; Doppalapudi, A. T.; Khan, M. M. K.; Hassan, N. M. S.; Gudimetla, P. A Landscape Review on Biodiesel Combustion Strategies to Reduce Emission. *Energy Reports* **2023**, *9*, 4413−4436.
(286) Altarazi, Y. S.M.; Abu Talib, A. R.; Yu, J.; Gires, E.; Abdul Ghafir, M. F.; Lucas, J.; Yusaf, T. Effects of Biofuel on Engines Performance and Emission Characteristics: A Review. *Energy* **2022**, *238*, 121910.
(287) Kumar, P.; Rehman, A. Bio-Diesel in Homogeneous Charge Compression Ignition (HCCI) Combustion. *Renew. Sustain. Energy Rev.* **2016**, *56*, 536−550.
(288) Saiteja, P.; Ashok, B. A Critical Insight Review on Homogeneous Charge Compression Ignition Engine Characteristics Powered by Biofuels. *Fuel* **2021**, *285*, 119202.
(289) Karre, A. V.; Garlapalli, R. K.; Jena, A.; Tripathi, N. State of the Art Developments in Oxidation Performance and Deactivation of Diesel Oxidation Catalyst (DOC). *Catal. Commun.* **2023**, *179*, 106682.
(290) Doppalapudi, A. T.; Azad, A. K.; Khan, M. M. K. Advanced Strategies to Reduce Harmful Nitrogen-Oxide Emissions from Biodiesel Fueled Engine. *Renew. Sustain. Energy Rev.* **2023**, *174*, 113123.
(291) Shi, Z.; Peng, Q.; Jiaqiang, E.; Xie, B.; Wei, J.; Yin, R.; Fu, G. Mechanism, Performance and Modification Methods for NH3-SCR Catalysts: A Review. *Fuel* **2023**, *331*, 125885.
(292) Luo, J.; Zhang, H.; Chen, X.; Ye, L.; Li, M.; Tie, Y.; Xu, S.; Chen, G.; Jiang, C. The Evaluation of Catalytic Activity, Reaction Mechanism and Catalyst Classification in Diesel Particulate Filter: A Review. *Clean Technol. Environ. Policy* **2024**, 1−43.
(293) Zhang, Z.; Dong, R.; Lan, G.; Yuan, T.; Tan, D. Diesel Particulate Filter Regeneration Mechanism of Modern Automobile Engines and Methods of Reducing PM Emissions: A Review. *Environ. Sci. Pollut. Res.* **2023**, *30* (14), 39338−39376.
(294) Leach, F. C. P.; Davy, M.; Terry, B. Combustion and Emissions from Cerium Oxide Nanoparticle Dosed Diesel Fuel in a High Speed Diesel Research Engine under Low Temperature Combustion (LTC) Conditions. *Fuel* **2021**, *288*, 119636.
(295) Arca Bati, Z.; Altun, S. Investigation of the Effect of Barium-Based Additive on Smoke and NO x Emissions of a Diesel Engine Fueled with Conventional and Biodiesel Fuels. *Clean Technol. Environ. Policy* **2020**, *22*, 1285−1295.
(296) Truex, T. J.; Pierson, W. R.; McKee, D. E.; Shelef, M.; Baker, R. E. Effects of Barium Fuel Additive and Fuel Sulfur Level on Diesel Particulate Emissions. *Environ. Sci. Technol.* **1980**, *14* (9), 1121−1124.
(297) Saikia, S.; Kumar, D.; Bhoumik, S.; Paul, A. Influence of Fuel Injection Timing and Pressure on the Performance, Combustion and Exhaust Emissions of a Compression Ignition Engine Fueled by Titanium Dioxide-Doped Biodiesel. *J. Therm. Anal. Calorim.* **2023**, *148* (13), 6515−6525.
(298) Shaafi, T.; Velraj, R. Influence of Alumina Nanoparticles, Ethanol and Isopropanol Blend as Additive with Diesel-Soybean Biodiesel Blend Fuel: Combustion, Engine Performance and Emissions. *Renew. Energy* **2015**, *80*, 655−663.
(299) Hoseini, S. S.; Najafi, G.; Ghobadian, B.; Ebadi, M. T.; Mamat, R.; Yusaf, T. Performance and Emission Characteristics of a CI Engine Using Graphene Oxide (GO) Nano-Particles Additives in Biodiesel-Diesel Blends. *Renew. Energy* **2020**, *145*, 458−465.
(300) Singh, G.; Singh, A. P.; Agarwal, A. K. Experimental Investigations of Combustion, Performance and Emission Characterization of Biodiesel Fuelled HCCI Engine Using External Mixture Formation Technique. *Sustain. Energy Technol. Assessments* **2014**, *6*, 116−128.
(301) Gowthaman, S.; Sathiyagnanam, A. P. Investigate the performance and Emission Characteristics of Temperature Charged methyl Ester Fuelled Homogeneous Charge Compression Ignition (HCCI) Engine. *Int. J. Appl. Eng. Res. 10* (13), **2015**, 11033−11047.
(302) Lavande, N. R.; More, R. K.; More, P. M. Mg Modified MnOx-CeO2-δ Catalyst for Low Temperature Complete Oxidation of Simulated Diesel Engine Exhaust. *Appl. Surf. Sci.* **2020**, *502*, 144299.
(303) Fan, R.; Li, Z.; Wang, Y. Y.; Wang, Y. Y.; Ding, Z.; Zhang, C.; Kang, N.; Guo, X.; Wang, R. Promotional Effect of ZrO2 and WO3 on Bimetallic Pt-Pd Diesel Oxidation Catalyst. *Environ. Sci. Pollut. Res.* **2022**, *29* (4), 5282−5294.
(304) Seo, Y.; Lee, M. W.; Kim, H. J.; Choung, J. W.; Jung, C.; Kim, C. H.; Lee, K.-Y. Effect of Ag Doping on Pd/Ag-CeO2 Catalysts for CO and C3H6 Oxidation. *J. Hazard. Mater.* **2021**, *415*, 125373.
(305) Liu, C.-H.; Chen, J.; Toops, T. J.; Choi, J.-S.; Thomas, C.; Lance, M. J.; Kyriakidou, E. A. Hydrothermally Stable Pd/SiO2@ Zr Core@ Shell Catalysts for Diesel Oxidation Applications. *Chem. Eng. J.* **2021**, *425*, 130637.
(306) Fan, L.; Sun, Q.; Zheng, W.; Tang, Q.; Zhang, T.; Tian, M. A Novel One-Step Hydrothermal Preparation of Ru/SnxTi1-xO2 Diesel Oxidation Catalysts and Its Low-Temperature Performance. *Nanoscale Res. Lett.* **2020**, *15*, 1−15.

AQ

(307) Li, P.; Chen, X.; Li, Y.; Schwank, J. W. Effect of Preparation Methods on the Catalytic Activity of La0. 9Sr0. 1CoO3 Perovskite for CO and C3H6 Oxidation. *Catal. Today* **2021**, *364*, 7−15.
(308) Heo, J. G.; Ullah, M.; Chun, M.-P.; Chu, Y. S.; Seo, S. G.; Seo, M. C.; Choe, Y. S.; Kim, D.-S. Low-Temperature Shift DeNOx Activity of Nanoflake V2O5 Loaded WO3/TiO2 as NH3-SCR Catalyst. *Inorg. Chem. Commun.* **2022**, *137*, 109191.
(309) Chen, X.; Liu, Q.; Wu, Q.; Luo, Z.; Zhao, W.; Chen, J.; Li, J. A Hollow Structure WO3@ CeO_2 Catalyst for NH3-SCR of NOx. *Catal. Commun.* **2021**, *149*, 106252.
(310) Zhu, H.; Wang, R. Rational Design of Porous CexNb1-x Oxide Hollow Nanospheres as a Novel NH_3-SCR Catalyst. *J. Mater. Chem. A* **2022**, *10* (22), 12269−12277.
(311) Zhang, K.; Wang, J.; Guan, P.; Li, N.; Gong, Z.; Zhao, R.; Luo, H.; Wu, W. Low-Temperature NH3-SCR Catalytic Characteristic of Ce-Fe Solid Solutions Based on Rare Earth Concentrate. *Mater. Res. Bull.* **2020**, *128*, 110871.
(312) Li, L.; Ji, J.; Tan, W.; Song, W.; Wang, X.; Wei, X.; Guo, K.; Zhang, W.; Tang, C.; Dong, L. Enhancing Low-Temperature NH3-SCR Performance of Fe-Mn/CeO_2 Catalyst by Al2O3Modification. *J. Rare Earths* **2022**, *40* (9), 1454−1461.
(313) Chen, C.; Xie, H.; He, P.; Liu, X.; Yang, C.; Wang, N.; Ge, C. Comparison of Low-Temperature Catalytic Activity and H_2O/SO_2 Resistance of the Ce-Mn/TiO_2 NH3-SCR Catalysts Prepared by the Reverse Co-Precipitation, Co-Precipitation and Impregnation Method. *Appl. Surf. Sci.* **2022**, *571*, 151285.
(314) Zhang, X. X.; Zhang, X. X.; Yang, X.; Chen, Y.; Hu, X.; Wu, X. CeMn/TiO_2 Catalysts Prepared by Different Methods for Enhanced Low-Temperature NH3-SCR Catalytic Performance. *Chem. Eng. Sci.* **2021**, *238*, 116588.
(315) Liu, S.; Yao, P.; Lin, Q.; Xu, S.; Pei, M.; Wang, J.; Xu, H.; Chen, Y. Optimizing Acid Promoters of Ce-Based NH3-SCR Catalysts for Reducing NOx Emissions. *Catal. Today* **2021**, *382*, 34−41.
(316) Tang, X.; Shi, Y.; Gao, F.; Zhao, S.; Yi, H.; Xie, Z. Promotional Role of Mo on Ce0. 3FeOx Catalyst towards Enhanced NH3-SCR Catalytic Performance and SO2 Resistance. *Chem. Eng. J.* **2020**, *398*, 125619.
(317) Liu, X.; Jiang, P.; Chen, Y.; Wang, Y.; Ding, Q.; Sui, Z.; Chen, H.; Shen, Z.; Wu, X. A Basic Comprehensive Study on Synergetic Effects among the Metal Oxides in CeO2-WO3/TiO2 NH3-SCR Catalyst. *Chem. Eng. J.* **2021**, *421*, 127833.
(318) Guillén-Hurtado, N.; García-García, A.; Bueno-López, A. Active Oxygen by Ce-Pr Mixed Oxide Nanoparticles Outperform Diesel Soot Combustion Pt Catalysts. *Appl. Catal. B Environ.* **2015**, *174*, 60−66.
(319) Tsai, Y.-C.; Lee, J.; Kwon, E.; Huang, C.-W.; Huy, N. N.; You, S.; Hsu, P.-S.; Oh, W. Da; Lin, K.-Y. A. Enhanced Catalytic Soot Oxidation by Ce-Based MOF-Derived Ceria Nano-Bar with Promoted Oxygen Vacancy. *Catalysts* **2021**, *11* (9), 1128.
(320) Govardhan, P.; Anantharaman, A. P.; Patil, S. S.; Dasari, H. P. H.; Dasari, H. P. H.; Shourya, A. Effect of Ag Loading on Praseodymium Doped Ceria Catalyst for Soot Oxidation Activity. *Korean J. Chem. Eng.* **2022**, *39*, 328.
(321) Uppara, H. P.; Singh, S. K.; Labhsetwar, N. K.; Murari, M. S.; Dasari, H. The Catalytic Activity of Ce-Hf, Ce-Hf-Mg Mixed Oxides and RuO2/HfO2 Deposited on CeO2: Role of Superoxide/Peroxide in Soot Oxidation Reaction. *Korean J. Chem. Eng.* **2021**, *38* (7), 1403−1415.
(322) He, J.; Zhang, H.; Wang, W.; Yao, P.; Jiao, Y.; Wang, J.; Chen, Y. Soot Combustion over CeO 2 Catalyst: The Influence of Biodiesel Impurities (Na, K, Ca, P) on Surface Chemical Properties. *Environ. Sci. Pollut. Res.* **2021**, *28*, 26018−26029.
(323) Wang, M.; Zhang, Y.; Yu, Y.; Shan, W.; He, H. Cesium as a Dual Function Promoter in Co/Ce-Sn Catalyst for Soot Oxidation. *Appl. Catal. B Environ.* **2021**, *285*, 119850.
(324) Vinodkumar, T.; Kumar, J. K. P.; Reddy, B. M. Supported Nano-Sized Ce0. 8Eu0.2O2-δ Solid Solution Catalysts for Diesel Soot and Benzylamine Oxidations. *J. Chem. Sci.* **2021**, *133* (3), 68.
(325) Raj, S.; Patra, P. K.; Debasish, D.; Ozawa, M.; Singh, S. K. Hydrothermally Prepared Ag-CeZrO2 Nanocomposite for Efficient Diesel Soot Oxidation. *Mater. Today Proc.* **2021**, *47*, 1163−1166.
(326) Xing, L.; Yang, Y.; Cao, C.; Zhao, D.; Gao, Z.; Ren, W.; Tian, Y.; Ding, T.; Li, X. Decorating CeO_2 Nanoparticles on Mn_2O_3 Nanosheets to Improve Catalytic Soot Combustion. *ACS Sustain. Chem. Eng.* **2018**, *6* (12), 16544−16554.
(327) Fang, F.; Zhao, P.; Feng, N.; Wan, H.; Guan, G. Surface Engineering on Porous Perovskite-Type La0. 6Sr0.4CoO3-δ Nanotubes for an Enhanced Performance in Diesel Soot Elimination. *J. Hazard. Mater.* **2020**, *399*, 123014.
(328) Uppara, H. P.; Dasari, H.; Singh, S. K.; Labhsetwar, N. K.; Murari, M. S. Effect of Copper Doping over GdFeO3 Perovskite on Soot Oxidation Activity. *Catal. Lett.* **2019**, *149*, 3097−3110.

https://doi.org/10.1021/acs.energyfuels.4c00705
Energy Fuels XXXX, XXX, XXX−XXX